Doxycycline-inducible overexpression of *NANOG* in bovine fibroblasts and nuclear transfer embryos

A thesis submitted in partial fulfilment
of the requirements for the degree
of
Masters of Science (Research)
in Biological Sciences
at
The University of Waikato
by

Alice Margaret Chibnall

The University of Waikato
2015

THE UNIVERSITY OF
WAIKATO
Te Whare Wānanga o Waikato

Abstract

Naïve pluripotent embryonic stem cells (ES cells) have the ability to give rise to all cell types including functional gametes. These cells have been well established in mice and rats. The potential for biomedical and agricultural applications of pluripotent stem cells in livestock are vast. Having this resource will make *in vitro* techniques more achievable for research purposes and commercial use. Their use for chimera formation will increase the production of high quality embryos, resulting in a faster inclusion of desirable traits in breeding lines.

The aim of this study was to investigate the molecular characteristics of pluripotency in bovine embryos. This is an incremental step to aid our understanding of the greater system which will encourage the derivation of ES cells within the bovine species. An initial target was the key pluripotency transcription factor NANOG. Nanog has thousands of targets and orchestrates the regulation of the naïve pluripotent molecular environment. This thesis will investigate the overexpression of *NANOG* with a doxycycline-inducible system in bovine female fibroblasts and nuclear transfer (NT) embryos derived from these. It was hypothesised that the overexpression of *NANOG* would stimulate the pluripotency network, increasing pluripotency. It has previously been recognised that the re-activation of the X-chromosome in females is an indicator of naïve pluripotency in mouse. Notably, the gene *Xist* which is important for the inactivation of the X-chromosome is directly repressed by Nanog. It was hypothesised that this would hold true in the bovine system.

Both the cell line and embryos were analysed for mRNA and protein expression of ectopic *NANOG* using quantitative PCR (qPCR) and immunocytochemistry. Eight pluripotency-related genes (endogenous *NANOG*, *OCT4*, *SOX2*, *KLF4*, *PDGFRα*, *SOX17*, *SOCS3* and *FGF4*) were quantified using qPCR to investigate the impact of increased NANOG in the NT embryo at day 8. Expression of *XIST* mRNA was analysed using qPCR and the inactive X-chromosome was identified using immunocytochemistry to understand the role of NANOG in the re-activation of the X-chromosome in the bovine system.

It was found that the inducible system significantly increased the expression of ectopic *NANOG* mRNA and protein within the fibroblasts used for NT. A two-fold significant increase of total *NANOG* mRNA was achieved in the NT embryo, although no additional NANOG protein was identified. The increased *NANOG* had no effect on the eight pluripotency-related genes investigated. The increased *NANOG* had no effect on the expression of *XIST* in the bovine system. No inactive X-chromosomes were identified via immunocytochemistry during this project. Subsequent to this research, details of an alternative overexpression technique using CRISPR technology were published. Use of this system will make research in this field achievable to a higher quality in a shorter timeframe.

Acknowledgements

I would like to thank the University of Waikato for the use of their facilities and for the lecturers who guided me through my undergraduate degree and the first year of my Masters' degree. The Bachelor of Science Technology degree has shaped my career and enabled me to be where I am today. In saying this, I would like to thank my placement co-ordinator Susan McCurdy for the connection she made between me and AgResearch. You encouraged me into a field which I am truly passionate about. I would also like to thank the Scholarships Office for their financial support in selecting me for the University of Waikato Masters Research Scholarship. This money has funded my living expenses for the last 15 months and was greatly appreciated.

In terms of my project work, I would like to specifically thank Dr Linda Peters. Your motivation and support throughout the past two years has kept me confident and excited about my research and future career opportunities. Thank you so very much for all the many versions of drafts you meticulously looked over and promptly returned.

I would also like to give a huge thanks to Dr Björn Oback for such a great opportunity. I would not have attempted a Masters' degree in such an awesome field, without your encouragement and inspiration. Your critical feedback on my research and writing was crucial for me to achieve a thesis I did not believe I was capable of. I would like to thank the wider team at AgResearch, in particular the reproductive technologies team. You were so welcoming and supportive of new students. I always felt I could ask any question about techniques being used and you all were so willing to teach me new things. I feel confident in a laboratory environment and that I can attempt any protocol thrown at me.

I would like to give a special thanks to all the lab mums. Andria Green, the cell culture lab mother, thank you for all the work that you did with the derivation of the EOG_TET_NANOG cell line prior to my research. Thank you for teaching me cell culture skills and being so helpful with new protocols. Fleur Oback, the

embryology lab mother, thank you for you're the hours and hours you spent at the micromanipulation microscope, enucleating hundreds of oocytes for me throughout my project. Pavla Turner, the molecular lab mother, thank you for your help with molecular lab protocols and the location of nearly every solution, reagent and sample in the building. I would like to thank my predecessor, Daina Harris, for teaching me nearly everything I know, when I first started at AgResearch way back in 2012. The other students and I were incredibly lucky to have you to ease us in to such a complicated field. I would like to thank all these wonderful women and Ljiljana Popovic for their friendship, advice and emotional guidance throughout my project. You all are inspirational.

I have not undertaken this feat on my own. There were many other students who went through this challenge alongside me. I would like to thank the other students from the University of Waikato for their friendship throughout this project, especially those who spent their days with me at AgResearch. Thanks to Zach McLean, and Pjotr Middendorf. An extra special thanks to Sarah Appleby for our time spent together during our cloning days and all your help with little details of my document and to Brooke Wilson who sat next to me throughout the 15 months of this project, for your friendship and support all the way.

Finally, I'd like to thank my family. Thanks to my father for housing me for the two years and for your financial support. I'd also like to thank you for your initial inspiration into the field of science and your confidence in my abilities. Your belief that I can do my best at anything and that will be enough has driven me through my education. To my mother for supporting me in my abilities and being a shoulder to cry on when times got tough. Thank you for your proof reading of my thesis it was very helpful although you couldn't understand a word in it! Finally, to my sister Grace, you were a very special support for me and I do not believe I could have achieved this without your love and friendship.

Table of Contents

List of Figures

List of Tables

List of Abbreviations

-Dox	Sample control not exposed to doxycycline
+Dox	Sample exposed to doxycycline
2i	Two inhibitors
3G	Third generation
3i	Three inhibitors
BLAST	Basic local alignment search tool
BMPs	Bone morphogenetic proteins
cDNA	Complementary DNA
CP	Crossover
CRISPR	Clustered regularly interspaced short palindromic repeats
COC	Cumulus-oocyte complexes
EOG	EF5_EF1α_OCT4-GFP
EOG_TET	EF5_EF1α_OCT4-GFP_TET3G_TRE3G
EOG_TET_NANOG	EF5_EF1α_OCT4-GFP_TET3G_TRE3G_NANOG
EPA	Environmental protection agency
ER	Endoplasmic reticulum
ERK	Extracellular signal-regulated kinase
ES cells	Embryonic stem cells
FACS	Fluorescence-activated cell sorter
FGF	Fibroblast growth factor
GFP	Green fluorescent protein
GSK3	Glycogen synthase kinase 3
HSNO	Hazardous substances and new organisms
ICC	Immunocytochemistry
ICM	Inner cell mass
IVC	*In vitro* culture
IVF	*In vitro* fertilisation
IVM	*In vitro* maturation
IVP	*In vitro* production
IRES	Internal ribosomal entry site
iPS cells	Induced pluripotent stem cells

LIF	Leukemia inhibitory factor
lncRNA	long non-coding RNA
mCherry	monomeric (m) red fluorescent protein (RFP)-reporter
MEFs	Mouse embryonic fibroblasts
MEK	Mitogen-activated protein kinase
mRNA	Messenger RNA
NCBI	National Centre for Biotechnology Informatics
NT	Nuclear transfer
NTC	No-template control
PC2	Physical containment level 2
PGCs	Primordial germ cells
PTC	Positive template control
qPCR	quantitative PCR
RNA FISH	Fluorescence RNA *In Situ* Hybridization
RNAi	RNA interference
RT	Room temperature
Rtta	Reverse tet transactivator
RU	Relative units
SEM	Standard error of the mean
ss	Serum starvation (Only used in figures and graphs)
Stdev	Standard deviation
TetR	Tetracycline repressor
WNT	Wingless-Type MMTV integration site family member
Xic	X-inactivation centre
Zona	Zona pellucida

Chapter 1: **Literature Review**

1.1 **The discovery of stem cells**

A stem cell is an undifferentiated cell which has not specialised into a cell type. A pluripotent stem cell can develop into any cell type in the body and can proliferate indefinitely. Pluripotency occurs during the reprogramming of the genome; it wipes the epigenetic history and allows a fresh start for the genome to begin development of a new organism. In 1981, the first embryonic stem (ES) cells were derived from 3-4 day old mouse (*Mus musculus*) embryos. In theory, a developing embryo must go through a phase of pluripotency to allow the subsequent development to occur; this event should take place across all animal species. However, only mouse has shown naïve pluripotency. Naïve pluripotency is stably pluripotent as opposed to primed pluripotency in which the cells is more responsive to differentiation cues. Most species investigated have only demonstrated putative pluripotency (Figure 1).

The first population of ES cells was derived from the inner cell mass (ICM) of a pre-implantation mouse blastocyst. All mammalian embryos have a blastocyst phase and go through the same initial developmental pattern. After initial fertilisation of the mammalian oocyte, the cytoplasm begins to cleave. It goes through a series of stages, 2, 4, and 8-cell, at which point the cells compact and form a tight morula [1] (Figure 1). A fluid-filled cavity is then formed and some cells compact into a small cluster known as the ICM [1] (Figure 1). The trophoblast will develop into the placenta, where the ICM is comprised of two populations of cells; the hypoblast and the epiblast. The hypoblast forms extra-embryonic components whereas the epiblast forms the embryo proper [1]. These populations are molecularly distinct from one another within the ICM. This development is similar across mammalian species. However, it differs in the duration of each stage (Figure 1). It is not until after the development of the blastocyst that there is a morphological distinction between species.

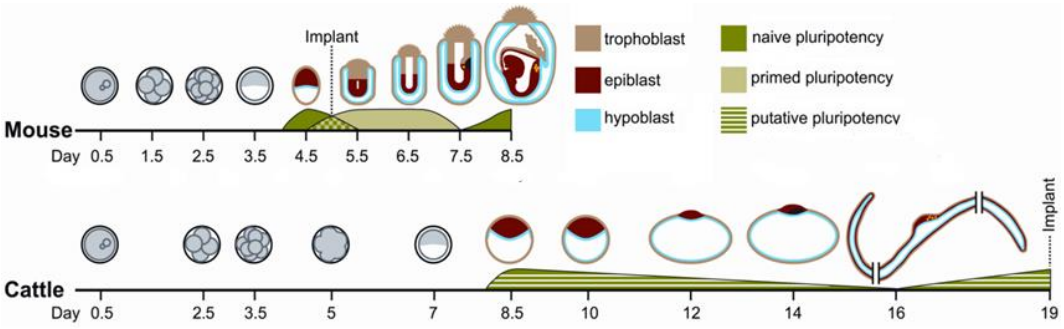

Figure 1: Early embryonic developmental stages of mouse and cattle in relation to its pluripotent state. Adapted from [1].

For a cell to achieve pluripotency status there are three validating assays. The first assay to verify pluripotency is to investigate the cells ability to develop into a teratoma, a tumour containing the germ layers mesoderm, ectoderm and endoderm. In this assay, the ES cell is placed *in vivo* and analysed for its abilities to derive cells from all three germ layers. The next assay is the chimera assay which tests the ES cells ability to contribute to an embryo once injected. This results in the creation of a chimera, where the organism contains two separate genomes. Cells that have a high pluripotentiality can also form germline chimeras in which the ES cell contributes to the formation of the germline. This is a more stringent assay as the germline is established prior to gastrulation of the three germ layers. The final and most rigorous assay is the tetraploid complementation assay which involves the combination of a tetraploid and a diploid embryo. A positive assay would result in an embryo that is completely comprised of the diploid genome where the extraembryonic tissue is derived from the tetraploid genome.

The search for the existence of these cells in other species intensified after the mouse ES derivation. In 1998, human ES cells were derived when the cells achieved the successful formation of a teratoma, suggesting they are pluripotent [2]. However, scientists still remain sceptical about their validity since chimera and tetraploid complementation assays were not completed. Due to the nature of these experiments, ethical boundaries prevent them from ever being conducted in the human species [3]. Therefore, the human ES cell cannot be truly validated as naïvely pluripotent. These three tests are considered ethically acceptable in

mammalian species other than human. However, ES cells derived from other species do not have the capacity to successfully achieve these assays.

When the mouse ES cell was derived it was found to require serum and mouse embryonic fibroblasts (MEFs) as feeder cells, which provided optimal culture media for the maintenance of pluripotency [4]. It was later discovered that the essential component produced by the feeders was leukemia inhibitory factor (LIF) [5,6]. Also, it was discovered that the serum could be replaced with bone morphogenetic proteins (BMPs), and in combination with feeder cells improve ES cell culture conditions [7]. These conditions have been attempted in the culture of other species' ES cells and have failed to stimulate pluripotency and allow indefinite cell proliferation. It is clear that these conditions are optimised for mouse ES cell growth and need to be modified to improve the culture conditions that support pluripotency in other species.

Recently, rat (*Rattus rattus*) ES cells have achieved all three pluripotency validating assays [8,9]. Thus, mouse and rat are the only animals to date that have demonstrated true pluripotency *in vitro*. Although it was initially believed that the ES cell requires extrinsic cues to promote the self-renewal pathways involved [10], it was later discovered that the ES cell also requires the block of the differentiation pathways to remain in a pluripotent state [11]. This resulted in the development of a variety of culture medias engineered to do so, such as 3i (three inhibitors). This contains the inhibitors for three cellular pathways, the three molecules; PD184352, PD173074 and CHIR99021. The CHIR99021 component is a small molecule inhibitor of glycogen synthase kinase 3 (GSK3) [12] which is a part of the Wingless-Type MMTV Integration Site Family Member (WNT) pathway. Whereas PD173074 and PD184352 are pharmacological inhibitors of fibroblast growth factor (FGF) [13] and mitogen-activated protein kinase (MEK) which is within the FGF pathway [14]. This media has allowed the production the rat ES cell, which have achieved true pluripotency. Unfortunately, this treatment was not as successful when applied in other species but does demonstrate the notion that the molecular environment of the cell can be modified to achieve the pluripotent status.

Over all after decades of research, these cells have really only been developed in mouse, rat and human. To truly understand pluripotency, the understanding of the molecular pathways involved must be extensively characterised, along with how these function to develop and maintain the pluripotent state.

1.2 Development and maintenance of pluripotency

The molecular mechanisms in place to develop and maintain the pluripotent state have been thoroughly investigated in the mouse model yet they are not greatly understood. There are four key extrinsic stimuli which activate four pathways that are known to play a role in the establishment and maintenance of pluripotency in the mouse model. These are BMP, LIF, FGF and WNT. They promote either self-renewal or differentiation by regulating the transcription of the three essential pluripotency regulators, SRY (Sex Determining Region-Y) Box-2 (Sox2) [15], Octamer Binding Transcription Factor-4 (Oct4) [16] and Nanog homeobox (Nanog) [17-19]. These factors are regulated depending on the stage of pluripotent development [20], which is governed by the four pathways involved.

Boosting the LIF pathway ultimately causes an up-regulation in the three key pluripotency regulators, which in turn increases the pluripotency of a cell. The BMP pathway acts by forming a balance between the FGF signalling and LIF signalling which maintains pluripotency by blocking ES cell neural differentiation [21]. The pathway FGF is involved in a number of processes such as cell survival, migration, proliferation and differentiation [22]. The FGF pathway also plays a role in lineage segregation within the embryo and ultimately also is one of the key regulators of pluripotency. When the FGF/extracellular signal-regulated kinases (ERK) pathway is inhibited, ES cells are able to maintain their pluripotency [23]. The FGF pathway is involved in the transition from the naïve pluripotency state, into the primed pluripotency state. The primed pluripotency state is a population of cells specific to the epiblast which do express many of the pluripotency indicators. However, they cannot achieve the stringent experimental requirements that naïve stem cells can [24]. This pathway is the key pathway involved in the transition into differentiation and is therefore a target for inhibition, in attempts to sustain pluripotency. Finally, the WNT pathway which regulates the differentiation of the cell into the three germ layers, has also been shown to

regulate self-renewal [25]. The activation of WNT results in an up-regulation of the three pluripotency regulators [26].

These four pathways have an impact on the regulation of *Oct4*, *Sox2* and *Nanog*. This triumvirate orchestrate thousands of target genes [27]. When this network is functioning the differentiation genes are switched off and the self-renewal genes are switched on. The reverse is true when this network is switched off [20,27]. Within the Nanog, Oct4, Sox2 network are a series of feedback loops. The Nanog protein binds to the promoter regions of *Sox2* and *Oct4*, as well as binding to its very own promoter region which can either result in expression or suppression of itself (Figure 2). *Oct4*, *Sox2* and *Nanog* are also individually regulated by the Oct4 and Sox2 heterodimer (Figure 2). This results in a core of transcription regulation (Figure 2).

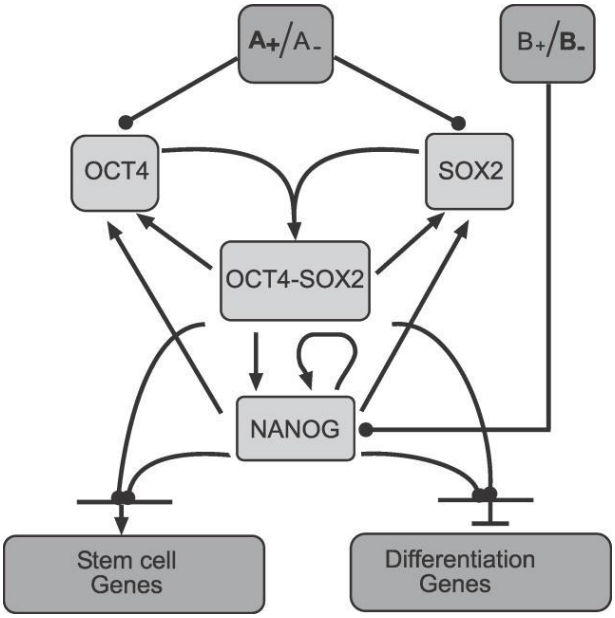

Figure 2: Core transcription factor network's regulation of pluripotency or differentiation. A and B represent two different pathways involved (Either LIF, BMP, FGF or WNT). In this example when A and B are switched on (+), the network is switched on resulting in the up-regulation of stem cell related genes and the intricate feedback loops of this system maintain pluripotency. Alternatively, A and B are switched off (-), it blocks Nanog's function and the core network dissolves resulting in differentiation [20].

With a greater knowledge of these mechanisms, other techniques such as 3i culture could be developed, allowing a greater potential to achieve the correct

culture conditions for ES cells for a variety of species. Many of these molecular markers described can be used in the identification of the time point in embryo development for pluripotency. This method allows research teams to hone in on a point in development which is more likely to achieve the culture of a truly pluripotent cell. A candidate molecular indicator for the development of pluripotency is X-chromosome inactivation.

1.3 Nanog's role in pluripotency

Although *Nanog* is not one of the genes required to maintain pluripotency [28,29], it is still heavily involved in "ground state pluripotency" [17]. It has also been theorised that *Nanog* may be the gene which initiates the development of pluripotency and may act as a transcriptional organiser of the other key pluripotent factors [30]. However, it is not required to maintain pluripotency once it has been established [17]. This was shown when *Nanog* was not required during dedifferentiation in the establishment of induced pluripotent stem cells (iPS cells) [28,29] but is the "gate keeper" for transition into "ground state" or naïve pluripotency in both ES and iPS cells [31]. When *Nanog* was removed from the mouse system the ICM was unable to generate an epiblast, and was incapable of maintaining pluripotency and differentiated into endoderm like cells [19].

In 2003, a group led by Professor Austin Smith from the University of Cambridge, identified *Nanog* [18]. The complementary DNA (cDNA) libraries of ES cells were functionally screened, which resulted in the detection of a homeobox gene which was only expressed in the early embryo. This homeoprotein was involved in cell self-renewal. The group therefore named this gene *Nanog*, after Tir na nOg, the mythological Celtic land of the ever young [18]. In a concurrent study, Dr Shinya Yamanaka from Kyoto University, used the *in silico* differential display technique to identify a series of genes that may be involved in pluripotency [19]. This was conducted on mouse ES cells and pre-implantation embryos. This also resulted in the discovery of the homeoprotein Nanog [19]. It was found that this protein allowed the cells to self-renew even in the absence of LIF [19,32]. In addition, when *Nanog* was deficient, the ICM did not generate an epiblast and in ES cells with Nanog deficiency, pluripotency could not be maintained, so the cells

differentiated [19]. This indicated that *Nanog* was essential in the development and maintenance of pluripotency [19].

After these two initial studies highlighted the significance of *Nanog* in the pluripotent system, the investigation of its finer workings within the system began. Surprisingly, the generation of iPS cells did not require *Nanog* to induce pluripotency [28,29], However, *Nanog* is important in the development of naïve pluripotency or "ground state" pluripotency, by orchestrating the core pluripotency factors to bind to their ES cell targets [31]. This is why *Nanog* was dubbed the "gatekeeper' of pluripotency. The next challenge was to understand if this models function is conserved across species.

When *Nanog* was removed from human ES cells via RNA interference (RNAi), there was an increase in the expression of genes associated with the extraembryonic endoderm and trophectoderm [31]. Alternatively, when *Nanog* was overexpressed in human ES cell culture it allowed the cells to propagate over a number of passages without the need for feeder cells. The *Nanog* overexpressing cells also no longer required media conditioned by MEFs which were usually required to provide the right environment for the cells to grow [33]. This is an indication that at least some of the workings of the *Nanog* system are conserved across mammalian species.

The function of *NANOG* in bovine is very similar to its role in the mouse model system. Again it is expressed in the bovine blastocyst in the ICM [34]. *NANOG* was also up-regulated from the morula to the blastocyst phase [35] and has a mosaic form of expression at day 7 [36] similar to that in mouse. It was also found that use of the 2i treatment (a treatment similar to 3i with two inhibitors) in bovine significantly up-regulates the expression of *NANOG* [37,38]. This indicates that NANOG's role in pluripotency is conserved throughout mammalian species and within the bovine system.

Nanog regulates the expression of thousands of genes by binding to their promotor regions [39]. The studies analysing the structure of the Nanog protein

elucidated how this function was preserved. The Nanog protein has three functional domains [40]. There is a homeodomain, which allows it to control the expression of other genes spatially and temporally [41]. The homeodomain is a 60 amino acid sequence which the protein uses to bind to its targets. This domain is highly conserved between vertebrate species [41].The Nanog homeodomain was found to bind to the TAAT(G/T)(G/T) motif [40]. Nanog also contains N and C terminal regions [40]. It has been confirmed that both regions undertake transcriptional actions [42]. The N terminal region is less active than the C terminal region seven-fold. This distinctive organisation of transactivators may allow Nanog to achieve the specificity and plasticity to interact with genes involved in pluripotency and differentiation [42]. There are multiple isoforms of Nanog found in the ES cell due to alternative splicing. In mouse, the longest isoform reported is a 2185 bp messenger RNA (mRNA) transcript encoding 305 amino acid protein [41] with a molecular weight of 34 kDa [43]. The Nanog protein has a brief half-life of 120 minutes [44] which allows tight regulation within the ES system.

Nanog plays a role in the four extrinsic signals relevant to the pluripotency network, LIF, FGF, BMP and WNT [45]. This was shown when increased levels of Nanog can allow human ES cells to grow feeder free [33] and mouse ES cells to be maintained without LIF [19]. There are also intrinsic pathways in which Nanog is involved such as the pluripotency trio Nanog, Oct4 and Sox2 [20]. Another important target of Nanog is *Xist* and their partnership in the re-activation and inactivation of the X-chromosome [46].

1.4 X-chromosome inactivation

There are a number of features of ES cells which can be used to identify whether they are truly pluripotent. One of these is double X-chromosome activation [31]. This is a stage of the process of X-chromosome inactivation [47]; a method of epigenetic silencing of the X-chromosome that has been extensively analysed in the mouse. This mechanism is required in female mammals as a form of dosage compensation for X-chromosomal genes which are only expressed from one X-chromosome in male mammals [48,49]. Females must effectively silence one

of their X-chromosomes from transcription and translation throughout their entire body [48].

There are a number of regulators of the X-chromosome inactivation process. It is largely controlled by the X-inactivation centre (*Xic*) [50] which contains multiple long non-coding RNAs (lncRNA) [51] that interact with one another to orchestrate the process of X-chromosome inactivation and reactivation. This is where the *Xist* gene is located, which encodes a 17 kb lncRNA which works in *cis* [50,52,53]. *Xist* forms a cloud around the inactive X-chromosome which prevents it from transcription and translation [52]. It does this by orchestrating heterochromatin changes, for example the recruitment of the Eed-Enx1 Polycomb group complex [54] which is required to establish methylation such as $H_3K_{27}me_3$ [55]. The silencing of the X-chromosome ultimately creates a balance between males and females in the expression of X-chromosome genes. Within the *Xic* also lies the *Xist* antisense *Tsix* [56]. *Tsix* is a 40 kb lncRNA, which is transcribed from both active X-chromosomes prior to inactivation. The expression of *Tsix* becomes monoallelic at the onset of X-chromosome inactivation and is expressed on the future active X-chromosome and cannot be detected on the inactive X-chromosome [56]. *Tsix* silences *Xist's* promoter and effectively supresses *Xist* expression [57,58]. It would be a simple mechanism if *Tsix* was the sole repressor of *Xist* and these two genes worked together to activate and inactivate the X-chromosomes. However, it has been characterised that there is a lack of *Tsix* in the reactivation of the inactive X-chromosome in the primordial germ cell (PGCs) which occurs later in development (Figure 3) [46]. This coupled with the suppression of *Xist* during the development of ES cells (Figure 3) encourages the idea that the factors involved in the regulation of pluripotency also play a role in the reactivation process via the suppression of *Xist* expression [46].

During this process there is a time point in which the silencing of the X-chromosome is reversed and for a brief period both X-chromosomes are active [59]. This is the result of a genome wide epigenetic wipe, in which all epigenetic elements such as methyl groups are removed from the genome as if to refresh the genome for its development into a new organism. This wipe also causes a small

population of cells to become naively pluripotent [59]. The most obvious marker for this event is the disappearance of *Xist* and its cloud around the inactive X-chromosome [59,60]. These clouds are very clear markers leading up to the development of ES cells, which disappear for the brief window when ES cells are established and develop again soon after. Therefore, with the use of a technique such as RNA fluorescence *in situ* hybridisation (RNA FISH), the process can be visualised taking place during the development of an embryo, where the absence of the *Xist* clouds can be used as an indicator for the presence of ES cells [59]. The timeline of the mouse X-chromosome inactivation and reactivation is illustrated in Figure 3 [46].

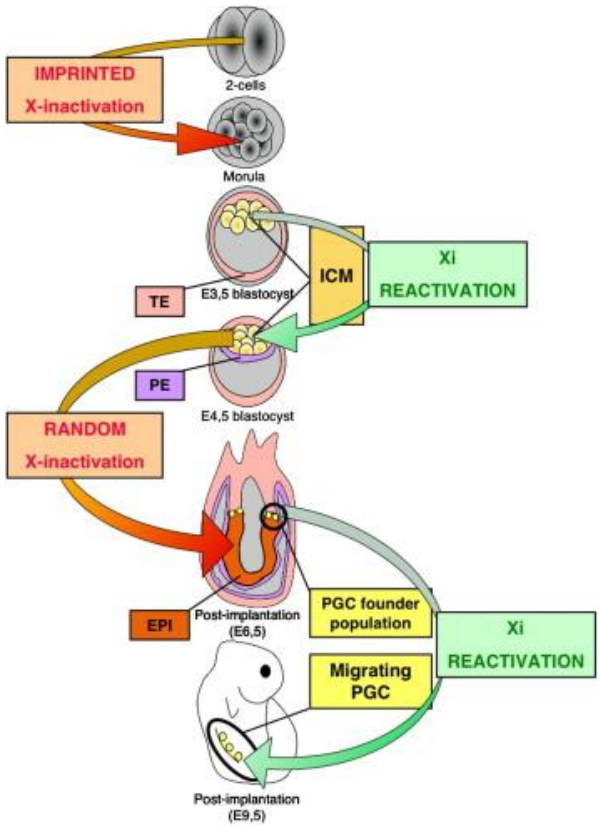

Figure 3: X-chromosome inactivation and reactivation in early mouse embryo development. Trophectoderm (TE, in pink), primotive endoderm (PE, in purple), inner cells mass (yellow), inactive X (Xi), epiblast (EPI, in orange), primordial germ cells (yellow). Image from:[46].

After initial fertilisation there is an imprinted X-chromosome inactivation. This is always the paternal X-chromosome [46] and it remains inactive until the embryo reaches the blastocyst phase. At this point, day 3.5 in mouse, the inactive X-chromosome switches back on for a brief period before a random

X-chromosome is selected and silenced at day 4.5. At the post implantation stage (day 6.5), the PGCs develop and again the inactive X-chromosome is reactivated until the PGCs have migrated, when finally one X-chromosome is randomly inactivated from then on [46].

When the activities of the pluripotency regulating transcription factors are evaluated in terms of *Xist* expression and X-chromosome reactivation, the elaborate mechanisms are revealed. It was previously assumed that the suppression of *Xist* and subsequent reactivation of the inactive X-chromosome was a by-product of the profound epigenetic reprogramming that occurs during pluripotency and was not the primary target [61,62]. However, recently it has been established that Oct4, Nanog and Sox2 maintain the suppression of *Xist* by binding to the chromatin of the *Xist* gene during the development of ES cells [63]. *Xist* is targeted by the pluripotency triumvirate and is actively suppressed during pluripotency [46]. The reactivation of the X-chromosome and the pluripotent status of the cell are intimately linked in that the stages of reprograming are directly related to degree of X-chromosome silencing [64].

There have been multiple theories as to how this may occur. One of which is depicted in Figure 4 [46]. Oct4 and Sox2 are active throughout the earlier development then later become more localised to the ICM. The reactivation of the X-chromosome does not occur until there is an increase in *Nanog* expression during the development of the blastocyst and the PGCs. This indicates that Nanog may be the predominant influence of the repression of *Xist* [46]. As demonstrated by iPS cells, *Nanog* is not required to maintain pluripotency [28,29]. However, it is required to produce the naïve ground state pluripotency seen in ES cells [31]. This shows *Nanog's* role as a regulator, only required to establish pluripotency but not essential to sustain it [46]. This may be the same way in which it acts in regards to *Xist* suppression. This is why the reactivation of the X-chromosome is only seen in the Nanog positive cells of the ICM and PGCs [46]. In relation to the model (Figure 4), Nanog may be able to bind to *Xist* intron 1. This could orchestrate a remodelling of the chromatin which allows the binding sites for *Oct4*

and *Sox2* to be unveiled. Finally, Oct4 and Sox2 can bind to *Xist* intron 1 and actively supress its expression [46].

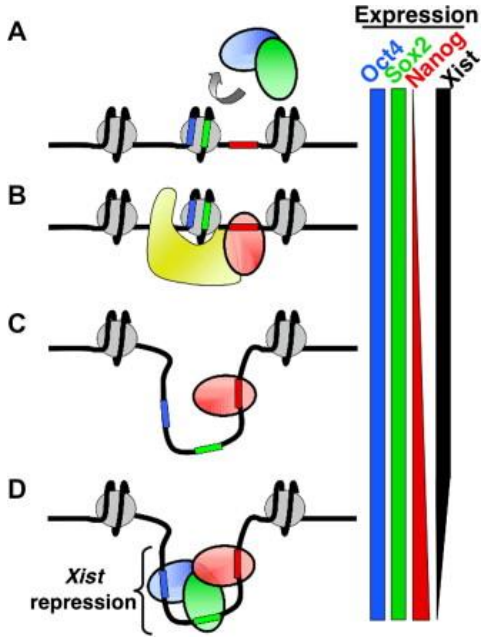

Figure 4: One theorised model of *Xist* repression via the action of the pluripotency factors Nanog, Oct4 and Sox2. A) Early cleavage stages express Oct4 (blue) and Sox2 (green). However, these cannot bind to Xist (black) intron 1 and *Xist* mRNA expression remains high. Oct4 and Sox2 binding sites remain tightly bound around nucleosomes (grey) B) As *Nanog* (red) begins to be expressed it employs chromatin remodelling complexes (yellow). C) These restructure the chromatin which exposes the binding sites for *Oct4* and *Sox2*. D) Once these have successfully bound to *Xist* intron 1 *Xist* is repressed. Image from:[46].

In describing the development and maintenance of pluripotency, many of the pathways involved had a direct impact on the regulation on the gene *Nanog*.

1.5 Nanog's role in X-chromosome reactivation

It is clear that the process of X-chromosome inactivation and reactivation is intimately linked with pluripotency in the mouse. This is why in these experiments the presence of the *Xist* clouds and its notable absence during the development of ES cells was used as an indicator for the function of Nanog and the timing of ES cell development in the bovine species. In the mouse, the interplay between *Nanog* expression and *Xist* expression was demonstrated by a team led by Professor Austin Smith in 2009 [31]. At day 3.5, the expression of Oct4 and Nanog is stronger in the ICM and trophectoderm (Figure 5). Also at this

time point, the expression of Eed, a constituent of the Eed-Enx1 Polycomb group complex used to establish epigenetic methylations on the inactive X-chromosome, is present within each cell throughout the embryo, representing the inactive X-chromosome. At day 4.5, there is an up-regulation in *Nanog* expression in a small population of cells within the ICM. The correlating cells in the Eed panel no longer possess their inactive X-chromosome. Both X- chromosomes are active within these cells and this population can be defined as naïve "ground state" pluripotent ES cells.

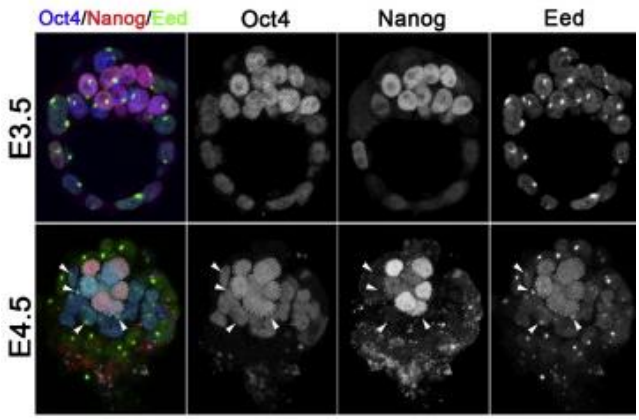

Figure 5: Expression of Oct4, Nanog and Eed at day 3.5 compared with day 4.5. E denotes embryonic day Arrows highlighting cells of the ICM. Image adapted from [31].

It has also been demonstrated that the increase in expression of *Xist* via a doxycycline-inducible system caused the suppression of the pluripotency associated genes, *Prdm14*, *Tcl1* and *Nanog* [65]. In the same study it was also confirmed that the double dosage of X-chromosome genes disrupts differentiation [65]. It is clear that the interplay between pluripotency and double X-chromosome activation is intimate [64].

It is hypothesised that this extensive link between *Nanog* and *Xist* (Eed) (Figure 3) may hold true in other species including bovine. Therefore, an analogous image using bovine ES cells as depicted in Figure 5 is the objective of the experiments conducted for the purpose of this thesis. To accomplish this requires a large number of female embryos, which overexpress the gene *NANOG*. This can be achieved via the technique of nuclear transfer (NT) cloning.

1.6 The history and utility of nuclear transfer cloning

In conducting any scientific experiment, it must be clear that the difference between the control group and the treatment group can only be a result of the treatment and not as a result of other factors. For many fields of research, this difference is easy to navigate. The use of identical twins in many human genetic studies has been valuable, as they possess the same genomic sequence and therefore can be used as control groups for one another [66]. This is where the cloning of animals serves the purpose of being able to produce such a set of genetically identical individuals for analysis of gene function, epigenetics and early developmental events [67].

The NT process is relatively simple in theory. A donor cell containing the desired DNA is fused with an unfertilised egg whose DNA was removed. The oocyte is then activated and begins normal embryonic development resulting in an adult animal [67] (Figure 6). The theory of nuclear transfer experiment was established in 1928 by Hans Spemann [68]. It was first put into practice in 1952 in experiments conducted by Robert Briggs and Thomas King [69] using embryonic blastula cells. The first time a somatic cell was transplanted and successfully reprogrammed was by Sir John Gordon in 1958 at the University of Oxford in the Xenopus tadpole [70,71]. This was the first time it was demonstrated that an adult cell can reprogramme its DNA in order to orchestrate the genetic regulation required during embryo development and growth. This encouraged heavy interest in the idea, leading to the first successful mammalian clone, at Roslin Institute in Scotland, with the production of Dolly the sheep in 1996 [72]. After this ground breaking achievement the number of cloned mammalian species increased, with many other species of mammals being successfully cloned [73-85], including the first successful bovine clone in 1998 [86,87]. All species have slight modifications to the NT method to increase efficiency. The standard method used for cow NT is shown in (Figure 6).

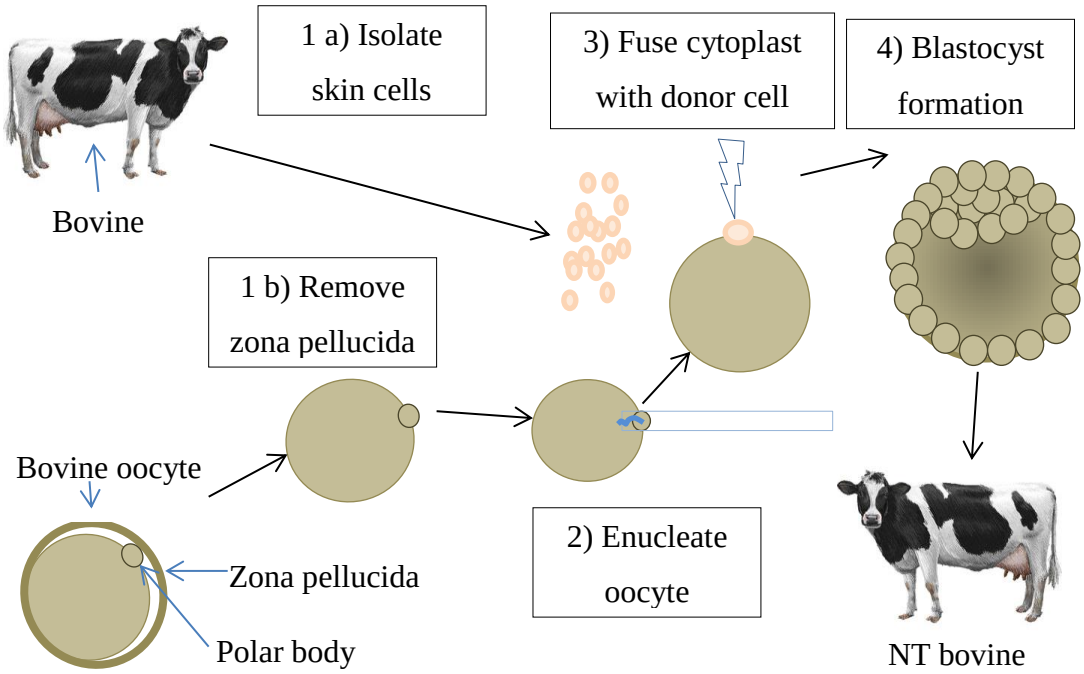

Figure 6: Somatic cell nuclear transfer method for bovine. 1 a) Skin cells are isolated from an adult animal. 1 b) Oocytes retrieved from an adult animal have their zona pellucida removed and they are enucleated (2)..Enucleated oocytes are fused with the isolate skin cells (3). Normal embryonic development then follows (4). The embryo develops into an adult.

This technique also allows the formation of genetically modified organisms [88] which during the culture of somatic cells may be transfected with vectors to overexpress or remove genes that are already present or to add genes that are not present in that organisms system. This allows the understanding of how that specific gene functions during the embryonic development of the organism and can elucidate a genes role. Animals that do not have pluripotent ES cells, but do have an established NT method, use NT to generate transgenic animals. This has become common practise for research in species such as bovine and porcine [88-90].

NT cloning was employed for the research conducted in this thesis. A transgenic cell line was created for the use in NT experiments to analyse the response of the overexpression of a gene. The cell line was transfected with a doxycycline-inducible vector which will be explained in more detail in section 1.7.

1.7 Tet-3G system and how it functions

Numerous techniques can be used to overexpress a gene in the mammalian cell. The most efficient technique is the production of the chimera, as explained in section 1.9. However, this technique requires the truly pluripotent ES cell, which the bovine does not have, thus, a different technique must be employed. Another overexpression technique is the use of the Tet-On 3G tetracycline inducible gene expression system (Tet-3G system) [91]. This was the system which was employed for this research. It uses the antibiotic tetracycline or a derivative (doxycycline, which is much more stable) to control gene expression by either turning transcription on or off.

This system involves the naturally occurring Tetracycline-repressor (TetR) which results in tetracycline resistance for some gram-negative bacteria [92]. TetR regulates the expression of TetA (the protein that moves tetracycline out of the cell) [92]. The expression of TetA and TetR are blocked by the presence of two homodimeric TetR molecules which bind to two DNA operator regions of the resistance determinant [92]. When tetracycline is present it forms a stable complex with TetR which prevents it from binding to the operators. This allows the expression of TetR and TetA. When TetA is present it can then export the tetracycline away from the ribosome before it can inhibit ribosomal activity [92].

This prokaryotic expression system can be used in the eukaryotic cell to induce or silence the expression of genes as a part of a vector sequence [93]. Doxycycline is simply added to the culture medium of the tissue. It binds to the Tet-On 3G transactivator, which as a result binds to the promoter region of the vector and commences transcription (Figure 7). The vector sequence can also contain a reporter protein, such as monomeric (m) red fluorescent protein (RFP)-reporter (mCherry), to indicate induction by visualisation of red fluorescence (Figure 7). The internal ribosome entry site (IRES) is located 5’ to the gene of interest which allows the translation of the protein to be initiated at this point, resulting in two separate protein constructs from a single mRNA sequence [94]. There are a few different types of this system that are commercially available, including those which switch off expression and others switch on expression when doxycycline is

present. The system used for the purposes of this research was the third generation (3G) system. This system is an improved system of the method originally developed by Hermann Bujard, Wolfgang Hillen and Manfred Gossen. It has increased sensitivity and reduced background by the addition of a new transactivator protein and promoter [91].

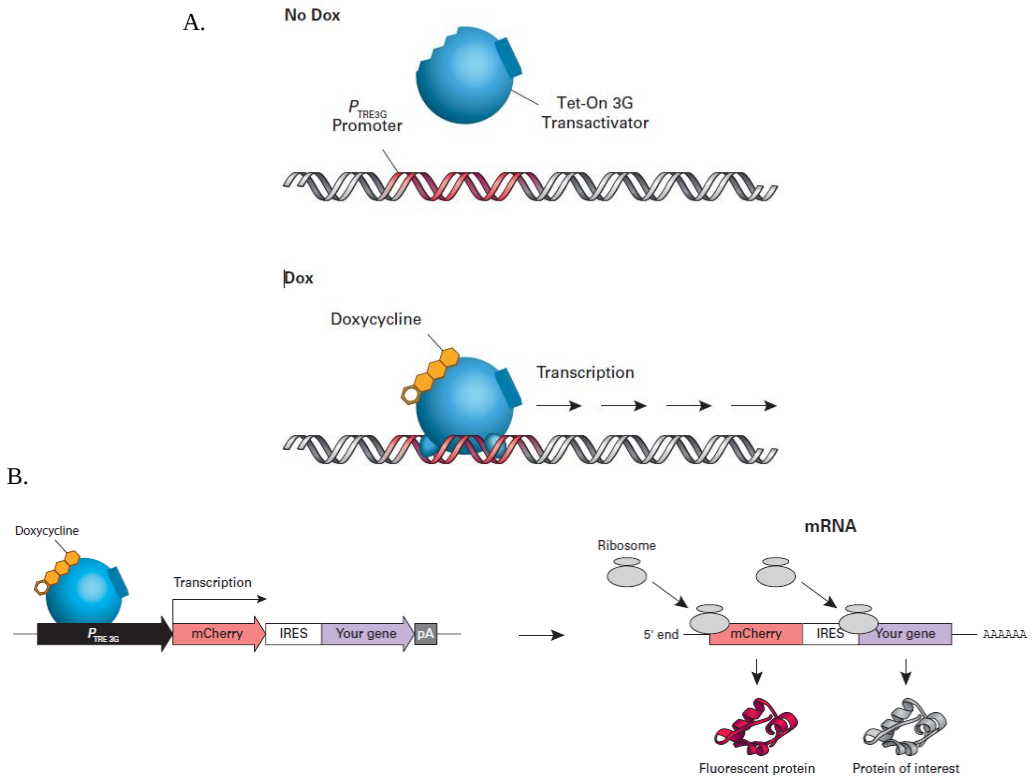

Figure 7: The Tet-On 3G system. A. Representation of the system in the absence of doxycycline, compared with in the presence of doxycycline. B. The Tet-On 3G system as a part of a vector containing mCherry as a reporter protein and a representation of the gene of interest [91].

The advantage of developing a cell line containing the Tet-On 3G system is that it has the ability to be able to induce the cells or embryos at any stage of development or growth [93]. This allows the gene to be switched on or off for any duration at any time point during embryonic development and can provide insight into how the gene functions at the different stages of development or at what time point the gene is essential or detrimental. This is critical for pluripotency studies as the development of pluripotent embryonic stem cells occurs for one brief time point during embryo development. Therefore, temporal investigation into gene

regulation during embryonic development is required to understand when the key genes are activated and when they are repressed.

1.8 Current status of bovine stem cell research

To date there has been no successful isolation of pluripotent stem cells in bovine or any other domestic ungulate [1]. This is because the understanding of how the bovine genome functions is still relatively low [95]. There are a number of reasons for this. Firstly, there are problems caused by the lack of an *in vitro* culture for the post hatching stages of development (where the development of pluripotent ES cells may arise) [1]. This means that the collection of embryos at such a stage requires *in vivo* culture and recovery via the flushing of the uterine tract. This in turn limits the number of embryos recovered and creates obstacles for certain treatments such as altering culture conditions and media composition. Secondly, there are issues in finding specific probes for bovine, such as primers and antibodies, because bovine work is not conducted on such a large scale as human or mouse [1]. Our lack of knowledge of the mechanics of pluripotency means we cannot yet produce the ideal conditions which could encourage the production bovine stem cells. The lack of stem cells slows our knowledge of the functioning of genes in the bovine system, creating an endless loop of hurdles for this field of research. Progress is currently slow, but there have been many advances in the 20 years of research in this field.

This research began with the development of an *in vitro* fertilisation (IVF) protocol to produce large quantities of early bovine embryos. The attempts to isolate ES cell cultures from these embryos then quickly began [96]. The culture of cell lines derived from the embryos ICMs were more successful in the later stages after hatching [97]. Many of the protocols employed within the mouse or human species were applied to attempt to produce a similar pluripotent state, including LIF supplementation, serum and feeders. Similar to human ES cell culture, LIF supplementation did not stimulate pluripotency [98,99]. In the genetic analysis of these cells cultures it was found that *OCT4* was expressed but there was a down-regulation in *SOX2* and *NANOG* after few passages, although they were initially expressed [100]. Also many of the key components for the

signalling factors of the murine system were also detectable in these cultures, such as, LIF, BMP, and WNT [100].

When bovine ES-like cells were analysed against the stringent pluripotency validating experiments, they were able to achieve teratoma formation from the epiblast of *in vivo* embryos at day 14, but not from the day 8 to day 10 stages [101]. Although no undifferentiated stem cells were identified in any of the tumours produced [101]. They have also achieved a chimera after only brief cell culture (passage 3-13) [102], although none of these were successful in populating the germ line [102]. Ultimately, the bovine ES cell has shown no naïve pluripotency. There is clearly much more to be done in terms of bovine ES cell derivation. More of what is already known of the mouse and human model can be used to identify a timeframe in which the naïvely pluripotent ES cells are formed within the early bovine embryo. This project integrated the knowledge discussed to do so.

1.9 The utility of embryonic stem cells and its potential in cattle

The biomedical and agricultural applications of pluripotent stem cells are vast. To date ES cells have only been derived from mouse [4] and more recently, in rat in 2008 [8]. The derivation of human ES cells has taken a different path in terms of research and will only be referred to here as a molecular model, as it is the one that most closely resembles the bovine (*Bos taurus*) model [1]. Since the discovery of ES cells in the mouse species in 1981 [4], our understanding of the mouse genome and its functioning has increased at an unprecedented rate [103] and this is currently in progress with the rat genome. However, the progression from mouse to rat was slow, and there have even been difficulties in developing ES cells for alternative mouse strains. Regardless, many research teams quickly began attempting to develop these cells in a variety of agricultural species such as goat [104], horse [105], pig [106-108], sheep [107], and cattle [96].

The reason for this interest is because the stem cell can be used as a scientific tool. For example, its use in the development of genetically modified mouse lines [103]. The first step of which is to isolate a clonal population of ES cells which contain

the desired mutation. The desired mutation is introduced by transfecting the cells with a DNA vector sequence. The cell population is then enriched via antibiotic selection, as the cells are also transfected with an antibiotic resistant gene. These cells are then used to generate chimeras which are whole animals comprised of two different sets of genomes, via the injection of the ES cell into a pre-implantation embryo. The embryo is then transferred into a foster mouse and is carried to full term. The ES cell then incorporates into the adult animal, if by chance it produces the population of gametes, then the next generation will contain the desired genotype. When these are mated with one another they produce a breeding line of mouse which contains the desired genetic modifications. This is the technique used to create "knock-in", "knock-out" or "knock-down" lines, where a gene is added, removed, or down-regulated within the system. This allows understanding of the function of the gene within the organism [103]. The ability for the ES cell to be capable of forming a chimera is one of the criteria of the naïve pluripotent stem cell. There have been no such ES cells identified in the bovine species [1].

The lack of bovine stem cells has become a barrier against our understanding of the bovine genome and is exacerbated by the fact that the bovine generation time (approximately 4-6 years [109]) is much longer than that of a mouse (eight to nine weeks [110]). Therefore the development of transgenic animals in bovine, although achievable, is incredibly challenging, costly and time-consuming to understand the function of just one gene. Once bovine stem cells are derived, the use of these cells as tools will allow the analysis of genes, which will rapidly increase our knowledge of how the bovine genome functions. This will give relevance and understanding to the genotyping that dairy and beef farmers are already conducting on their herds. In addition, this will culminate in gene targeting as it will be applied to enhance the genetic quality of New Zealand's national herd. Ultimately it will increase the productivity of New Zealand's largest industry, the dairy industry. This is the goal of the reproductive technologies team at AgResearch; to identify and isolate naive pluripotent stem cell in the bovine species. This is just one of the many applications for bovine ES cells, more of which will be discussed in section 1.10.

1.10 **Research rationale and objectives**

The research conducted in accordance with this thesis was an incremental step towards the derivation of naïve pluripotent stem cells in bovine. There are a number of applications for these cells once they have finally been harvested successfully. The bovine system shows higher similarity to the human system than the mouse [1] and therefore understanding of the bovine system can give insight into how these mechanisms are evolutionarily conserved and ultimately comprehension into the human system [1] in which many research experiments are unethical.

Because the stem cell can be used to engineer the genome of the bovine, giving rise to genetically modified animals in just one generation, there will also be many applications available with the use of genetic modification [1]. One opportunity for bovine would be the idea that they could be used as bioreactors to produce biopharmaceutical proteins [1]. The stem cell population could be modified to overexpress a specific gene, producing a desired protein in large quantities. This protein could be harvested in their milk and therefore be produced in bulk without harming the animals in any way. Similar projects to this have already been conducted, such as the recent study which produced Daisy, a cow that produces milk that does not contain the common allergen β-lactoglobulin [111]. This cow contains an RNAi knock-down which down-regulates β-lactoglobulin, a protein that is a major contributor [112] to the 2% of the populations milk allergies [113]. Without the availability of bovine stem cells this project took six years. With the availability of stem cells many steps such as creating a stable cell line and NT cloning can be avoided and the desired cow can be produced much faster.

Another possibility is the use of these animals for human disease modelling, as there are many shortcomings for rodents in this function. The much larger size of bovine better resembles the human body and modifications to its genome can produce a more similar disease model than is achievable by the mouse, giving us a better picture of how the disease functions [1]. Also with slight modifications to specific genes within the bovine surrounding its immune system, there is the possibility of xenotransplatation, which is where bovine could be used as organ

donors for humans as long as they have been altered to become immunocompatible [1]. They will also make the production of "knock-out" and "knock-in" animals much quicker to produce by allowing germline chimera formation, which will result in the understanding of the function of a gene in the bovine system to be uncovered in a much shorter timeframe. This will culminate in a rapid increase in knowledge of the functioning of the bovine system, which will mean that genotyping results of elite animals will be better understood.

Most importantly from an agricultural perspective, the isolation of bovine ES cells will improve the way animals are selected for breeding. The conventional technique was to phenotype the progeny of an animal [114]. This would take six years for the course of two generations in bovine, ultimately delaying genetic gain. With improvements in DNA sequencing, the genotyping of offspring is now possible, although still relatively new, it will allow the selection of embryos that have high genetic quality during the IVF procedure, shortening the selection time to just one week. Since *in vitro* procedure (IVP) has a low chance that each embryo will survive until calving, the use of ES cells will be of great benefit. If an embryo is identified to have desirable genetics, it could be harvested for ES cell culture. ES cells are able to generate multiple embryos with the desirable DNA through chimera generation. This will rapidly increase the speed of genetic gain in the bovine species and has the potential to increase milk yield, decrease disease, increase meat quality and decrease environmental impacts of farming, overall increasing productivity for the dairy industry.

The overexpression of *NANOG* was hypothesised to have an effect on related pluripotency factors as it has shown this in a number of other models such as mouse, pig and human [18,33,115]. Understanding the effects of *NANOG* overexpression in the bovine system was the first objective for this research. To investigate this, eight pluripotency-related genes were studied. A series of genes that collaborate to produce pluripotency were investigated along with markers of the hypoblast. This was to see if there is a decrease in the size of the hypoblast as opposed to the epiblast which is identified by *NANOG* expression [31].

One interesting NANOG target is itself. NANOG can bind to its own promotor and either stimulate or supress expression [20]. Therefore, analysis of endogenously expressed *NANOG* versus ectopic *NANOG* was conducted. Also an investigation into the core pluripotency network, OCT4 and SOX2 was performed to see if overexpression of *NANOG* stimulated this network. One of the iPS cell factors was also evaluated, Krupple-like factor 4 (KLF4). Klf4 binds directly to the promotor region of Nanog [116] and is one of the four factors required in the dedifferentiation of cells used in iPS cell generation. It was theorised that the increase in *NANOG* expression would increase the expression of *KLF4*. *FGF4* is another gene of interest, in recent 2i studies in bovine, both *NANOG* and *FGF4* were up-regulated when embryos were cultured in 2i media [37]. The link between NANOG and FGF4 is intimate and it was expected that the overexpression of *NANOG* would result in the up-regulation of *FGF4*.

Consistently in mouse, Nanog has been shown to supress hypoblast markers [31]. The hypoblast can be identified by SRY (Sex Determining Region Y)-Box 17 (*Sox17)* and platelet-derived growth factor receptor, alpha polypeptide (*Pdgfrα)* [117-119]. *Sox17* is a marker for differentiation and directly interacts with the pluripotency network as overexpression of *Sox17* directs cells into differentiation. [117]. It was previously found that *SOX17* was significantly down-regulated with the use of the 2i treatment in bovine, which also resulted in an up-regulation of *NANOG* [37]. This is likely because Nanog and Sox17 compete for the same binding locations [117]. *PDGRFα* is also a marker for the hypoblast and is essential for the proliferation of the hypoblast lineage [118]. This was also down-regulated during 2i treatment in bovine [37]. Suppressor of cytokine signalling 3 (Socs3) is also a differentiation marker that negatively regulates the LIF pathway [120]. It is down-regulated by Nanog and results in an enhanced LIF signal transduction. Therefore, with the overexpression of *NANOG* it was expected to result in a decrease in *SOCS3* expression.

It was also theorised the inactivation and reactivation of the X-chromosome would occur in all mammalian females. Investigation of bovine ES cells and the analysis of their X-chromosomes reactivation may illuminate a time point in

which ES cells may be targeted for collection in bovine. Based on research conducted in the mouse model, showing Nanog's role in down-regulating *Xist*, it was hypothesised that overexpression in *NANOG* via the Tet-on 3G system would cause a down-regulation in *XIST* levels. It was theorised that this would result in either an increased duration of the double X-chromosome active signal and/or it would more completely remove the *XIST* clouds surrounding the inactive X-chromosome. Investigation of the effects of increased *NANOG* on *XIST* expression was the second objective of this research.

Chapter 2: **Materials and Methods**

2.1 **Materials**

2.1.1 Commercial kits

All reagents within the commercial kit were used as stated by the protocol provided by the manufacturer. Table 1 gives information regarding suppliers.

Table 1: Kits used for experiments in accordance with the work conducted in this thesis.

Kit	Method	Source
E.Z.N.A® kit	Gel elution (2.2.11.1.5)	E.Z.N.A OMEGA, bio-tek, Thermo Fisher Scientific, (USA)
***RNA*GEM ™ Tissue PLUS kit**	*RNA*GEM Tissue Plus (2.2.11.1.5)	ZyGEM, #RTP0500, (New Zealand)

2.1.2 Specific equipment and instruments

All equipment and instruments used for the purposes of this research (Table 2).

Table 2: Equipment and instruments used for the purposes of this research.

Equipment	Method	Make and Manufacturer
AMG Evos microscope	Preparation of cells (2.2.5)	AMG Evos, Advanced microscopy group, Millenium Science, (Australia)
Autoclave	Sterilisation of plastic and glassware (Various)	Tuttanauer autoclave, Tuttanauer, (USA)
Bench centrifuge	Molecular analysis (Various)	Mini spin, Eppendorf (Germany)
Cell culture centrifuge	Tissue culture (Various)	Biofage Primo Centrifuge, Heraeus, (Germany)
Cell culture laminar flow	Tissue culture (2.2.4)	Hera guard, Heraeus, (Germany)
Cell culture incubator	Tissue culture (2.2.4)	Series II water jacketed CO_2 incubator, Therma Forma, Thermo Scientific, (USA)
Cell microscope	Cell counting (2.2.4.4)	Nikon TMS, Nikon (Japan)

Counter	Cell counting (2.2.4.4)	BSI ISO9001, Up Green Counters, (Taiwan)
Deep freezer (-80° C)	Sample storage	Forma 900 series, Thermo Fisher Scientific Inc, (USA)
Electro cell manipulator	Cell Fusion (2.2.6.5.2)	BTX ECM 200, Biotechnologies and Experimental Research Inc, (CA, USA)
Electrophoresis power supply	Gel electrophoresis (2.2.13)	Power station 300, Labnet international Inc, (NJ, USA)
Electrophoresis unit	Gel electrophoresis (2.2.13)	Sub-Cell ® GT, BIO-RAD, (CA,USA)
Embryology incubator	Embryo culture (2.2.6.6)	Contherm biocell 1000 incubator, 38° C, Contherm, (New Zealand)
Embryology Laminar Flow	Embryo generation (2.2.6)	Model CF 43/40, Gelman Sciences, (Australia)
Embryology mini centrifuge	Embryo Culture (Various)	Spectrafuge mini C1301, Labnet International INC., NJ (USA)
Embryology vortex	Enucleation (2.2.6.4)	SM1 minishaker IKA ®, (Germany)
Enucleation pipette	Enucleation (2.2.6.4)	24 µm diameter, blunt cut open end, House made
Freezer (-20° C)	Sample storage	Chest freezer, Fisher and Paykel (New Zealand)
Gel doc	Gel electrophoresis (2.2.13)	Gel doc 2000, BIORAD (USA)
Hand pipettes	Various	1 mL, 200 µL, 20 µL, 10 µL, 2µL, Eppendorf (Germany), Gilson (Switzerland)
Heating block	*RNA*GEM (2.2.7)	Accublock™ Digital Dry Bath, Labnet International Inc, (NJ, USA)
Haemocytometer	Cell counting (2.2.4.4)	Bürker Counting Chamber, Neubauer, Weber, (UK)
Ice machine	Molecular analysis (Various)	Hoshizaki Cube Star FM-120D, Hoshizaki, (Japan)

Liquid nitrogen tank	Sample storage	Chart MVE Biological systems (USA)
LightCycler	mRNA qPCR (2.2.11)	LightCycler 2.0, Roche, (Germany)
LightCycler carousel centrifuge	mRNA qPCR (2.2.11)	LC Carousel Centrifuge 2.0, Roche, (Germany)
Micromanipulation microscope	Enucleation (2.2.6.4)	MO-188, Nikon Narishige, (Japan)
Microwave oven	Gel electrophoresis (2.2.13)	The time saver MX145, Samsung, (China)
Milli-Q water production unit	Various	Purelab Ultra Elga Reservoir 75 L, Milipore H2O-production unit Milli-Q plus, Bio Lab, (USA)
Mr Frosty	Freezing cells (2.2.4.3)	Cryo 1° C Freezing container, Nalgen, Thermo Scientific, (USA)
NanoDrop spectrophotometer	Gel elution (2.2.11.1.5)	Nanodrop 1000, Thermo Scientific (USA)
Olympus fluorescent microscope	Photography of immunocytochemistry (Section 2.2.14.1)	Olympus BX50, Olympus (Japan)
PCR machine	End point PCR (2.2.12)	Master cycler gradient, Eppendorf, (Germany)
Scale	Gel electrophoresis (2.2.13)	Mettler AT250, Mettler-Toledo International Inc, (Switzerland)
Separation needle	Enucleation (2.2.6.4)	100-150 µm diameter, blunt closed ended, House made
Suction system for cells	Cell culture (2.2.4)	Air Cadet, Thermo Scientific, (USA)
Vacuum	Sourcing oocytes (2.2.6.2)	IVF Ultra Quiet VMAR-5100, Cook veterinary products, (Switzerland)
Vortex	*RNA*GEM (2.2.7)	Grant-bio, Biolab, Thermo Scientific, (USA)
Water bath	Cell culture (2.2.4)	GD100, Grant, Global Sciences, (New Zealand)

2.1.3 Plastic and glass ware

All plasticware was purchased clean and sterile. All glassware was autoclaved at 121° C for 15-20 minutes time at high pressure. A detailed list of all plastic and glassware used can be seen in Table 3.

Table 3: Detailed list of plastic and glassware used for the purposes of this research.

Item	Method	Make and Manufacturer
15 mL Conical tube	Various	15 mL Conical tube, Corning ® Centristar ™ (USA)
18 gauge needle	Sourcing oocytes (2.2.6.2)	BD PrecisionGlide ™ Needle, Sigma Aldrich (Switzerland)
96 well Conical plate	Immunocytochemistry (2.2.14)	TC Microwell 96U W/WD NUNCLON D, Thermo Scientific, (Denmark)
Circular coverslips	Immunocytochemistry (2.2.14)	10 mm Coverglass No. 1, Pro Sci Tech, (Australia)
Cryovials	Freezing cells (2.2.4.3)	Cryotube ™ Vials, Thermo Scientific, (Denmark)
Filter paper	Immunocytochemistry (2.2.14)	150 mm diameter filter paper, Whatman Internation Ltd, (UK)
Gilmont ® Micrometer syringe	Enucleation (2.2.6.4)	0.2 mL Gilmont, Cole-Parmer Instruments, (IL USA)
Gridded dish	Sourcing oocytes (2.2.6.2)	House made, Petri dish with an etched in 1 cm grid
LightCycler Capillaries	mRNA qPCR (2.2.11)	LightCycler Capillaries, Roche, (Germany)
Microcentrifuge tube	Various	0.6 mL, 1.5 mL Graduated microcentrifuge with flat top cap, Quality Scientific Plastics, (USA)
Modular incubation chamber	Embryo culture (2.2.6.6)	Modular incubation chamber, QNA International Pty Ltd., Australia
Mouth pipette	Embryo culture (2.2.6.6)	House made, Tubing with mouth piece, filter and puller Pasteur pipette
Parafilm	Immunocytochemistry (2.2.14)	Parafilm, Bemis flexible packaging, (WI, USA)

Pasteur pipettes	Various	Disposable glass Pasteur pipettes D810, Poulten & Graf (UK)
PCR tube	End point PCR (2.2.12)	200 µL Snapstrip II PCR tubes, Scientific Specialties Inc, (USA)
Petri dish	Embryo culture (2.2.6)	3 cm, 6 cm, 9 cm Easy grip Petri dish, Falcon, (NY,USA)
Thermos	Sourcing oocytes (2.2.6.2)	Nippon, (Japan)
Tissue culture dish	Cell culture (2.2.4)	3 cm, 6 cm, 9 cm, Easy grip Tissue culture dish, Falcon (NY, USA)
Vacucap filter unit	Solution preparation	Vacucap® Filter Unit w/0.2 µm Supor® Membrane, Pall Corporation, (New Zealand)
Volumetric flask	Various	Various, Schott Duran, (Germany)

2.1.4 Computer software and outsourced services

A series of computer software was used for the purposes of this research; a detailed list can be seen in Table 4. This table also contains outsourced services such as primer synthesis.

Table 4: Computer software and outsourced services.

Software	Method	Manufacturer
Excel	Graph formation and statistical analysis	Microsoft, (USA)
Geneious	Bioinformatics (2.2.9)	Biomatters Ltd, (New Zealand)
ImageJ	Photography of immunocytochemistry samples (2.2.14.1)	National Institute of Health, (USA)
LightCycler software	qPCR (2.2.11)	4.1.1.21, LightCycler, Roche, (Germany)
NanoDrop software	Gel elution (2.2.11.1.5)	NanogDrop 1000 3.8.1, ThermoScientific, (USA)
Nucleotide search	Primer design (2.2.9)	NCBI, (USA)
Pick primers	Primer design (2.2.9)	NCBI, (USA)

Primer synthesis	Primer design (2.2.9)	Integrated DNA technologies IDT, (USA)
Quantity one software	Gel electrophoresis (2.2.13)	Quantity one 4.4.0, BIORAD, (USA)
Spot Basic Software	Photography of immunocytochemistry samples (2.2.14.1)	Spot imaging solutions, (USA)
Spot RT3 camera	Photography of immunocytochemistry samples (2.2.14.1)	Spot imaging solutions, (USA)

2.1.5 Reagents and media for tissue culture

All solutions (Table 5) were prepared using Milli-Q water sourced from the Milli-Q water production unit. Solutions containing non-sterile components were filtered using Vacucap filter units. Solutions with "house made" were prepared within AgResearch facilities.

Table 5: Reagents used for tissue culture.

Common Name	Make and Manufacturer	Composition
1 x PBS	House made	Phosphate buffered saline
Cell culture media	DMEM/F12+GlutaMAX I 1x , GIBCO, Life Technologies, (USA)	2.438 g/L Sodium Bicarbonate, Sodium Pyruvate
Cryoprotectant	House made	80% FCS, 20% DMSO
DMSO	Sigma Aldrich, (Switzerland)	Dimethyl sulfoxide
Doxycycline	Sigma Aldrich, (Switzerland)	Stock with 2 mg/mL
Fetal bovine serum (FBS)	Moregate, (Australia)	-
Fetal calf serum (FCS)	GIBCO, Life Technologies, (USA)	-
Gelatin	Sigman Aldrich, (Switzerland)	0.1% in dsMilliQ
Hygromycin	Hygromycin B #10687-010, Life Technologies, (USA)	Maintenance level 200mg/mL
Low serum media	House made	0.5% FCS, 99.5% cell culture media
TrypLE	TrypLE Express, GIBCO, Life Technologies, (Denmark)	-

2.1.6 Reagents for nuclear transfer and embryo culture

A list of reagents used for nuclear transfer can be found in Table 6. All reagents with the make and manufacturer stated as "house made" were prepared within AgResearch facilities.

Table 6: List of reagents used for nuclear transfer and embryo culture.

Common name	Make and manufacturer	Composition
Aspiration media	House made	H199 medium + 925 IU/mL Heparin, CP Pharmaceuticals, (UK) + 2% (w/v) foetal calf serum, Life Technologies, (USA)
B199	House made	Bicarbonate-buffered medium M199 with 25 mM $NaHCO_3$, 0.2 mM Pyruvate and 0.086 mM Kanamycin monosulfate
Bovine Serum Albumin (BSA)	Sigma Aldrich, (Switzerland)	-
D-MAP	House made	6-dimethylaminopurine, Sigma Aldrich (Switzerland), 74.62 mg/mL in DMSO
ESOF (Early synthetic oviduct fluid)	House made	107.7 mM NaCl, 7.15 mM KCl, 0.30 mM KH2PO4, 25 mM NaHCO3, 0.33mM C3H3O3Na, 1.71 mM CaCl2:2H20, 0.15 mM C6H12O6, 3.32 mM C3H5O3Na, 0.04 mM C18H36N4O11H2SO4, and 0.081 g/L Non Essential Amino Acid, 1 mM Gluta-Max, and 8 mg/mL BSA.
ESOF –Ca + 10% FCS	House made	-
H199	House made	Hepes-buffered M119 with 15mM Hepes, 5 mM $NaHCO_3$, and 0.086 mM kanamycin monosulfate
H199 + 3 mg/mL BSA	House made	H199 + 3 mg/mL BSA
H199 + 0.5% FCS	House made	H199 + 0.5% FCS
H199 + 10% FCS	House made	H199 + 10% FCS
HSOF (Hepes buffered synthetic oviduct fluid)	House made	107.7 mM NaCl, 7.15 mM KCl, 0.3 mM KH_2PO_4, 5 mM $NaHCO_3$, 3.32 mM sodium lactate, 0.069 mM kanamycin monosulfate, 20 mM Hepes, 0.33 mM pyruvate, 1.71 mM $CaCl_2.2H_2O$, 3 mg/mL fatty-acid free bovine albumin
HSOF -Ca + 10% FCS	House made	-

Hyaluronidase	House made	Hyaluronidase, Sigma Aldrich (Switzerland), 0.1% in H199 -BSA.
Hypoosmolar fusion buffer	House made	165 mM mannitol, 50 µM $CaCl_2$, 100 µM $MgCl_2$, 500 µM Hepes, 0.05% bovine albumin [ABIVP, ICP], pH 7.3
Ionomycin	House made	Ionomycin Ca salt, Sigma Aldrich, (Switzerland), 1 mg in 268 µL DMSO
IVM media	House made	B199 with 10 µg/mL ovine follicle stimulating hormone, Ovagen; Immuno-Chemical Products, (New Zealand), 1 µg/mL ovine lutenizing hormone, 1 µg/mL 17-β-estradiol, 0.1 mM cysteamine
Lectin	House made	Phytohaemagglutinin PHA-P, Sigma Aldrich (Switzerland), 2 mg/mL in H199 + 3 mg/mL BSA
LSOF (Late synthetic oviduct fluid)	House made	107.7 mM NaCl, 3.99 mM KCl, 1.20 mM KH2PO4, 25 mM NaHCO3, 0.33 mM C3H3O3Na, 1.71 mM CaCl2:2H20, 0.49 mM MgCl2:6H2O, 3.32 mM C3H5O3Na, 0.04 mM C18H36N4O11H2SO4, 1.5 mM C6H12O6, 1 mM DNP (2-, 4-dinitrophenol) and 0.081 g/L Non Essential Amino Acid, 1 mM Gluta-Max, 0.22 g/L BM Essential Amino Acid and 8 mg/mL BSA.
Pronase	House made	Protease, Sigma Aldrich, (Switzerland), 0.5% in HSOF + Ca + Mg + 1 mg/mL PVA
M199	House made	Medium 199 with L- glutamine, Earle's salts, Life Technologies, (USA)
Mineral oil	Sigma Aldrich, (Switzerland)	Sterile-filtered, BioXtra

2.1.7 Reagents for molecular biology

A comprehensive list of reagents used for molecular biology can be found in Table 7.

Table 7: List of reagents used for all molecular biology protocols.

Reagent	Method	Manufacturer
1 Kb ladder	Gel electrophoresis (2.2.13)	1 Kb Plus DNA ladder, Invitrogen, Life Technologies, (USA)
5 x RT-buffer	cDNA synthesis (2.2.7.4)	5 x First Strand buffer, Invitrogen, Life Technologies, (USA)
dNTP	cDNA synthesis (2.2.7.4)	10 mM diluted from 100 mM dNTP Set, Invitrogen, Life Technologies (USA)
Loading dye	Gel electrophoresis (2.2.13)	House made, 15 mL 30 % glycerol in H_20, 35 mL H_20 + 0.5 g 1% Orange dye, Sigma (Switzerland)
Lysis Buffer	DNA extraction (2.2.8)	Tris pH8 100 mM, EDTA 1 mM, Tween-20 0.5% (v/v), TX-100 0.5% (v/v), House made
MgCl	cDNA synthesis (2.2.7.3)	25 mM stock solution, Roch diagnostics, (Germany)
Proteinase K	DNA extraction (2.2.8)	Proteinase K, Sigma Aldrich, (Switzerland)
Random Hexamer primers	cDNA synthesis (2.2.7.4)	5 nmoles, Applied Biosystems, Roche (Germany)
RNAse out	cDNA synthesis (2.2.7.4)	RNAse OUT ™ Recombinant Ribonucleas Inhibitor 5,000 U, Invitrogen, Life Technologies, (USA)
Superscript III	cDNA synthesis (2.2.7.4)	Superscript ® III, Reverse Transcriptase, Invitrogen, Life Technologies, (USA)
SYBR safe	Gel electrophoresis (2.2.13)	SYBR® Safe DNA Gel stain, Life Technologies, (USA)
Takara	qPCR (2.2.11)	SYBR Premix Taq II (Tli RNAse H Plus), Norrie Biotech, (New Zealand)

2.1.8 Reagents used in immunocytochemistry

Reagents used for the immunocytochemistry protocol are listed in Table 8. All reagents with the make and manufacturer stated as "house made" were prepared within AgResearch facilities.

Table 8: Table of reagents used in immunocytochemistry.

Reagent	Details	Make and Manufacturer
Donkey Serum	5% work concentration in PBS	Sigma Aldrich, (Switzerland)
Goat Serum	5% work concentration in PBS	Life Technologies, (USA)
Hoechst stain (H33342)	5 µg/mL working concentration, Bis-Benzimide in 1 mg/mL Mili-Q water	Sigma Aldrich, (Switzerland)
Mounting media	-	ProLong Gold Antifade or ProLong Diamond Antifade (Dependent on availability), Life Technologies, (USA)
NH_4Cl	50 mM	Sigma Aldrich, (Switzerland)
Paraformaldehyde (PFA)	4% depolymerised (w/v) PFA, 4% (w/v) sucrose, 1 M NaOH in PBS with phenol red indicator	Sigma Aldrich, (Switzerland)
PBS-PVA	5% 1 mg/mL PVA in PBS	House made
Triton X-100	-	Sigma Aldrich, (Switzerland)

2.1.9 Primary and secondary antibodies used in immunofluorescence

Primary and secondary antibodies used in immunocytochemistry are listed in Table 9.

Table 9: Details of primary and secondary antibodies used for immunocytochemistry.

Antibody	Dilution	Cloniality	Species	Manufacturer
Primary				
$H_3K_{27}me_3$	1:10,000	Polyclonal	Rabbit	Millipore #NM_003493
NANOG	1:100	Monoclonal	Mouse	eBiosciences (USA) #14-5768
SOX2	1:30	Polyclonal	Goat	R & D Systems (USA) #AF2018
Secondary				
Donkey anti Mouse Alexa Fluor® 488 (Green)	1:1000	-	-	Invitrogen (USA) #A21202
Donkey anti Goat Alexa Fluor® 568 (Red)	1:1000	-	-	Invitrogen (USA) #A11057
Donkey anti Rabbit Alexa Fluor® 488 (Green)	1:1000	-	-	Invitrogen (USA) #A21206

2.1.10 Frequently used reagents

Commonly used reagents used throughout the range of protocols can be found in Table 10. All reagents with the make and manufacturer stated as "house made" were prepared within AgResearch facilities.

Table 10: List of commonly used reagents.

Reagent	Details	Manufacturer
50 x TAE buffer	241.2 g 2M Tris, 15.01 mL 250 mM Glacial acetic acid, 18.61 g 50 mM EDTA	House made
DEPC	0.1% (v/v) diethyl procarbonate in Milli-Q water. Mixed overnight and autoclaved	House made
dH_2O	-	Distilled water, Nalgene
Ethanol	70% diluted in DEPC	Fisher Chemicals,
Milli-Q water	18.2 MΩ	From Milli-Q reservoir
PBS	8.4 mM disodium hydrogen orthophosphate 2-hydrate, 1.9 mM sodium dihydrogen orthophosphate 1-hydrate, and 150 mM sodium chloride in MQ-H2O	House made
TAE buffer	1 x TAE diluted from 50 x stock	House made

2.1.11 Primers

A series of primers was used for both qPCR and PCR analysis of samples. The sequence and additional information about these primers can be seen in Table 11.

Table 11: List of primers describes sequences, melting peak and amplicon size.

Gene	Sequence (5'-3')	qPCR Melting peak (°C)	Amplicon size (bp)
18S	F:GACTCATTGGCCCTGTAATTGGAATGAGTC R: GCTGCTGGCACCAGACTTG	80	87
DDX3Y	F: GGACGTGTAGGAAACCTTGG R: GCCAGAACTGCTACTTTGTCG	81	225
Ectopic *NANOG*	F: CACGGGGACGTGGTTTTCCTTT R: CTGCAGGGACACGTAGGATTCCTC	88	166
Endogenous *NANOG*	F: TCACACCCGGAGATCTTCAC R: TCCATGGAGGAGGGAAGAGG	84	274
FGF4	F: TACGGCTCGCCTTTCTTCAC R: TTCTTGGCCTTGCCGTTCTT	89	131
GAPDH	F: GGCGTGAACCACGAGAAGTATAA R: CCCTCCACGATGCCAAAGT	84	118
KLF4	F: TCCCACCGCTCCATTAC R: ATGAGAACTCTTCGTGTAGG	88	158
OCT4	F: GGTTCTCTTTGGAAAGGTGTTC R: TGGCGACGGTTGCAAAACCA	89	333
PDGFRα	F; CCCCGACGTGGAAATCAGAA R: CATCTGGGTCTGGCACGTAG	88	179
SOCS3	F: CCAGCCTGCGCCTCAAGACC R: AAAGTGGCGCTGGTCCGAGC	91	185
SOX2	F: CTATGACCAGCTCGCAGA R: GGAAGAAGAGGTAACCACG	90	152
SOX17	F: ATGCTGGGCAAGTCGTGG R: CTTTAGCCGCTTCACCTGCTT	93	147
USP9Y	F: GCCAGATGACCAAGAAGCCCCA R: GGACTGTAAGGCCTAATAGCCTGGT	-	285
XIST	F: AGCATTGCTTAGCATGGCTC R: TGGCTGTGACCGATTCTACC	85	466
ZRSR2Y	F: GTCAGTTGCAACCTGGAACC R: GCCATATTCCATTGGGTCAC	-	158

2.1.12 Cell line details

All cell lines used for the purposes of this project were bovine. Their names and cell type details can be seen in Table 12.

Table 12: Details of all bovine cell lines used for the purposes of this research.

Cell line common name	Cell line full name	Cell type	Source
EFC1B	Elizabeth Follicular Cells, Line 1B	Follicular isolated from adult ovary	AgResearch [121]
EOG	EF5_EF1α_OCT4-GFP	Foetal fibroblasts isolated from day 45 embryo	AgResearch [122]
EOG_TET	EF5_EF1α_OCT4-GFP_TET3G_TRE3G	Foetal fibroblasts isolated from day 45 embryo	AgResearch
EOG_TET_NANOG	EF5_EF1α_OCT4-GFP_TET3G_TRE3G_NANOG	Foetal fibroblasts isolated from day 45 embryo	AgResearch
LFC2	Lady Follicular Cell, line 2	Follicular isolated from adult ovary	AgResearch [123]
LJ801	Limousine Jersey 801	Skin fibroblast isolated by ear biopsy	AgResearch [124]
SNAZY	SNAZY	Skin fibroblast isolated by ear biopsy	AgResearch [124]

2.2 Methods

2.2.1 Ethics statement

All research was exempt from animal ethics approval as the research conducted was on early stage embryo or *in vitro* culture of cell lines. No approval was required from the University of Waikato animal ethics committee or AgResearch animal ethics committee. This project had environmental protection agency (EPA) approval under the hazardous substances and new organisms (HSNO) act. The EPA approval number for this project is GMO05/ARR003.

2.2.2 Cell culture

Cell culture is the removal of cells from the organism as a whole and growing of these cells *in vitro* under controlled conditions [125]. The bovine fibroblast cell line used for the purposes of this research thesis was named EOG_TET_NANOG.

This cell line was derived within AgResearch, New Zealand. The history of the cell line is described in section 2.2.3.

2.2.3 Background information about the cell line

The EOG_TET_NANOG cell line was prepared prior to the work conducted in this thesis. The bovine cell sample was initially taken from the embryo of a natural mating of a dairy cow with a high breeding index and a high genetic quality sire. The embryo was recovered at day 60 and was originally called EF5LG, describing that it was a bovine embryonic fibroblast derived from the foetal lung.

This cell line was then transfected with a bovine OCT4- green fluorescent protein (GFP) promoter construct and used for NT to determine the expression of OCT4 within the cloned bovine blastocyst [122]. A transfected clone from this cell line was used for NT and a resulting embryo was recovered at day 45. The re-derived tissue from this foetus was then used to develop a new foetal fibroblast cell line called EOG (Table 9). The OCT4-GFP vector sequenced was silenced over this period but is on occasion reactivated unpredictably. Therefore, its GFP signal was visualised and recorded during these NT experiments.

The EOG cell line was transfected via Neon-electroporation with the Tet-3G system by Clone-tech. This contained the reverse tet transactivator (rtta) which drives gene transcription by binding to tetO in the presence of doxycycline. This was a minimal promoter sequence which means it was less likely to be silenced. This also had a pEF-1α promoter which was linked to a Neomycin resistance marker that was derived by a separate SV40 promoter. The clones were then selected with Neomycin and tested for inducibility. The best clones were then selected and expanded. The cell line was then used for NT. A day 45 embryo was recovered and a new cell line was created. This was again tested for inducibility. At this stage the cells were named EOG_TET (Table 12). This cell line was often used as a control treatment for the EOG_TET_NANOG cell line as it was parental and constitutively expressed the Tet-activator but did not contain NANOG sequence.

The cell line was then transfected again with a vector from GeneArt. The vector contained the tetracycline responsive element of the third generation (TRE3G). This contained a mCherry reported protein to indicate that the vector was on, where the sequence was being transcribed. The sequence also contained codon-optimised *NANOG* sequence which was optimised based on which codon was most efficient at transcription and translation for that particular amino acid. Therefore, there was a difference between the mRNA sequence of the vector and the endogenously expressed *NANOG* which allowed them to be distinguished. The protein sequence was the same for both ectopically and endogenously expressed *NANOG*. The comparison between the codon-optimised and endogenous Nanog nucleotide sequences can be seen in section 3.1 along with a comparison of the corresponding protein sequences. The pTRE3G-mCherry vector also contains an internal ribosomal entry site (IRES), which allows the *mCherry-NANOG* mRNA hybrid sequence to be translated, but then are transcribed separately to form separate proteins (Figure 7). A plasmid map for this sequence can be seen in Figure 8. The cells were also simultaneously transfected with a Hygromycin resistant vector and were selected based on mCherry expression and Hygromycin resistance by SV40 promotor.

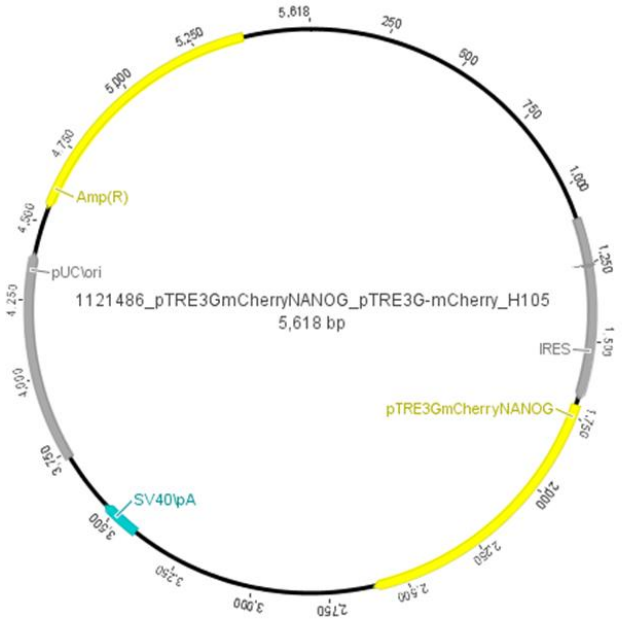

Figure 8: Plasmid map for pTRE3G-mCherry vector. The location for IRES, ampicillin (AmpR), SV40 promotor and fused tetracycline responsive element-*mCherry* reporter protein-*NANOG* gene are depicted in the 5618 bp vector.

The line was then again rejuvenated via NT. Only those embryos with mCherry expression at day 7 were selected for embryonic transfer. A day 45 embryo was then recovered and the cells were harvested. Doxycycline was added to the cells and it was found that around 33% of them were positive for mCherry (Unpublished data). At this point, a number of NT runs were conducted and qPCR analysis of embryos was used to analyse *NANOG* expression. The results for these NT runs can be seen in results section 3.2. A diagram of the work conducted up until this point can be seen in Figure 9. This cell line was then given the common name EOG_TET_NANOG (Table 12).

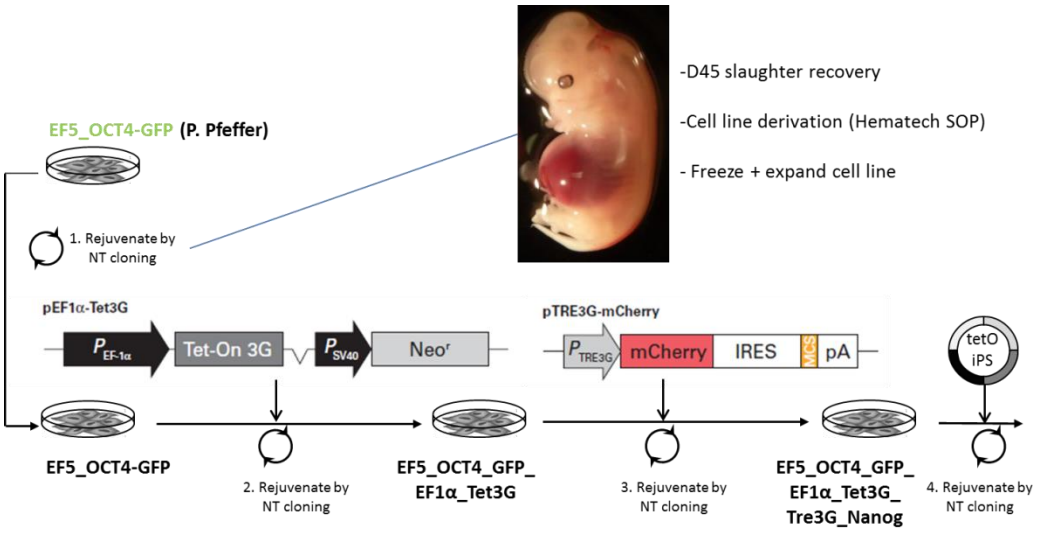

Figure 9: History of EOG_TET_NANOG cell line. Details of parental cell lines Table 12. Contains image of day 45 embryo and each step of the derivation of the EOG_TET_NANOG cell line. Diagram from Björn Oback (unpublished).

After these initial NT runs, it was concluded that the cell line did not contain a high enough concentration of mCherry positive cells. It was then sorted for the mCherry signal by a fluorescence-activated cell sorter (FACS) at University of Auckland, New Zealand. The percentage of cells expressing mCherry after sorting was 98% (Unpublished data). The cells were then expanded and frozen down to be analysed via immunocytochemistry (ICC) and qPCR for *NANOG* expression.

2.2.4 Routine cell culture protocols

All mammalian cell culture work was conducted with in the cell culture laminar flow using aseptic technique. Cells were grown in the cell culture incubator which was kept at 38.5° C, with a gas composition of 5% CO_2.

2.2.4.1 Thawing cells

Cryovial tubes containing frozen cells were stored in a liquid Nitrogen storage tank in order to preserve them for future use, as they are able to recover from cryopreservation and continue to proliferate. To thaw these cells liquid Nitrogen was poured into a polystyrene box and a cryovial was quickly removed from the storage tank with forceps and placed into the liquid nitrogen. The cryovial was then incubated in a 38° C waterbath in order for the cells to thaw. The thawed cells were added to a 15 mL conical tube containing pre-warmed cell culture media. The tube was then centrifuged using the cell culture centrifuge for 3 minutes at 1000 rpm at room temperature (RT) to pellet the cells. The supernatant was then aspirated using a Pasteur pipette attached to a suction system. The cells were then re-suspended in pre-warmed cell culture media, where they were well mixed and then transferred into a tissue culture dish. The dishes were labelled with the cell line name, date of thawing, the number of cells plated and the passage number.

2.2.4.2 Passaging cells

Each passage number reflects when cells have outgrown the dish they were cultured in and have been transferred into a new dish, giving them more space and fresh nutrients to continue proliferation. Before passaging, cells could be visualised based on morphology to observe any potential changes as a result of induction or culture conditions. Firstly, the cell culture media was aspirated off the dish. The cells were then washed with pre-warmed 38° C 1 x PBS. The PBS was aspirated and warm trypLE was added to the dish. The dish was then incubated for 3-5 minutes in the cell culture incubator, which dislodged the cells from the surface of the dish. Large clumps of cells were disrupted by gently pipetting the cells up and down. The media containing the cells was transferred to a centrifuge tube containing pre-warmed media. The tube was centrifuged for 3-5 minutes at 1000 rpm at RT. The supernatant was aspirated and the cell pellet was loosened by lightly tapping the tube on the bench. The pellet was then diluted in the required volume of media and transferred into a new tissue culture dish. The culture dish size requirements for seeding density and media volume can be seen in Table 13. The cells were then incubated at 38° C until the cells reach a

confluency of 70-90%, at which time they must be passaged again or frozen for future use.

Table 13: Seeding density and media requirements for each size of tissue culture dish.

Dish size	Seeding density (cells)	Volume of media (mL)	Volume of trypLE (mL)
4 well plate	50,000	0.8	0.2
35 mm dish	200,000	2	0.5
60 mm dish	500,000	5	1
90 mm dish	1,000,000	10	2

2.2.4.3 Freezing cells

Since these cells are not immortal, and require time and resources to continue growth, it was often necessary to freeze the cells, until they are needed again. Cells were frozen when they reached 70-90% confluency as this was when the cells were at a log phase. Therefore, they could recover quickly after thawing and begin proliferation again. The cells were lifted off the tissue culture plate with warm trypLE. They were then suspended in pre-warmed media and centrifuged at 1000 rpm for 3 minutes. A cryoprotectant solution was prepared immediately prior to use. The media the cells were frozen in was comprised of 50% Cryoprotectant and 50% cell culture media. Once the cells had formed a pellet they were then re-suspended in cell culture media. The cryoprotectant was then added slowly and the entire solution was mixed to produce homogeneity across the sample. The cryovial was labelled with the cell line name, the date of freezing, the passage number, the cell count and the technician's initials. The cells were then placed into a Mr Frosty freezing container, which was then placed into a -80° C freezer. The Mr Frosty controlled the temperature decrease to one degree per minute, which is the optimal rate of freezing to keep the cells viable. After a 24 hour period the cells were transferred into a liquid nitrogen tank for future use.

2.2.4.4 Cell counting

A haemocytometer was used to determine the cell count. A cell count must be conducted in a number of different steps as cells must be passaged at densities as stated in Table 13, since this is crucial to continue healthy cell growth. A 10 µL volume of media containing cells was pipetted onto a haemocytometer, to fill the counting area. Under the cell microscope at 10 X objective the cells were counted using a 10 - X cell counter on phase contrast.

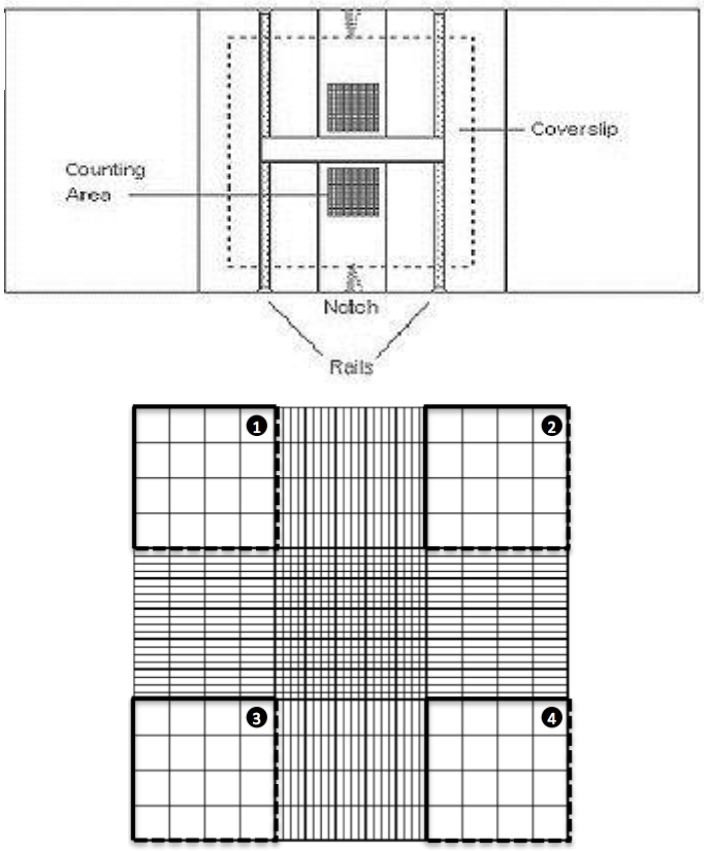

Figure 10: Haemocytometer diagram. A) An aerial view of the haemocytometer, highlighting the counting area, the notch in which the cells are added and the coverslip. B) An enlarged view of the counting area.

The cells in the grids numbered one to four, and the centre grid (Figure 10) were counted and the numbers were entered into Equation 1.

Equation 1: Cell count formula

$$\frac{Cell\ count}{Number\ of\ squares\ counted} \times Volume\ of\ media \times 10{,}000 = Number\ of\ cells$$

The count was set up in duplicate as there were two grids on the haemocytometer and the results were averaged to obtain an accurate estimation. The cell solution could then be diluted to produce the appropriate seeding density.

2.2.5 Preparation of cells for ICC, RNA extraction and qPCR analysis

Cells were thawed (2.2.4.1) and were passaged at an appropriate seeding density into a tissue culture dish containing sterile circular cover slips. To induce the cells doxycycline was added to the EOG_TET_NANOG + Dox treatment immediately after seeding the cell at a quantity of 1 µL/mL. The cells were incubated for 48 hours which resulted in a confluency of approximately 80% which is ideal for ICC.

After 48 hours, the cells were analysed for confluency and induction. They were initially visualised under the AMG EVOS microscope. Once the cells were 80% confluent and the EOG_TET_NANOG + Dox treatment showed a strong positive mCherry signal then the cells were collected for ICC and *RNA*GEM. For ICC the coverslips were removed and placed into a new 3 cm dish in which the ICC protocol was to be carried out (Section 2.2.14). Once they were removed the remaining cells were lifted off the plate with TrypLE, they were then washed in PBS. A cell count (Section 2.2.4.4) was conducted as the *RNA*GEM protocol (Section 2.2.7) can only process 500,000 cells at a time. If the cell count was above 500,000 the excess cells were discarded. The remaining pellet was re-suspended in 50 µL of *RNA*GEM solution. Once the cell line was validated for the presence of *NANOG* expression, it could then be used as a donor cell line for nuclear transfer cloning.

2.2.6 Embryo generation via nuclear transfer

The production of bovine nuclear transfer embryos was carried out in a physical containment level 2 (PC2) embryology laboratory at AgResearch Ltd, Ruakura, Hamilton. All plates used in this procedure for IVP were made two hours prior to use, in the embryology laminar flow and then were gassed in a humidified incubator containing 5% CO2 at 38° C. Plates used for *in vitro* culture (IVC) were made 2 hours prior to use and were stored in humidified modular incubator chamber at 38° C with a gas composition of 7% O2, 88% N2 and 5% CO2.

Further information about the composition of media, solutions or reagents can be found in section 2.1.6. The information for each NT run was recorded on a on a fusion record sheet (Appendix 1), these were collected alongside mCherry and GFP record sheets (Appendix 2) and embryo grading sheets (Appendix 3).

2.2.6.1 Cell cycle coordination

The process of NT has been proven to most successfully generate embryos with cells that are in the G_0 phase of the cell cycle [126]. To synchronise into the G_0 phase, the cells must be serum starved. The cells were washed three times in 38° C PBS to remove remaining serum from previous media. A low serum media was then used, at 0.5% foetal calf serum and not replenished for the remaining 3-7 days prior to nuclear transfer. For the fibroblast cells used in these experiments, a five day serum starvation was sufficient to synchronise cells. For the duration of serum starvation the EOG_TET_NANOG +Dox treatment had the doxycycline replenished every 48 hours.

2.2.6.2 Sourcing oocytes and follicular aspiration (Day-1)

A population of oocytes primed for NT has been identified for follicular aspiration [127]. This population consists of oocytes matured via *in vitro* maturation until they are in metaphase II of meiosis. These are aspirated from follicles within a size range defined in Figure 11 [128]. For the purposes of these experiments, bovine ovaries (Figure 12) were retrieved from abattoirs in the Waikato region. Upon removal from the offal, these were placed into a thermos containing 0.9% saline solution warmed to 29.5-30.5° C. They were transported to AgResearch and aspiration was conducted no longer than 3 hours after collection. An 18-gauge needle under a 48 mm Hg vacuum was used to collect the follicular fluid containing oocytes of the appropriately matured follicles as indicated in Figure 11. The cumulus–oocyte complexes (COCs) were collected in a 15 mL centrifuge flask containing 2 mL 38° C aspiration media so they could be used for *in vitro* maturation.

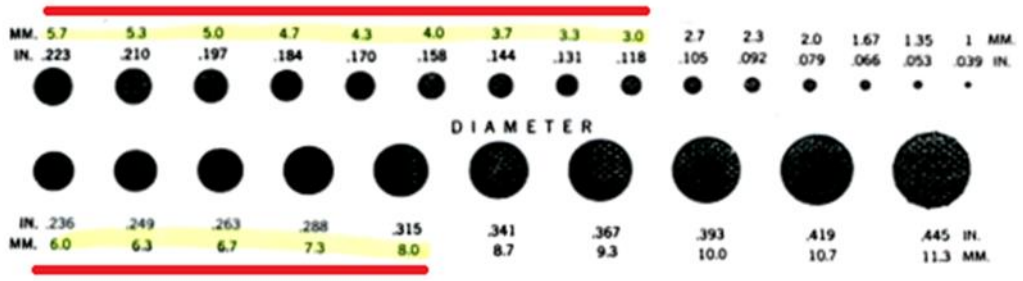

Figure 11: Potential sizes for bovine follicles with red lines indicating follicles prime for aspiration.

Figure 12: Bovine ovaries showing varied sizes of follicles and varied stages of follicular development.

2.2.6.3 *In vitro* maturation (IVM) (Day -1)

The IVM step allows the oocytes to mature to a state in which they are ready for enucleation. The COCs formed a pellet at the bottom of the 15 mL centrifuge tube which was removed with a Pasteur pipette and was then expelled into a 9 cm petri dish containing aspiration media. The dish was searched using a gridded 9 cm dish lid underneath for guidance. Oocytes were selected based on appearance, compact COCs, homogeneous ooplasm and a non-atratic cumulus oophorus-corona [129]. The selected COCs were then washed through two pre-warmed 3 cm dishes of H199 and finally through a 3 cm dish containing B199. Using a 10 µL pipette 10 oocytes in 10 µL were taken up and placed into each of the 40 µL IVM media drops arranged in three rows of four overlaid with mineral oil (Figure 13). These were then placed in an embryology incubator for 18-20 hours to allow them to mature.

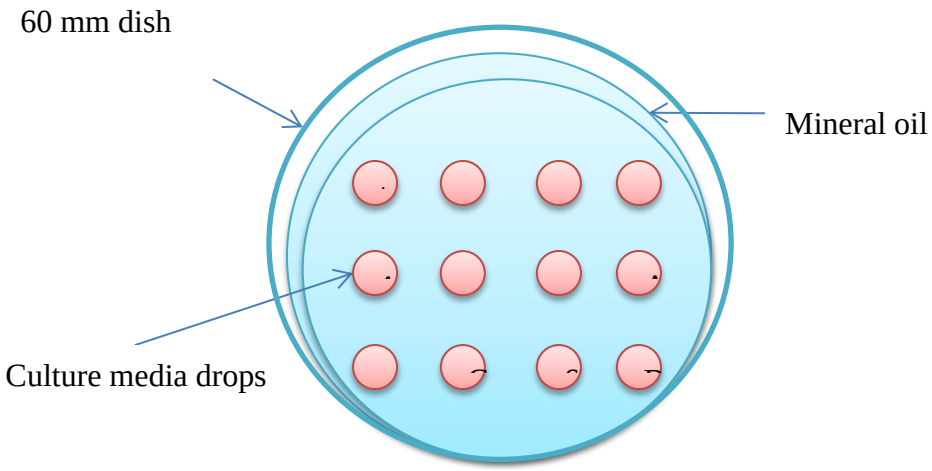

Figure 13: Standard culture dish layout. This layout was used for any multi-culture period, drop size may vary from 30-40 µL depending on culture requirements. Mineral oil overlays the culture drops to retain the heat and gas composition within the dish during the time in which the dish is worked on outside the incubator.

After maturation the cumulus corona were dispersed by the embryology vortex. Up to 180 COCs were placed into a 1.5 mL microcentrifuge tube containing 500 µL of bovine testicular hyaluronidase for two minutes at 2000 rpm. This removes the cumulus cells. The tube was then spun down for around three seconds with the embryology mini centrifuge in order to collect the oocytes. The oocytes were then washed two times in H199 + 10% FCS and then once in H199 + 3 mg/mL BSA. Oocytes which have a polar body present were identified; these went on to have their zona pellucida (zona) removed via a one-two minute incubation in pronase (5 mg / mL in H199). Once the zona begun to dissolve it was then washed in H199 + 3 mg/mL BSA. The zona was then dissolved completely and the oocytes were allowed to recover their spherical shape for five minutes before commencing the enucleation phase.

2.2.6.4 Oocyte enucleation

Enucleation is the removal of oocyte DNA to make way for the donor cell genome to enter the oocyte and begin embryonic development. For this process, 40

oocytes were processed at a time. These were collected and incubated in a plate of DNA stain (5 µg/mL Hoechst 33342 in H199 + 3 mg/mL BSA). Oocytes were then washed briefly in H199 + 3 mg/mL BSA. Once washed the oocytes were transferred into a 10 cm petri dish lid containing drops of H199 + 10% FCS overlaid with mineral oil. This dish was placed on the warm stage (32° C) of the micromanipulation microscope where three axis oil hydraulic hanging joy stick micromanipulators along with a 0.2 mL Gilmont ® micrometer syringe were used to manipulate the blunt aspiration pipette and the separation needle. The enucleation procedure was conducted using 100X total magnification, under constant UV light exposure. The aspiration pipette was used to remove the metaphase plate of the oocyte. Once the chromosomes where detected within the aspiration needle, the separation needle was used to move the cytoplast away and separate it from the karyoplast. The cytoplast was then quickly moved out of the UV light.

2.2.6.5 Nuclear transfer

The nuclear transfer step is the process that joins the donor cell and the enucleated oocyte together, and then fuses them, causing the donor cell's DNA to enter the cytoplast, allowing embryo development to begin.

2.2.6.5.1 Cell attachment

Cells prepared in 2.2.6.1 were lifted off their plates with trypLE and were re-suspended at 1 x 10^4 cell/mL in H199 + 0.5% FCS. This solution was then pipetted into 40 µL drops overlaid with mineral oil. From this drop, in groups of 5-10, the donor cells were removed and added to drop of 10 µg/mL Lectin in H199 + 3 mg/mL BSA. The cytoplasts (prepared in 2.2.6.4) were also placed into the same drop, five to ten at a time. The donor cells and cytoplasts were pushed together with a mouth pipette to form a couplet. The couplets were incubated for five minutes, and then transferred into a H199 + 3 mg/mL BSA wash.

2.2.6.5.2 Cell fusion

The couplets from step 2.2.6.5.1 were equilibrated in hypoosmolar fusion buffer in groups of ten at a time. At RT the couplets were then placed into a custom

made fusion chamber which was hooked up to an electro cell manipulator. An alternating current field (60-100 V/cm) was applied to the couplets for 5-10 seconds. This was conducted in order to align the couplets with the donor cell either at the top or the bottom of the cytoplast. Fusion was induced with two 10 µsec direct current pulses (1.5-2.0 kV/cm) immediately followed by an alternating current for between 5-10 seconds (60-100 V / cm). The couplets were then moved into a dish containing H199 + 3 mg/mL BSA. The couplets were visualised to detect potential cell lysis or detachment of the donor and cytoplast. These were washed through with HSOF- Ca + 10% FSC and then through two 40 µL drops of ESOF-Ca. Finally, ten reconstructs per drop in ESOF-Ca + 10% FSC were incubated for four hours until activation. The ESOF-Ca + 10% FCS plates contained doxycycline for the EOG_TET_NANOG +Dox treatment.

2.2.6.5.3 Activation

Activation is the step that stimulates the reconstruct to begin embryonic development; it does this by mimicking the process initiated by the sperm during fertilisation. This step occurs approximately four hours after fusion. The reconstructs were moved into 3 cm dishes containing HSOF + 1mg/mL BSA 30 minutes prior to fusion, one dish per treatment. The reconstructs were then transferred into fresh Ionomycin (1 µL/mL of HSOF + 1 mg/mL) for 4.5 minutes. They were then transferred into HSOF + 30 mg/mL BSA for 3 minutes. Then with a mouth pipette, each reconstruct was placed into single culture of D-MAP. The D-MAP plates contained doxycycline for the EOG_TET_NANOG +Dox treatment. The D-MAP plate was laid out to allow single embryo culture (Figure 14).

2.2.6.6 Embryo culture

2.2.6.6.1 Embryo culture

The reconstructs were then cultured in a media to promote normal embryonic development. ESOF is a synthetic oviduct fluid specific for the needs of the developing early embryo. This was used to culture the embryos for the initial culture period. Once the reconstruct had been activated, they were incubated in D-MAP for four hours. During this time the ESOF plates were made, in order to

ensure that the doxycycline was fresh and would last as long as possible through embryo culture. The ESOF plates were made with a layout (Figure 14) that allows single culture of the embryos, to prevent the embryos from joining together and forming aggregates. These were placed in a modular-incubation chamber for two hours to equilibrate. Each reconstruct was then moved from the D-MAP into a HSOF wash dish and then into a single culture ESOF plate, which contained doxycycline for the EOG_TET_NANOG +Dox treatment. These plates were placed into a modular-incubation chamber, which is a sealed container that was gassed with 5% CO_2, 7% O_2 and 88% N_2 at high pressure for 5 minutes. The chamber was then sealed and stored in a 38° C incubator until the doxycycline needed to be refreshed.

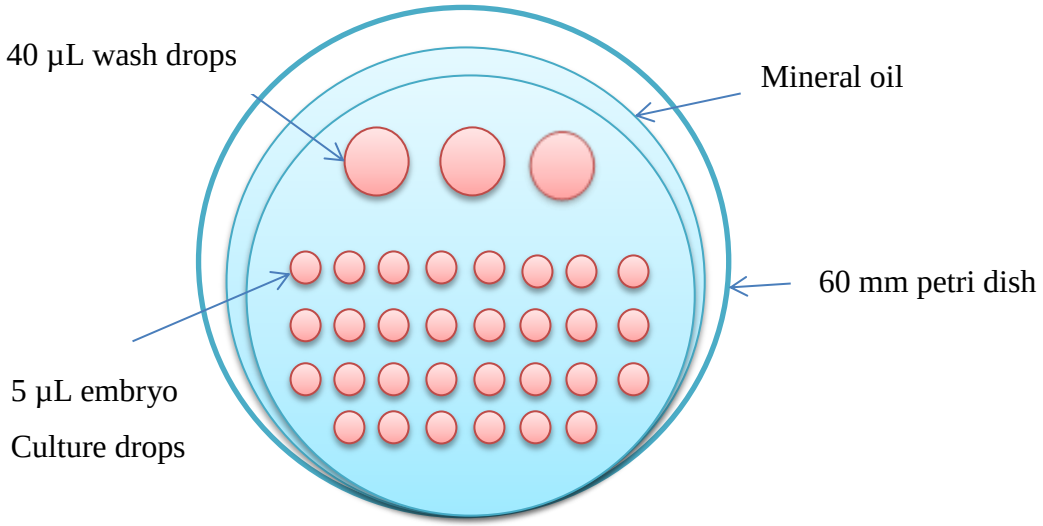

Figure 14: Single embryo culture dish for zona free NT embryos. Contains 3 x 40 µL wash drops in which the embryos were washed through before being placed individually into the 5 µL embryo culture drops.

2.2.6.6.2 Refreshing doxycycline in embryo culture

Doxycycline only remains active for 48 hrs at the 2 mg/mL concentration required. Therefore, it must be refreshed every 48 hours to maintain the induction of the pTRE3G-mCherry vector throughout embryo culture. For handling consistency between samples the EOG_TET_NANOG -Dox treatment was also moved into a new plate every time the doxycycline was refreshed. At days two and three the ESOF plates must be remade with freshly thawed doxycycline. These were gassed

for two hours prior to transfer in a modular-incubation chamber. The embryos were then moved into the new ESOF dish, which was returned to the modular-incubation chamber. This was gassed and placed into the incubator until the doxycycline needed to be refreshed again, or until step 2.2.6.6.3.

2.2.6.6.3 Change of embryo culture media (Day 5)

The media the embryo is cultured in is designed to best suit the embryos needs for healthy growth, by mimicking the environment *in vivo*. At day five of embryo culture, Late Synthetic Oviduct Fluid (LSOF) is required for optimal embryo growth. LSOF plates were made and gassed in the modular-incubation chamber for two hours prior to use. These plates contained fresh doxycycline for the EOG_TET_NANOG +Dox treatment. Whilst moving the embryos from the ESOF into the LSOF, they move through three 40 µL wash drops before being placed into single culture 5 µL drops. The LSOF plates containing the embryos were then placed back into the modular-incubation chamber for a further two days of culture.

2.2.6.6.4 Day 7 grading and doxycycline refreshing

A standardised part of embryo culture in the reproductive technologies lab is to grade all embryos at day seven to provide an understanding of IVP skills or NT development for personal records and as a further step of analysing the developmental success of the NT run. The embryo grading was always conducted by the same person for consistency using the standard grading regulations (Appendix 4). The embryos stage of development was recorded along with a number from one to three which represented the morphological quality of the embryo. Also at this stage the mCherry and GFP signal was visualised and recorded with the Olympus microscope. As the embryos required one further day of culture, this also meant that the doxycycline needed to be replenished. Another set of LSOF plates were made and gassed for two hours in a micro-incubation chamber containing fresh doxycycline in the EOG_TET_NANOG +Dox treatment as previously described in section 2.2.6.6.3. EOG_TET_NANOG -Dox plates were also made and both treatments were moved into the new plates to keep the handling of the embryos consistent.

2.2.6.6.5 Day 8 grading and embryo collection

On day eight, the embryos were at the stage of interest for the research objectives in this thesis. They were again graded following the same guidelines as in Appendix 4 and were analysed for mCherry and GFP signal. The embryos then underwent RNA extraction and cDNA synthesis for qPCR analysis (2.2.6.6.5) or were fixed with 4% PFA for ICC (2.2.14).

2.2.7 RNAGEMTM Tissue PLUS for cells and embryos

2.2.7.1 Solution preparation

An *RNA*GEM Tissue PLUS kit was used to extract RNA from the cells of embryos or cell culture tissue and preserved in preparation for cDNA synthesis. The *RNA*GEM mix was prepared before the sample was ready for collection. A cell line with a cell count between 50,000 and 500,000 cells requires 1 µL of *RNA*GEM, 5 µL 10x Buffer Silver in 44 µL of DEPC water. A blastocyst sample requires 0.5 µl, 1 µL Buffer Silver in 8.5 µL DEPC water.

2.2.7.2 Sample collection

The cells must then be prepared for *RNA*GEM in the tissue culture lab. Cells in culture had their media removed. They were washed once in PBS. TrypLE was then added to at a quantity which covered the base of the dish. The plate was tapped in order to ensure the cells had detached. The trypLE solution containing the cells was pipetted into a microcentrifuge tube and spun for 3 minutes at 1000 rpm. The supernatant is then removed and is replaced with the *RNA*GEM solution prepared earlier. These tubes were then placed on ice and were moved into the RNA molecular biology lab. For preparation of an embryo sample, microcentrifuge tubes containing the prepared *RNA*GEM solution were placed on ice in order to receive the sample in the embryo lab. Once the tissue was added the tubes were spun down using embryology mini centrifuge to ensure the sample was immersed in the solution. The microcentrifuge tubes were then placed back on ice and were transported to the molecular lab for further processing.

2.2.7.3 RNA extraction and DNAse treatment

The tubes were placed on a heat block for 5-10 minutes depending on cell quantity, at 75° C, at which *RNA*GEM is active. They then were placed back on ice where 0.4-2 µL of DNAse treatment was added to each sample, based on number of cells.1-5 µL of DNAse buffer was also added to each tube. Tubes were placed on a vortex and then briefly spun down. The next step was a five minute 37° C incubation to activate the DNAse followed by a five minute 75° C incubation to inactivate it. Samples were then placed back on ice and spun down before 1/10 of the volume of the sample of 10 x TE buffer was added. The samples could then be stored at -20° C or could be immediately processed for cDNA synthesis (2.2.7.4).

2.2.7.4 cDNA synthesis

To begin this process, all samples must be at a quantity of 9 µL. For samples containing a greater volume, 9 µL was removed and placed into a new tube for further processing and the remaining samples were stored at -80° C. To the tubes containing 9 µL of the sample prepared in 2.2.7.3, 1 µL of dNTP mix and 1 µL of Random Hexamer Primers were added. The tubes were then incubated at 65 °C for five minutes which denatures the secondary binding structure of the mRNA and then were plunged into ice for at least one minute which binds the primer. These were then spun down to receive the cDNA synthesis mix. This was 4 µL 5x RT buffer, 4 µL MgCl, 1 µL RNAse Out and 1 µL of SuperScript III. An RT-Negative sample was also prepared for each cDNA batch to analyse potential genomic contamination. The SuperScript III was replaced with water for this sample. The samples were then run on a cDNA programme in a PCR machine. This incubates the samples at 25° C for ten minutes, then, 50° C for 50 minutes and finally at 85° C for five minutes. These samples were then stored at -20° C and can be analyse using quantitative polymerase chain reaction (qPCR) or endpoint PCR.

2.2.8 DNA extraction

DNA extraction is a simple method of collecting genomic DNA for analysis. To an embryo sample or a cell pellet, 100 µL of lysis buffer and 2 µL of proteinase K were added. The samples were then incubated at 55° C for 15 minutes to digest

the sample, and then at 95° C for 15 minutes to heat inactivate the proteinase K. The samples can then be run on an end point PCR.

2.2.9 Primer design

Primers bind to the sequence of interest and amplify them to a testable level. A list of primers can be found in the materials section (2.1.11). For the purposes of this research, primers specific for the pTRE3G-mCherry vector sequence and endogenous NANOG sequence were generated to identify the difference in mRNA expression. Homologs were identified through the nucleotide section of the National Centre for Biotechnology Informatics (NCBI) website. The basic local alignment search tool (BLAST) function was used to identify *Bos taurus* homologs. Once one was selected, the "pick primers" tool was then used. The default settings were used except the primer preference was set to a minimum PCR amplicon size of 70 bp and a maximum of 300 bp, respectively. In addition the primer must span exon-exon junctions. Once the primers were generated, they were selected based on their specificity. The primer sequences were then sent for primer synthesis.

2.2.10 Primer re-suspension

The lyophilised primers were briefly spun down to ensure the pellet was at the bottom of the tube. The pellet was then re-suspended in DEPC water at a final concentration of 1 mM. A working stock of the combined forward and reverse primers was prepared at a final concentration of 10 µM. These were then stored at -20 ° C to be used for qPCR (2.2.11) or endpoint PCR (2.2.12).

2.2.11 Quantitative PCR (qPCR)

The qPCR method is used to amplify cDNA whilst measuring its amplification in order to calculate its original quantity. This allows the comparison of a genes expression across cDNA samples generated in section 2.2.7. For the work conducted in this thesis a variety of primers were used, the details of which can be seen in the methods section (2.1.11). For each qPCR reaction the reaction master mix was assembled via the quantities depicted in Table 14.

Table 14: Reaction mix components and quantities using Takara for the LightCycler2.0.

Reagents	X1
DEPC water	2.2 µL
Takara	5 µL
Primer F & R	.8 µL

LightCycler capillaries were arranged in order to receive the appropriate sample. The master mix was then pipetted into each capillary tube and the cDNA sample was then added. Samples were run in duplicate or triplicate when sample availability permitted. Capillaries were then centrifuged for 15 seconds using the LightCycler Carousel centrifuge ensuring the samples location at the end of the capillary. Samples were then loaded into the LightCycler and the programmed temperature regime shown in Table 15 was followed.

Table 15: LightCycler temperature regime.

Step	Temperature	Time
Denaturation	95° C	10 minutes
Cycling (x45)	95° C	20 seconds
	60° C	20 seconds
	72° C	20 seconds
Melting curve	95° C then decreasing to 65° C	20 seconds
	Heating to 95° C at 0.2° C s^{-1}	NA
Cooling	4° C	NA

The sample produces a number that can be compared to other samples. This is the crossover point (CP) in which the amplification of the primer product moves into a exponential style amplification increase. The identity of the resulting product was confirmed via analysis of the melting curve produced by the LightCycler software (2.2.11.1.1). The quantity expression was calculated using the CP and a standard curve (2.2.11.1.2) specific to the primer and was expressed as a ratio

over the house keeping gene *18S*. This works on the assumption that our experimental treatments do not impact the expression of *18S*.

2.2.11.1.1 Melting curve analysis

The melting peak of the product produced during the LightCycler's program was analysed at the end of each run. Each product produced has a specific melting temperature in which the strands separate based on base length and GC content. In the initial testing of the primer this temperature was revealed and all following experiments were compared to check the product was genuine. An inaccurate melting peak could be the result of genomic or cDNA contamination of the sample, or primer dimer, where the primer binds to itself and creates a subsequent sequence. For each primer run conducted a no-template control (NTC) was run in parallel. This sample either produced a flat line with no melting peak, or showed a standard primer dimer peak, consistent with that primer. A positive template control (PTC) was also run in parallel. This sample contained a gel elute of the band produced in section 2.2.11.1.5. The band length was checked against the expected length provided by the information pamphlet that came with the primer. The band was eluted using the E.Z.N.A gel elution kit (section 2.2.11.1.5), resulting in a concentrated solution of the primer product. These were often diluted 1/100 to achieve a reasonable CP. When this was run through the LightCycler it produced a melting peak to compare the cDNA samples to and also validated the experiment, showing that it worked.

All qPCR experiments throughout this research underwent melting curve analysis. Each CP produced by a sample was only analysed if the melting peak of that sample matched what was expected from that primer pair (Table 11). The result was discarded if it was not a match. A NTC was also run alongside all experiments. This was expected to flat line. If it produced a specific peak, the entire run of samples was discounted as the CPs could have been altered by the presence of something in the master mix.

2.2.11.1.2 Standard curve generation

A standard curve is used to provide a calculation in which the concentration can be determined for each CP. Primers were ordered as described in section 2.2.9. Once they arrived, they underwent analysis via qPCR to see if the CP and melting peak produced was consistent. They were then validated by running the result of the qPCR on a gel to check the band size they produced. Once the band was confirmed to be the correct size, it was extracted using the E.Z.N.A protocol (2.2.11.1.5). This gel elute is a highly concentrated solution of the primer product which was used to generate the standard curve. This was serially diluted to 5-log dilutions. A master mix for the primer was made following the reaction mix guidelines explained in Table 14. Each dilution set was run in duplicate, triplicate or quadruplicate depending on how dilute the sample was, as higher dilutions required more replicates to obtain a more accurate result. The standard program from the LightCycler was run (Table 15) and the curves were generated using the LightCycler software. The data generated by the LightCycler was exported to Excel. The data was graphed and a trend line equation and R value was generated for each graph. A graph with an efficiency within a 0.5% range of 2, was used to statistically analyse each CP in accordance with the gene analysed.

2.2.11.1.3 Statistical analysis of CPs using the standard curve

The relative units (RU) were generated via the use of the standard curve of each primer for each sample. The CP generated by the qPCR experiment on the samples was incorporated into an equation (Equation 2), along with the primers standard curve values.

Equation 2: **Relative units calculation**

$$\boldsymbol{RU = EXP\ (-(CP\ value - x\ value/y\ value)}$$

All samples were also analysed with a house keeper gene, either *GAPDH* or *18S*. The RU for the samples of the target gene was then expressed as a ratio over an RU from the house keeper gene. This samples number could then be compared to numbers generated for other samples and revealed which sample was expressing more or less of the gene of interest. These results were graphed and the data underwent a Students t-test or Fishers exact test to determine if the difference

between treatments was statistically significant ($P < 0.05$). Students t-tests were conducted on logged values. Samples were graphically presented in column graphs in either log or fold change format. Fold change graphs were generated by calculating the ratio of expression of the EOG_TET_NANOG +Dox treatment over the control; all genes were then presented on one fold change graph. Error bars were calculated based on the standard error of the mean (SEM) of all biological replicates. Log graphs were generated by unclogging logged values (generated for statistical analysis) and setting the graph to a log setting. SEM was calculated using Equation 3 and Equation 4.

Equation 3: Equation to calculate positive error in logarithmic graph.

$$Error\ up = Power(10, average\ log10 + stdev\ log10 - Power(10\ average\ log10\ value)$$

Equation 4: Equation to calculate negative error in logarithmic graph.

$$Error\ down = Power\ (10, average\ log10) - Power(10, average\ log10 - stdev\ log10)$$

2.2.11.1.4 Calculation of absolute copy number of mRNA transcripts from concentration

The molecular weight (bp) for the transcript of interest was converted into M [g/mol]. Then the ng/µL value of the primer gel elute derived in section 2.2.11.1.2 was entered into a table where the log-5 dilution series used to create the standard curve was recalculated into the ng/µL unit. This value was then multiplied by 1000 to derive the value of ng/mL. This value was then added to Equation 5 to calculate mol per mL.

Equation 5: Mol per mL calculation.

$$n = m/M$$

This value was again multiplied by 1000 to calculate the mols per litre. The number of molecules per litre was then calculated using Avogadro's constant $6.002214129 \times 10^{23}$. This was converted back into mL by multiplication of 0.001.

The concentration was calculated based on 2 µL of template in the 10 µL qPCR reaction mix. This was calculated using Equation 6 which resulted in mol/L.

Equation 6: Concentration calculation.

$$C = n/V$$

The number of molecules in the litre was calculated by again using Avogadro's constant. Finally the number of molecules per 10 µL reaction was able to be calculated by multiplying the mol/L in the 10 µL reaction mix by 1.00 E -05 to convert to the 10 µL volume, then multiplying that number by Avogadro's constant. For embryo samples the copy number was normalised over the number of embryos within each sample. Cell samples consistently contained 500,000 cells per sample so did not require normalisation.

2.2.11.1.5 Gel elution for positive template controls and standard curves

To generate enough PCR product to produce a standard curve, a DNA band of the product was extracted and eluted to produce a highly concentrated solution of the primer's product. End point PCR described in section 2.2.12 was used to amplify the primer product from a sample containing the target gene. The resulting solution was subject to agarose gel electrophoresis (2.2.13) to confirm that the band that was in the correct size range and was then carefully cut out of the gel using a scalpel blade. The gel section containing the DNA fragment was then placed into a pre-weighed 1.5 mL microcentrifuge tube. The tube containing the gel section was then re-weighed to calculate the weight of the gel section. The E.Z.N.A kit protocol was then followed. Binding buffer was added to the tube at 1 mL per 1 g of band. This was then added to a heated shaker at 60° C, until the gel had completely dissolved into the solution. The solution was then pipetted into a HiBind DNA spin-column which held the DNA as the dissolved gel moves through during a two minute spin at 14,000 rpm at RT. The DNA in the column was then washed with a wash buffer and eluted into a new tube with an elution buffer. The concentration and purity of the solution was then measured using a NanoDrop Spectrophotometer. A 1 µL drop was pipetted onto the NanoDrop pedestal after it had been blanked with DEPC water. The DNA was measured at

Absorbance (A) of 260 nm and the concentration was reported in ng/µL. A pure DNA sample is expected to produce an $A_{260/280}$ ratio above 1.8. The solution can then be used to generate standard curves (2.2.11.1.2) or as a positive template control for qPCR analysis (2.2.11)

2.2.12 Endpoint PCR

End point PCR is a more primitive version of qPCR. It works on the same principles but an endpoint PCR machine does not have the capability of measuring the quantity of the gene as it is amplified. Instead it can only detect if a gene is present or absent in a tissue. This can only be visualised when the end product is run on through gel electrophoresis.

For each cDNA or DNA sample a 25 µL PCR reaction was prepared in a PCR tube. The reaction mix is outlined in Table 16. To each PCR tube, 1 µL of sample was added or 1 µL of water for a negative control.

Table 16: Endpoint PCR reaction mix.

Reagent	1x
10x buffer mix	2.5 µL
dNTPs	0.5 µL
F and R primers	1 µL
Taq DNA Polymerase	0.2 µL
H_2O	20.8 µL
Total	25 µL

The samples were then run on a PCR machine which has a number of different set programmes depending on how many cycles needed to be run and which primers were being used. The parameters are displayed in Table 17.

Table 17: Outline of standard endpoint PCR reaction parameters.

Step	Temperature (°C)	Time	Cycles
Initial denaturation	95	5 minutes	1
Denaturation	94	30 seconds	30-45 depending on primer
Annealing	50-60 (depending on the primer)	30 seconds	
Extension	72	30 seconds	
Final extension	72	7 minutes	1
Cooling	4	On hold	NA

Once the PCR reaction was complete, the samples were analysed using gel electrophoresis (section 2.2.13) to determine whether or not a band is present.

2.2.13 Gel electrophoresis

Gel electrophoresis was used to visualise the product of end point PCR or qPCR and to identify the base pair length. First, the agarose gel mould was prepared. The size of the mould depended on the number of samples. The required 1 X TAE buffer to fill the gel mould was measured in a volumetric flask and the quantity of agarose powder was weighed. The gel can be made at a concentration anywhere between 1-2.5% agarose depending on the parameters of the experiment. The powder was then added to the TAE buffer and the solution was microwaved in order to dissolve the agarose crystals. Once the agarose was melted and the solution had cooled to a heat where it could be touched, 1 µL of SYBR safe was added per 10 mL of agarose solution. The solution was then poured into the mould and left to set at RT.

Once the gel had solidified, it was placed into a gel electrophoresis tank. A 1 kb ladder was added to each end well to act as a marker by which the samples bands could have their band length measured. A 10 µL sample of the PCR or endpoint PCR product was transferred onto a piece of Parafilm and was mixed with 2 µL of loading dye. Each sample was then loaded into its designated well. The lid was placed back on the tank and the voltage was set from 80-120 volts depending on

the thickness of the gel. Once the loading dye had travelled 3/4 of the way through the gel, electrophoresis was stopped. The bands were then visualised under UV light and photographed using the gel doc and Quantity one software.

2.2.14 Immunocytochemistry (ICC)

Immunocytochemistry (ICC) offers visualisation of the cellular localisation of gene expression via a fluorescent signal attachment to the target protein. Two methodologies were developed for ICC on cell lines and embryos. For cell lines, cells were grown on 10 mm circular coverslips which were previously placed on the bottom of a tissue culture dish prior to the cells culture. This allowed the cells to adhere and grow on the surface of the coverslip. The solutions are then placed on to the coverslip, in a dish with the cell side up or the coverslips can be placed cell side down onto a drop of solution. When this protocol is conducted on embryos, an embryo was placed into a 96 well conical plate where each solution is in a different well and the embryos are moved from well to well as required. The two day ICC protocol was carried out at RT unless otherwise stated. Wash steps were at a duration of five minutes and require PBS for cells and PBS-PVA for embryos to prevent the embryos from attaching to the plate.

Firstly, the sample must be washed three times from the media in which it has been growing to remove protein growth nutrients. This was achieved via three washes. The samples were then fixed in freshly depolymerized 4% PFA for 15 or 30 minutes at 4° C for cells and embryos respectively. The samples were washed three times. To reduce background staining, the samples were then incubated in NH_4Cl for 10 minutes which quenches the aldehyde groups. This was followed by one wash. Then, to increase the permeability of the cells, the samples were incubated in 0.1% Triton-X for 10 or 15 minutes for cells or embryo, followed by one wash. To avoid false positive staining the samples were blocked in 5% serum of the species in which the secondary antibody was raised for 30 minutes for a cell sample and 90 minutes for an embryo sample. This was commonly either donkey or goat serum.

The samples were then transferred to a humidified chamber and incubated with 50 µL of primary antibody overnight at 4° C. This binds to the protein of the gene

under investigation. The antibodies were diluted in blocking solution. A list of antibodies and dilutions used can be found in the materials section 2.1.9. A control treatment was included where no primary antibody was applied. This control determined the intensity of background fluorescence produced by the secondary antibody. This incubation must be conducted in a humidified chamber. For cells this means the antibody was pipetted in 50 µL drops onto Parafilm in a petri dish lined with damp filter paper. The petri dish is then wrapped with Parafilm. For embryos, the surrounding wells in the 96 well plate were filled with dH_2O, the plate was then wrapped in Parafilm. The primary antibody incubation was left overnight at 4° C.

On the second day, the samples were washed three times to remove unbound antibody before they are placed in the secondary antibody. The secondary antibody was also diluted in the blocking solution. The DNA stain Hoechst was also added to the secondary stain incubation. The secondary antibody was in a humidified chamber at 37° C for 30 minutes. The samples were then washed three times, followed by a brief wash in dH_2O.

The samples were then mounted. For cells, the coverslip was placed cell side down onto 3 µL of mounting media on a frosted slide. For embryos, 3 µL of mounting media was pipetted onto the frosted slide and the embryos were then mouth pipetted into the mounting media followed by the placement of a circular cover slip on top. The slides were stored in at 4° C until photographs were taken using a digital camera and microscope.

2.2.14.1 Photography of ICC samples

The fluorescent signal was visualised on the Olympus microscope. The images were taken using Spotbasic software. When possible, images were taken in black and white of three different wave length channels; 488, 568 and 405. The exposure time for all channels was established upon the first observation of the samples and this was kept consistent throughout the analysis of that run. This allowed the images to be comparable, and accurately demonstrates the background fluorescence from the secondary antibody shown in the control

treatment. The images were then re-coloured using the computer software programme ImageJ. From the look up tables menu a colour was selected based on the actual colour photographed. On occasion colour images were taken using the colour setting on the camera. A scale bar was added with the Spotbasic software. In addition, the three images taken were composed into a merge image to overlay the location of protein expression.

Chapter 3: **Results**

3.1 **Primers which distinguish between ectopically and endogenously expressed *NANOG***

A series of primers were designed using the NCBI BLAST function. These primers were to determine the difference between the ectopically and endogenously expressed *NANOG*.

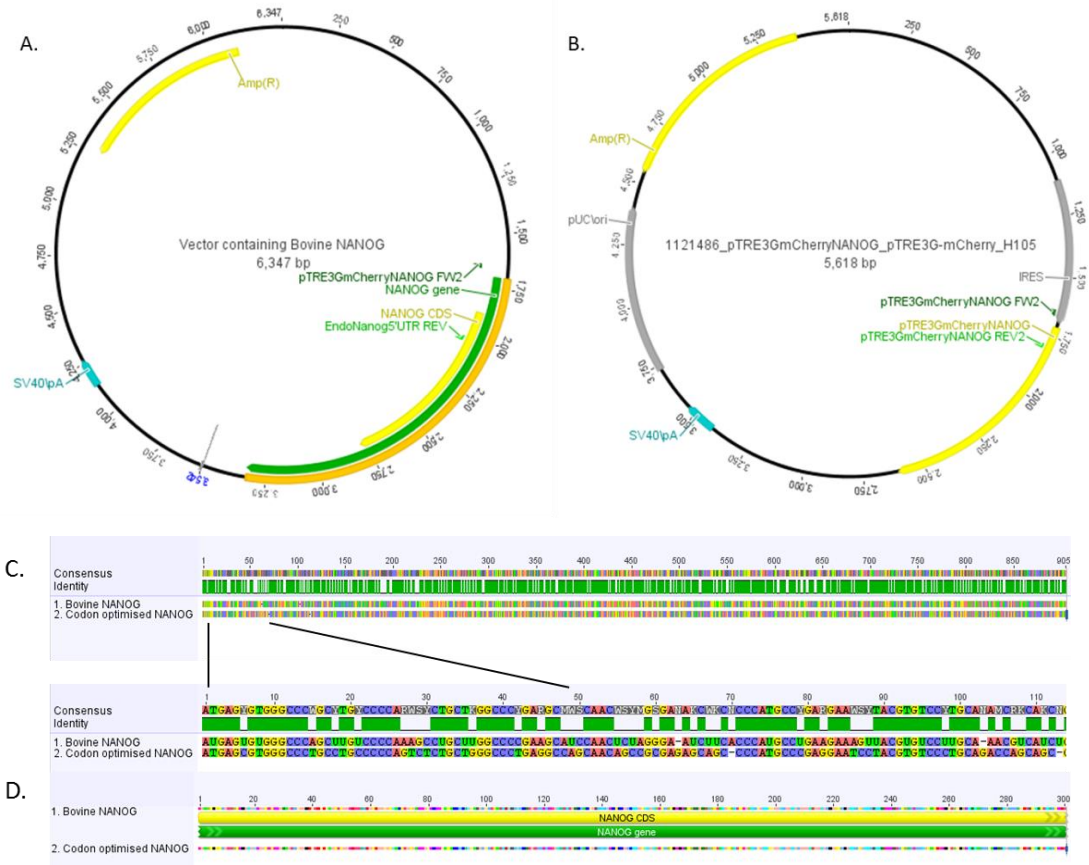

Figure 15: Vector maps of DNA constructs used in this study. A. Vector sequence containing bovine *NANOG* gene (green), with the endogenous *NANOG* primer and ectopic *NANOG* primer binding locations depicted with green arrows. B. pTRE3G-mCherry vector sequence containing codon-optimised bovine *NANOG* with the binding locations for the ectopic *NANOG* primers. C. Alignment of mRNA sequences for bovine *NANOG* (from vector sequence) and codon-optimised *NANOG*. The consensus sequence is 905 nt in length with the green bar indicating sequence sections that match with 100% identity, white indicates discrepancies between the two sequences. An enlargement of mRNA 1-50 illustrates 14 differences at the nucleotide level. D. Alignment of amino acid sequences for vector A bovine NANOG and vector B codon-optimised NANOG protein.

Image A. of Figure 15 shows the reverse primer for the endogenous *NANOG* sequence binding in the open reading frame of the bovine *NANOG* sequence. The forward primer binds in the bovine genomic sequence immediately prior to *NANOG* and does not bind to the pTRE3G-mCherry vector. Therefore, this primer will only bind the mRNA of *NANOG* expressed by the embryo. Image A. of Figure 15 also shows the forward primer for the ectopic *NANOG* binding the vector before the *NANOG* sequence. The reverse primer does not bind to the bovine *NANOG* sequence, but does bind to the codon-optimised *NANOG* sequence (Image B, Figure 15) Therefore, this primer will only bind the mRNA produced by the vector. Image C. of Figure 15 shows the differences in mRNA sequences for the bovine *NANOG* and codon-optimised *NANOG* sequences, where the amino acid sequences align 100%, forming the same protein structure (Image D, Figure 15).

3.2 NT with unsorted donor cells overexpress NANOG but do not affect targets

There were three NT runs conducted on the EOG_TET_NANOG cell line before it was sorted for high mCherry expression using FACS. The aim of these initial NT runs was to analyse how well the pTRE3G-mCherry vector was transcribed and translated within the embryo, to optimise the cell culture and embryo culture for most effective results, and to analyse how efficiently the cell line was reprogrammed.

.

A total of 60 bovine ovaries were aspirated for each run, generating approximately 200 oocytes. Of these, 140 were enucleated. The cell line was not induced prior to NT and was synchronised to cell cycle G_0 via a six day serum starvation. For each treatment, 30 embryos were derived. In an earlier analysis it was concluded that the day of doxycycline treatment was to be from day 0. At day 7, the embryos were graded based on morphology and the mCherry signal was visualised and graded based on strength (data not shown). The samples were then sorted and blastocysts grade 1-2 underwent RNA extraction and cDNA synthesis. These samples were then analysed via qPCR for ectopic *NANOG*, endogenous *NANOG* and *XIST* to understand the transcriptional effects resulting from the vector.

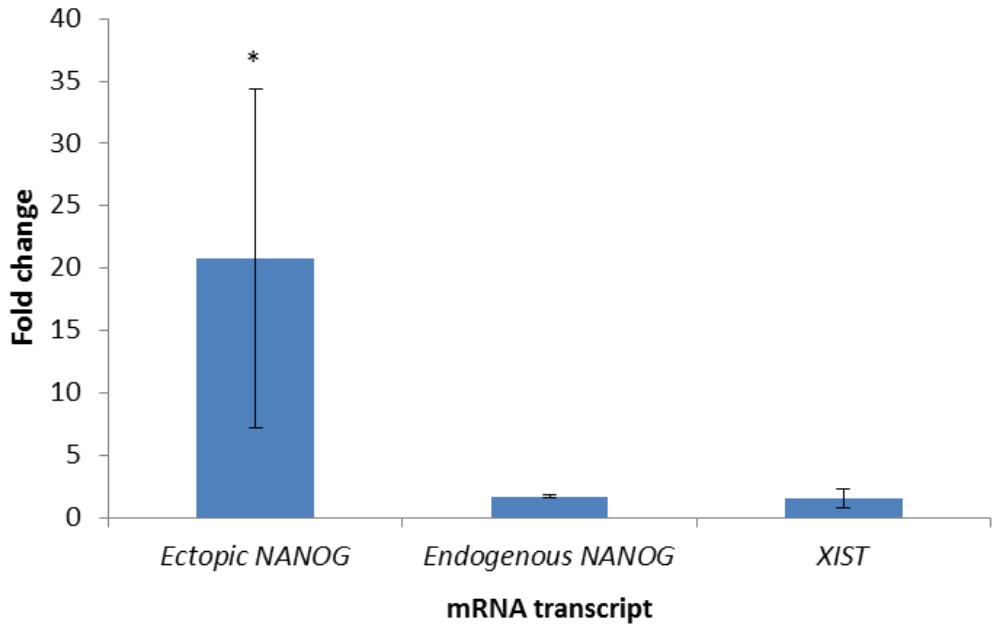

Figure 16: Fold change of ectopic *NANOG*, endogenous *NANOG* and *XIST* expression relative to *18S* EOG_TET_NANOG +Dox over control. cDNA was extracted from blastocysts grade 1-2 which were pooled in groups of 5-10. n= number of biological replicates, N= number of blastocysts. EOG_TET_NANOG +Dox n= 3 N= 19. EOG_TET_NANOG -Dox n= 3 N= 21.Target genes were normalised over *18S* expression in RU. Results were logged and averaged. Error bars indicate ± SEM. Students t-tests were conducted to conclude significance ($P<0.05$). * denotes significance ($P<0.05$).

The ectopic *NANOG* was significantly overexpressed in embryos exposed to doxycycline in comparison to non-induced embryos 20-fold ($P = 0.008$). The endogenous *NANOG* and *XIST* expression show no significant differences between treatments $P = 0.443$ and $P = 0.335$, respectively. Since there was no effect on NANOGs targets, it was decided that the EOG_TET_NANOG cell line should be sorted against mCherry expression in order to achieve a higher population of *NANOG* expressing cells.

3.3 Characterisation of FACS sorted donor cell line EOG_TET_NANOG

The developmental history of the FACS sorted doxycycline-inducible EOG_TET_NANOG cell line was explained in section 2.2.3. This cell line was derived in order for it to be used for the production of embryos which overexpress *NANOG* via NT. Prior to its use in NT it must be again validated (after sorting)

for its mCherry and *NANOG* expression via qPCR and ICC. When analysing the cell lines inducibility, a non-induced EOG_TET_NANOG control was important to test alongside. This was to analyse the difference in expression between the induced and non-induced treatments. However, a further control was also required for many experiments. This was the EOG_TET cell line described in section 2.2.3. This cell line is the parental line to EOG_TET_NANOG, it does not contain the *NANOG* gene but does constitutively express Tet activator (TET 3G). Cells were observed based on morphology to identify any possible changes as a result of culture conditions or induction.

3.3.1 Cell line gene expression analysis of overexpressed *NANOG* has no effect on targets

Cells were processed via the *RNA*GEM protocol to extract RNA, converted to cDNA and analysed via qPCR with ectopic and endogenous *NANOG* primers, along with *XIST*, *OCT4* and *SOX2* (Figure 17). Section A. of Figure 17 shows that the increase in ectopically expressed *NANOG* is four orders of magnitude higher in the non-induced treatment than in the non-induced EOG_TET control. The induced treatment is significantly higher than the non-induced EOG_TET and EOG_TET_NANOG treatments by ten and four orders of magnitude. No other genes were significantly affected by the over expression of *NANOG* (Figure 17, Section B. C. D. E.) The absolute copy number of the ectopic *NANOG* transcript was calculated, the results of this can be seen in Figure 18. The copy number of the induced EOG_TET_NANOG is significantly higher than the EOG_TET_NANOG and EOG_TET non-induced controls by five and ten orders of magnitude. Non-induced EOG_TET_NANOG is five orders of magnitude higher than the non-induced EOG_TET control.

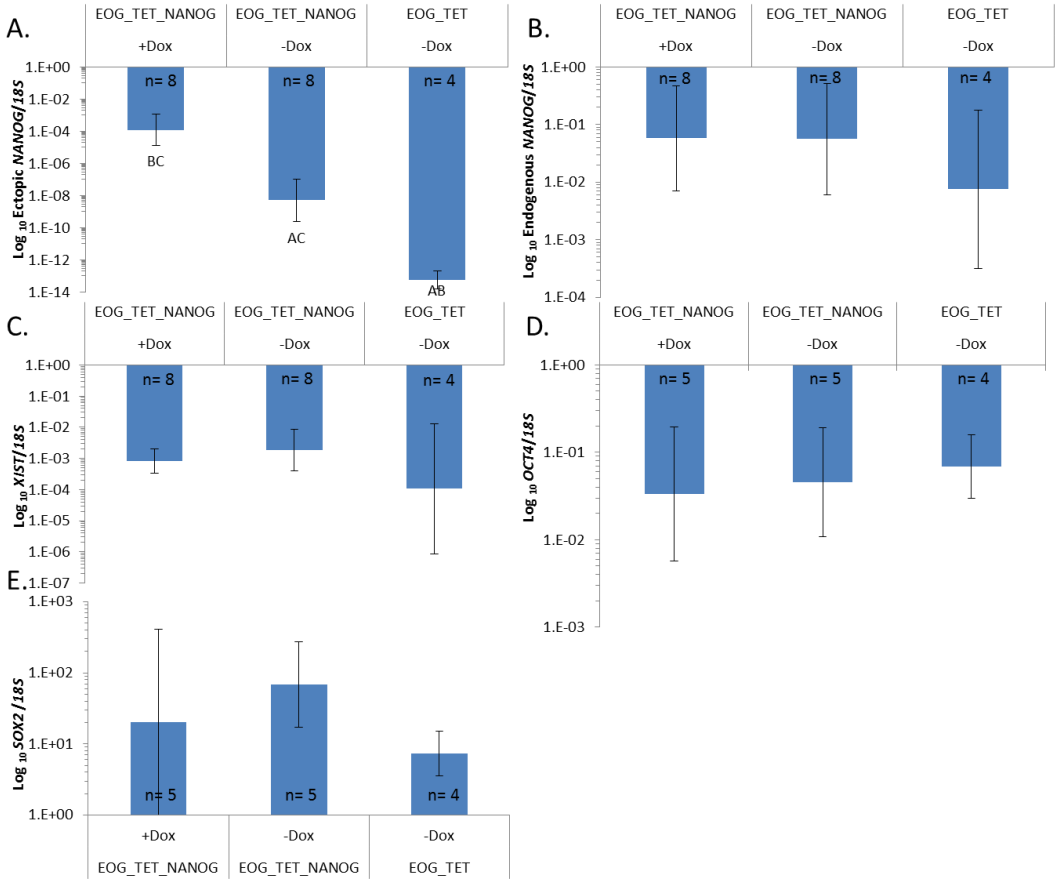

Figure 17: qPCR analysis of the EOG_TET_NANOG cell line, EOG_TET_NANOG +Dox compared to EOG_TETNANOG –Dox and EOG_TET -Dox controls. Target gene values were normalised against *18S* expression in RU. Results were logged and averaged. n= biological replicates. Error bars represent ± SEM. Students t-tests were conducted to test significance (P<0.05) A. Ectopic *NANOG* expression. B. Endogenous *NANOG* expression. C. *XIST* expression. D. *OCT4* expression. E. *SOX2* expression. Bars denoted with an A are significant from the EOG_TET_NANOG +Dox treatment. Bars denoted with a B are significant from the EOG_TET_NANOG -Dox treatment. Bars denoted with are C are significantly different from the EOG_TET treatment.

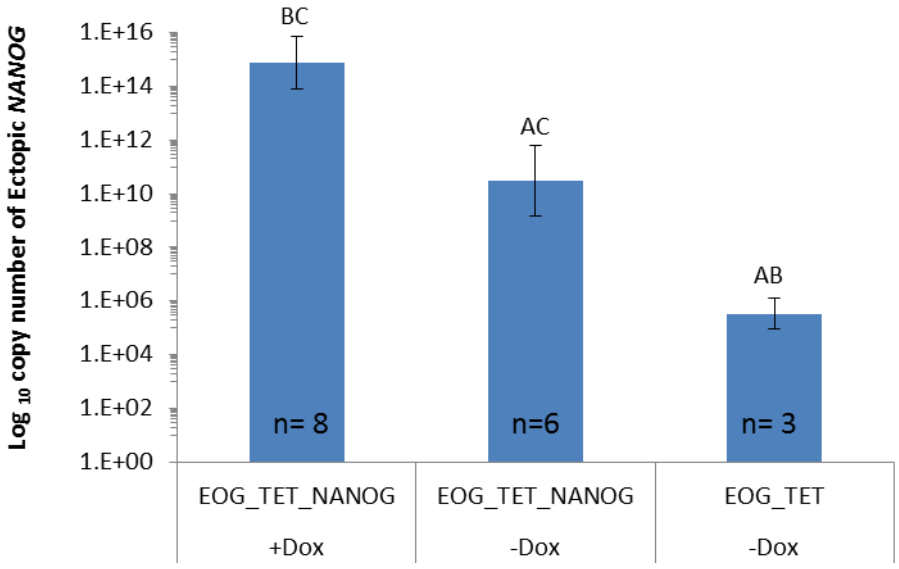

Figure 18: Copy number of ectopic NANOG transcript shows significance between all treatments. Copy number was calculated based on protocol outlined in section 2.2.11.1.4. n= number of biological replicates. Students t-test were conducted to evaluate significance ($P<0.05$). Bars denoted with A are significant from EOG_TET_NANOG +Dox ($P<0.001$), bars denoted with B are significant from EOG_TET_NANOG –Dox ($P<0.001$), bars denoted with C are significant from EOG_TET –Dox.

3.3.2 EOG_TET_NANOG cell line doxycycline-induced treatment positive for NANOG protein

Fibroblasts were thawed (2.2.4.1) into a tissue culture dish containing glass coverslips. They were cultured for 48 hours in which the induced EOG_TET_NANOG treatment was induced throughout. This was conducted in standard cell culture media. The fibroblasts were then stained for NANOG protein using the ICC protocol (section 2.2.14) (Figure 19). For the NANOG staining non-induced EOG_TET_NANOG and EOG_TET treatments were used as controls. A Donkey anti Mouse Alexa Fluor® 488 secondary antibody was used. Images of the mCherry signal were also taken to compare with NANOG protein localisation. The number of cells expressing NANOG and mCherry were counted in a blind analysis of ten different fields of view of each treatment (Figure 20). The treatment names were encoded and the party who conducted the count was unaware of the projects details.

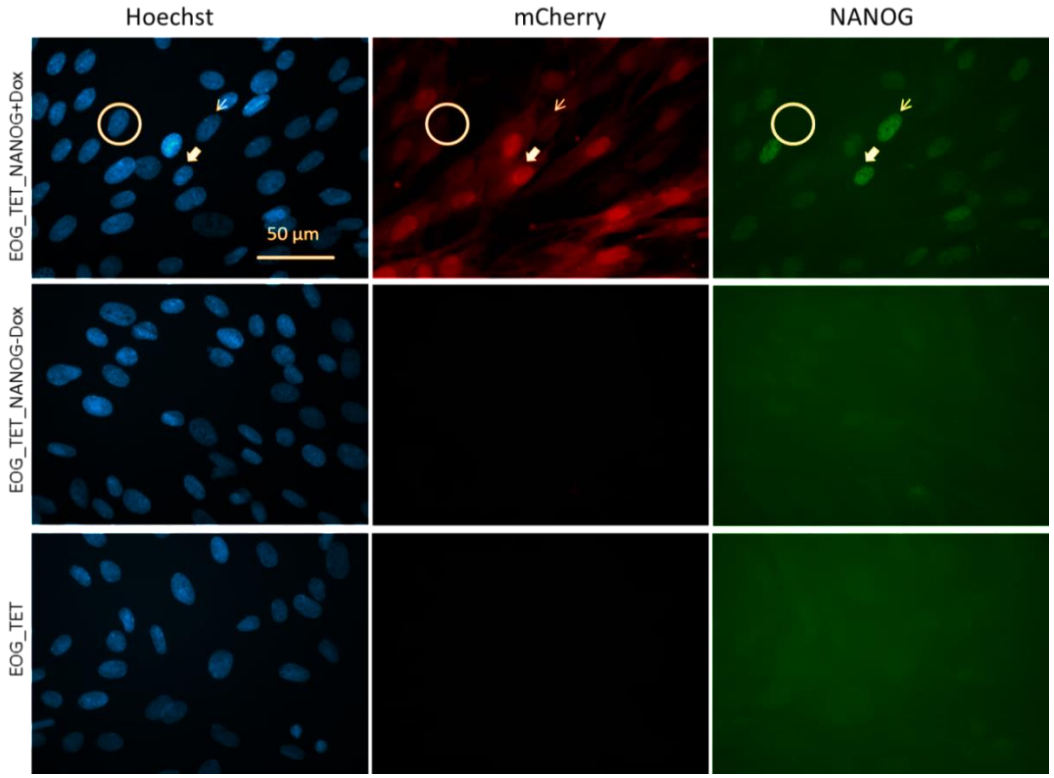

Figure 19: ICC analysis of NANOG protein in the EOG_TET_NANOG cell line. ⬋ Denote cells which are positive for all signals. ↙ Denote cells which have weak mCherry signal and strong NANOG. O Denotes a cell which has a Hoechst signal but is negative for both mCherry and NANOG. Images pseudo coloured with ImageJ. Hoechst DNA stain (blue), mCherry signal (red), Alexa Fluor® 488 secondary stain for NANOG (green).

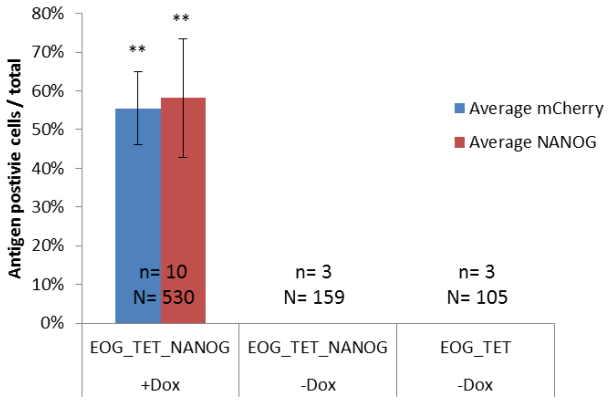

Figure 20: Significantly higher percentage of antigen positive cells for mCherry and NANOG in the EOG_TET_NANOG +Dox treatment than controls. Students t-tests were conducted to test significance ($P<0.05$). ** denotes significance from controls $P<0.001$. n= biological replicates. N= number of cells counted. Error bars represent ± SEM.

There was no mCherry or NANOG signal in the non-induced EOG_TET or EOG_TET_NANOG control. The mCherry count was 55 ± 15% which is much lower than what was seen in a flow cytometry reading just after cell sorting for the mCherry signal. The NANOG positive cells were higher than that of the mCherry signal, at 58 ± 9%.

3.4 Inactive X-chromosome analysis of seven cell lines

3.4.1 Sexing analysis confirms EOG_TET-NANOG as female compared with five control cell lines

The cell lines were analysed via PCR using sexing primers in order to confirm their sex. DNA samples for a seven cell lines were prepared via the genotyping technique as described in section 2.2.8, this consisted of the cell line focused on in this research, EOG_TET_NANOG and all its parental cell lines which were EOG_TET and EOG. The cell lines LFC2 and EFC1B were female controls of follicular cells isolated from adult ovaries and LJ801 was a male control of skin fibroblasts isolated form an ear biopsy. Seven PCR reactions were performed using DNA extracted from these cell lines with sexing primers (Figure 21) and or a multiplex of Y chromosome primers (Figure 22). Positive and negative controls were included. Finally, amplified products were run on a 2% agarose gel for 1 hour at 90 V.

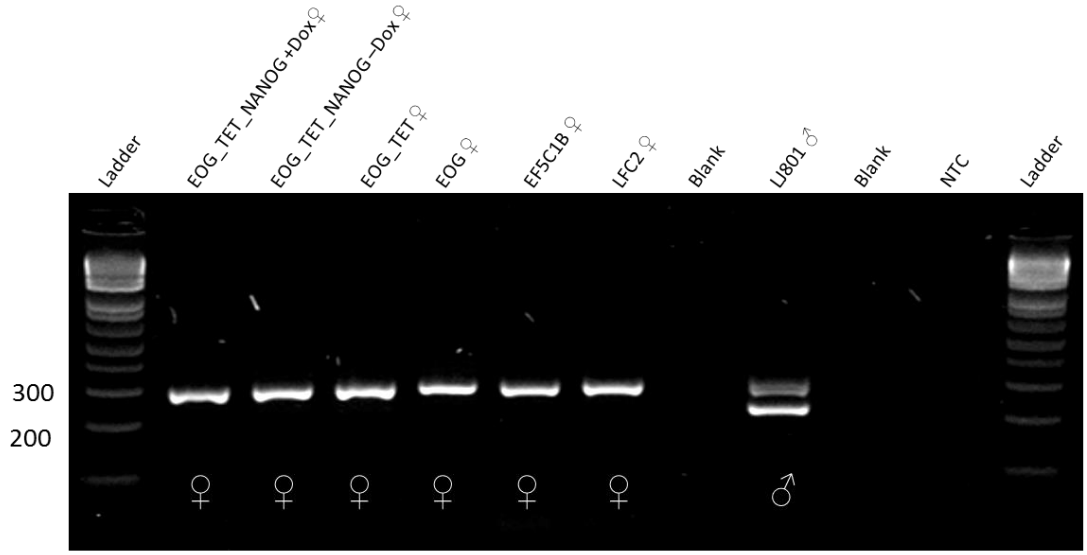

Figure 21: Agarose gel electrophoresis of DNA extraction of seven cell lines confirms six female and one male cell line. Run for 1 hour at 90 V, 2% agarose.

The sexing set of primers contains one primer pair specific for the X-chromosome and one primer pair specific for the Y chromosome. The expected PCR results using these primers is the observation of an X-chromosome band at 262 bp, and the Y chromosome band at 202 bp on the agarose gel. Cell lines that had both bands visible were confirmed to be male, cell lines that only have the X band visible were confirmed to be female. EOG_TET_NANOG, EOG_TET, EOG, EFC1B and LFC2 cell lines were female and the LJ801 cell line was male (Figure 21).

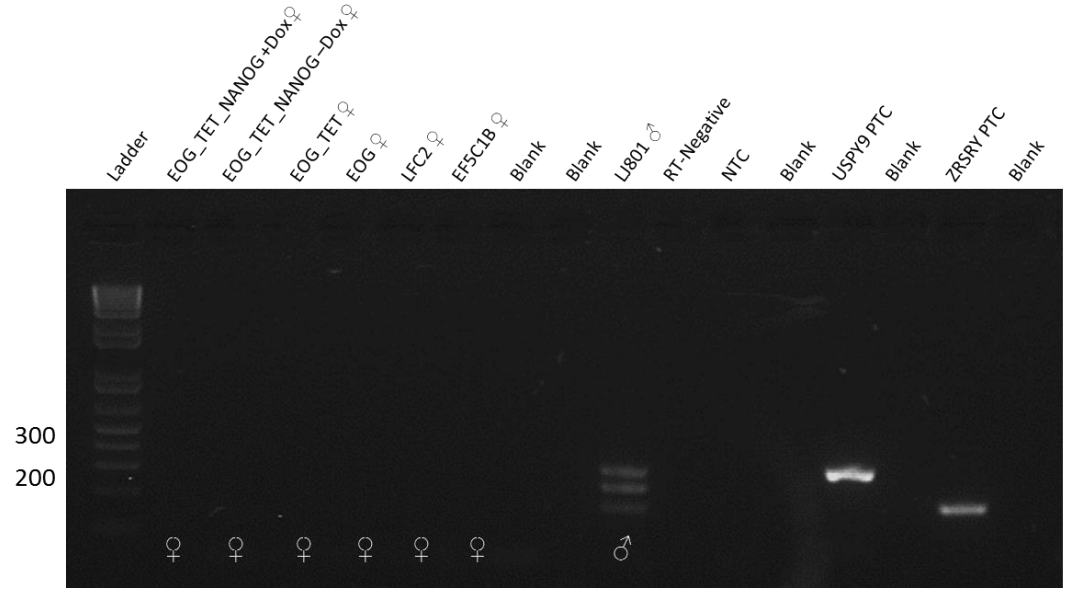

Figure 22: Agarose gel electrophoresis of multiplex PCR of seven DNA samples confirms six female and one male cell line. Run for 1 hour at 90 V, 2% agarose.

The Y chromosome specific primers used in this multiplex PCR were *DDX3Y*, *USPY9* and *ZRSRY*. The bands produced by each primer pair were 225, 285 and 158 bp respectively. Figure 22 shows the PTC for *USP9Y* and *ZRSRY* (*DDX3Y* PTC was unavailable). These were the result of a PCR experiment conducted on a gel elute of the DNA band produced by each primer pair, this is highly concentrated which is why these two bands are much brighter than the bands in the samples. The expected result is that female cell lines will produce no bands, where male cell lines will have three. LJ801 is the only male cell line. No cell lines confirmed female in Figure 22 contain any male contamination. In conclusion, EOG_TET_NANOG and all its parental cell lines were female, LJ801

was a male cell line and there was no contamination of male cells within EOG_TET_NANOG or any of its parental lines.

3.4.2 Male and female cell lines have significantly different Xist expression

The second objective for this research is an investigation into the expression of *XIST*, and if it is changed by the overexpression of NANOG in the induced EOG_TET_NANOG treatment. A series of male and female cell lines were analysed via qPCR for *XIST* and *DDX3Y* gene expression. This was to analyse if the *XIST* expression of the induced EOG_TET_NANOG treatment was significantly lower than other females as a result of the overexpression of NANOG. For this series of experiments the house keeping gene *18S* was initially used (Figure 23 A/B), but showed too much variation.

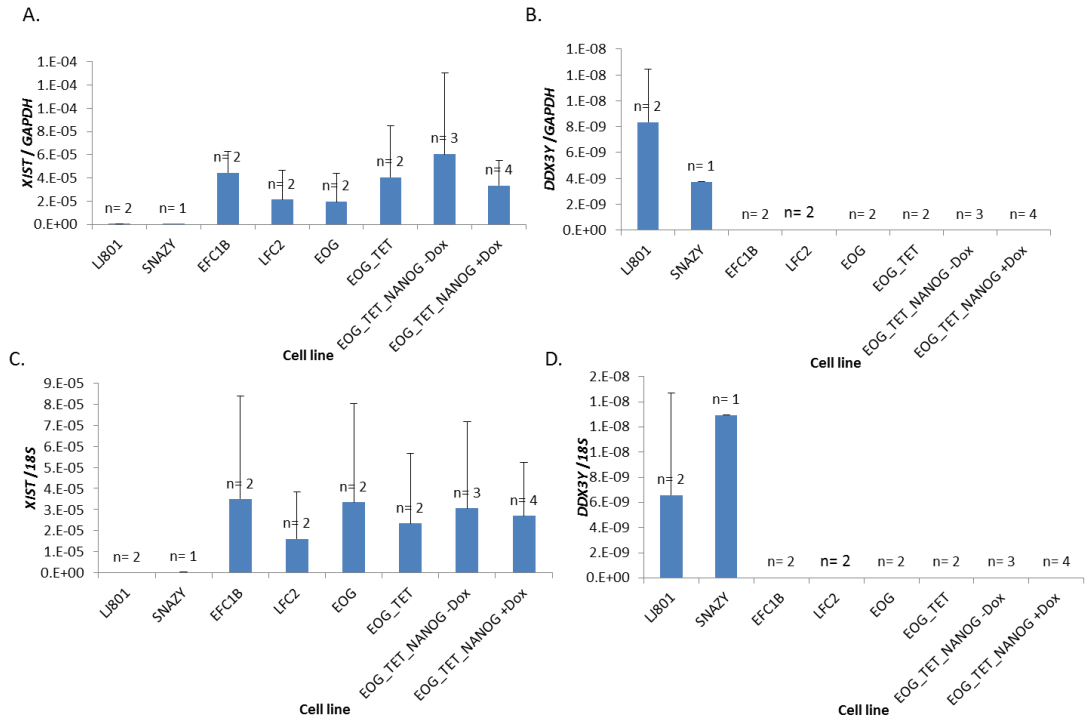

Figure 23: qPCR analysis of *XIST* and *DD3XY* expression of female and male cell lines show greater variability with *18S* housekeeper than *GAPDH*. *XIST* and *DDX3Y* expression was normalised against either *18S* or *GAPDH* expression in RU. Error bars represent + SEM. n= biological replicates. Figures A and B have *18S* as a housekeeping gene where figures C and D have the *GAPDH* house keeping gene. Cell lines LJ801 and SNAZY are male, cell lines EFC1B, LFC2, EOG, EOG_TET, EOG_TET_NANOG were all female.

GAPDH was then used as it showed less variation and gave a clearer picture of gene expression (Figure 23 C/D). For this series of experiments the same set of cell lines were used as in section 3.4.2, however, there was one more male control included. This was to be sure that the LJ801 was representative of normal male expression. The additional male cell line was SNAZY, a bovine skin fibroblast sample created from an ear biopsy.

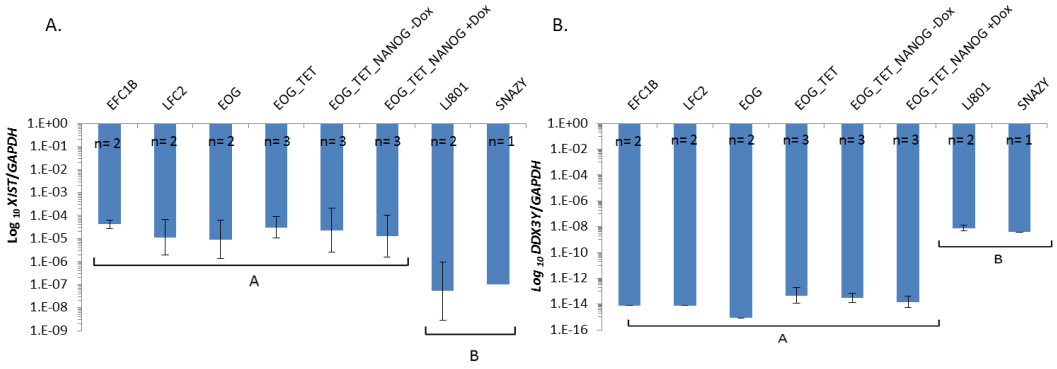

Figure 24: qPCR analysis of XIST and DD3XY on eight cell lines show significant differences between female and male lines. Target gene values were normalised against *GAPDH* expression in RU. Results were logged and averaged. n= biological replicates. Error bars show the ± SEM. Students t-tests were conducted to measure significance of pooled male and pooled female groups ($P<0.05$). Image A. A and B are significantly different from one another ($P<0.001$).Image B. A and B are significantly different ($P = <0.001$).

The *XIST* expression of the grouped female cell lines is significantly higher than the grouped male cell lines by around two orders of magnitude. The induced EOG_TET_NANOG treatment was not significantly different from the other female cell lines, nor is the EOG_TET_NANOG treatments when compared as a group. The expression of *DD3XY* was significantly higher by four orders of magnitude in the two male cell lines than in the female cell lines.

3.4.3 H3K27me3 staining does not identify inactive X-chromosome

An issue of interest was whether the inactive X-chromosome could be visualised in fibroblast cells and further more if the overexpression of NANOG would decrease the number of visible inactive X-chromosomes in the induced EOG_TET_NANOG treatment. In a literature search, no published data describing this phenomenon has been identified in this cell type before. Therefore,

an assay was set up with a series of female and male fibroblast controls to test this hypothesis. This consisted of EOG_TET_NANOG parental cell lines, EOG_TET, and EOG. LFC2 and EFC1B were female controls of follicular cells isolated from an adult ovary and LJ801 was a male control of skin fibroblasts isolated from an ear biopsy. Cells were thawed into tissue culture dishes containing glass cover slips and were cultured for 48 hours until they were between 60 and 90 % confluent. The ICC protocol was carried then out. As *XIST* is a lncRNA there was no direct protein to stain for. Instead an $H_3K_{27}me_3$ antibody was used as a proxy. $H_3K_{27}me_3$ is present across all chromosomes but is enriched around the inactive X-chromosome, which produces a clear dot or cloud around the inactive X-chromosome [130]. Cells were co-stained with a Hoechst DNA stain. A Donkey anti Rabbit Alexa Fluor 488 secondary was used. The staining protocol did work although the intense inactive X-chromosome $H_3K_{27}me_3$ cloud was never observed with 100 % certainty (Figure 25).

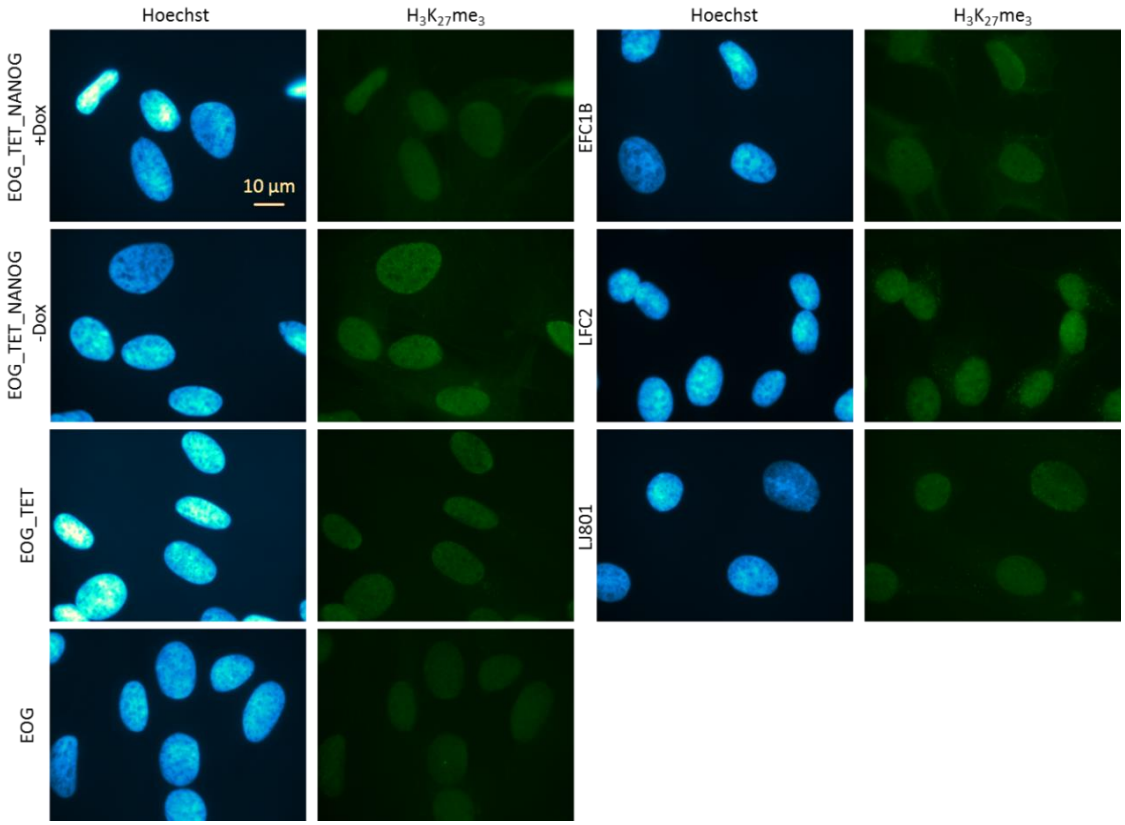

Figure 25: Seven cell lines stained for the inactive X-chromosome H3K27me3. Images pseudo coloured with ImageJ. Hoechst DNA stain (blue), $H_3K_{27}me_3$ stain with Alexa Fluor® 488 Fluor secondary (green).

A blind count was set up to determine if any of the potential $H_3K_{27}me_3$ cloud dots were valid. Three random fields of view from each treatment were counted and each potential dot was identified with a red arrow. The count was conducted with encoded cell names by a party who was unaware of the details of this project. An example of the potential $H_3K_{27}me_3$ clouds can be seen in Figure 26 and the results of this count can be seen in Figure 27.

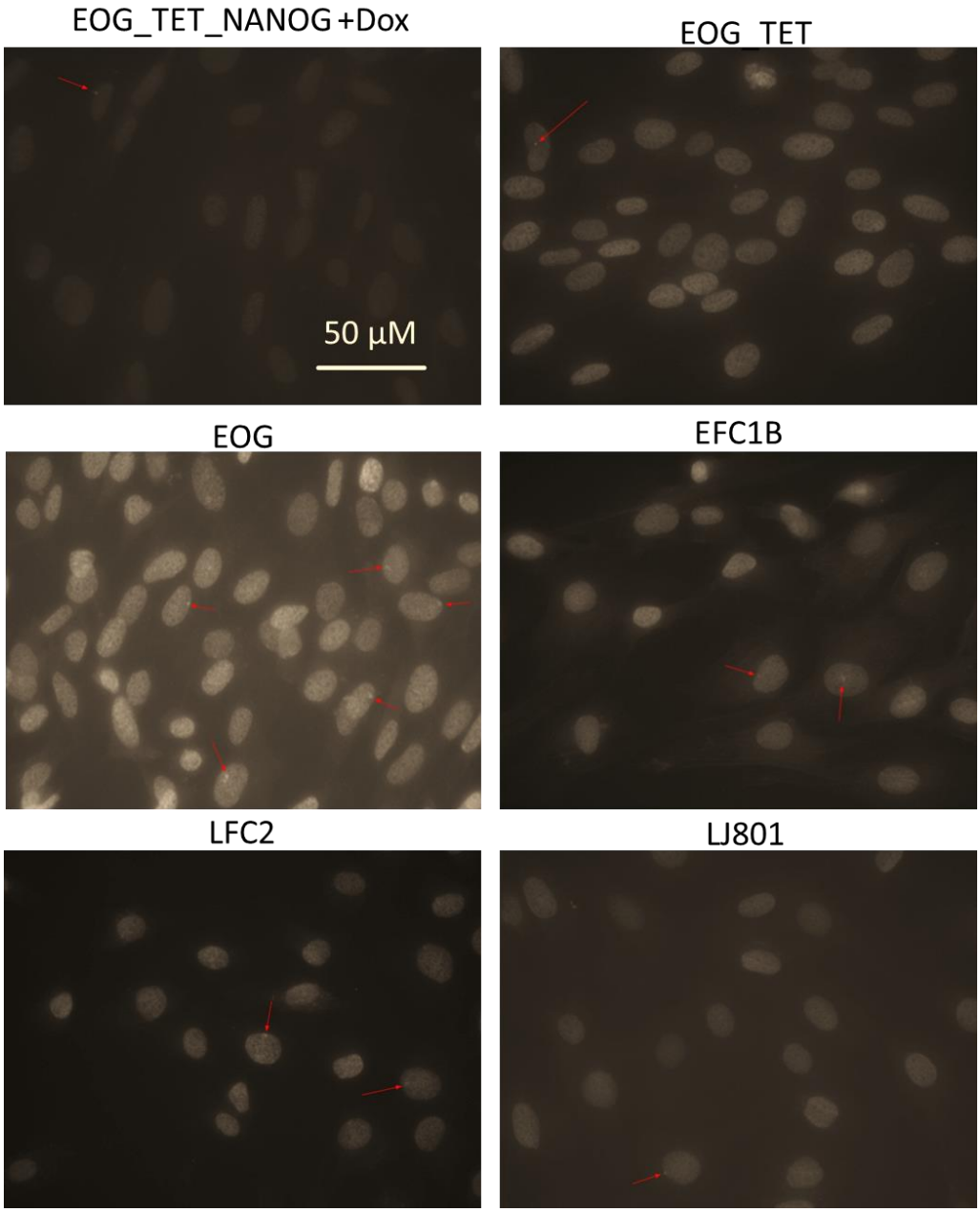

Figure 26: ICC staining of H3K27me3 of seven cell lines where potential H3K27me3 clouds are indicated with red arrows. EOG_TET_NANOG –Dox image did not contain arrows. Images are presented in black and white for better definition of potential $H_3K_{27}me_3$ clouds.

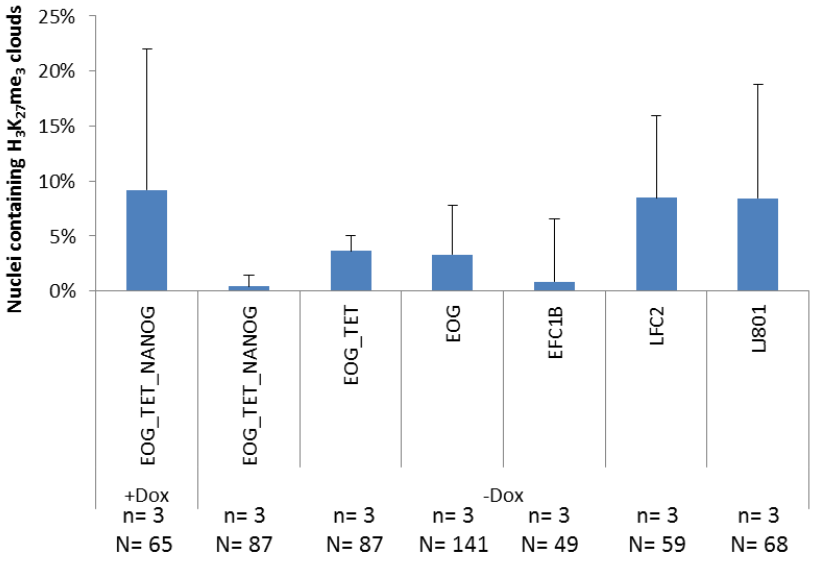

Figure 27: Bar graph depicting the percentage of cells containing a potential inactive X-chromosomes represented by H3K27me3 clouds. n= biological replicates, N= number of cells counted. Student t-test were conducted for significance ($P<0.05$). Error bars represent + SEM.

The statistical analysis of the count revealed that there was no significant difference in the number of potential $H_3K_{27}me_3$ clouds between the female cell lines and the male cell line control.

3.5 Characterisation of cell line after serum starvation

Prior to NT, the cell line must undergo serum starvation to synchronise all cells into the G_0 phase of the cell cycle, as this phase is optimal for NT. The initial characterisation of the EOG_TET_NANOG cell line was conducted under standard culture conditions as described in section 2.2.2. It was important to analyse if the expression of the pTRE3G-mCherry vector was altered by the low serum culture conditions for G_0 synchronisation. Cells were also observed on a morphological basis to identify any possible changes that may have occurred due to serum starvation.

3.5.1 Serum starvation causes a significant decrease in ectopic NANOG expression

The EOG_TET_NANOG cell line was analysed for the expression of the pTRE3G-mCherry vector sequence with the ectopic *NANOG* primer after 6 days of serum starvation (Figure 28). These cells were processed via *RNA*GEM and

cDNA libraries were derived from induced non-starved and serum starved induced and non-induced treatments.

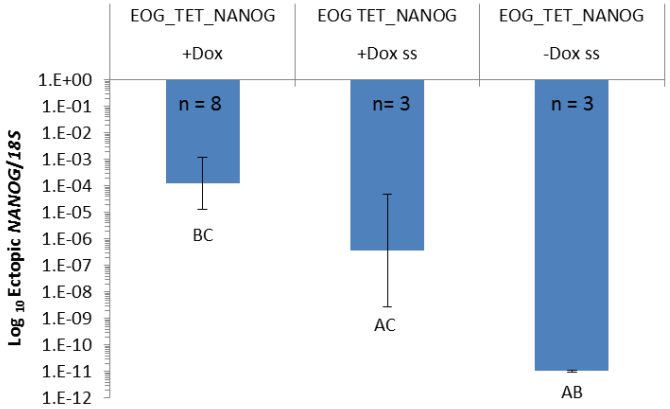

Figure 28: Ectopic NANOG expression is significantly decreased by serum starvation. ss denotes serum starved treatments. Ectopic *NANOG* values were normalised against *18S* in RU. Results were logged and averaged. n = biological replicates. Error bars represent ± SEM. Students t-tests were conducted to measure significance ($P<0.05$). A denotes significant difference from EOG_TET_NANOG +Dox, B denotes significant difference from EOG_TET_NANOG +Dox ss, C denotes significant difference from EOG_TET_NANOG -Dox ss.

Both the serum starved cell treatments had significantly less expression of ectopic *NANOG* than the induced non-starved treatment by two and seven orders of magnitude, respectively (EOG_TET_NANOG +Dox ss $P = 0.02$, EOG_TET_NANOG –Dox ss $P = <0.001$). Within the serum starved treatments the induced and non-induced treatment remains significantly different from each other ($P = 0.02$).

3.5.2 NANOG positive cells are present after serum starvation

The serum starved cells were stained for NANOG to see how the impact of serum starvation affected the ectopic NANOG on a protein level (Figure 29). The EOG_TET_NANOG cell line was thawed (section 2.2.4) into two tissue culture dishes containing glass cover slips. The cells were cultured in low serum media for 6 days of which the induced serum starved treatment was induced throughout. A serum starved non-induced treatment was a control. On day 4 a new vial of EOG_TET_NANOG cells was thawed and non-starved induced and non-induced treatments were made in standard cell culture media, of which the induced treatment was induced for 48 hours. Coverslips from all four treatments were

stained for the protein NANOG using the ICC protocol (section 2.2.14). A Donkey anti Rabbit Alexa Fluor® 488 (Green) secondary was used. Cells were co-stained for DNA with Hoechst. Images of the mCherry signal were also taken.

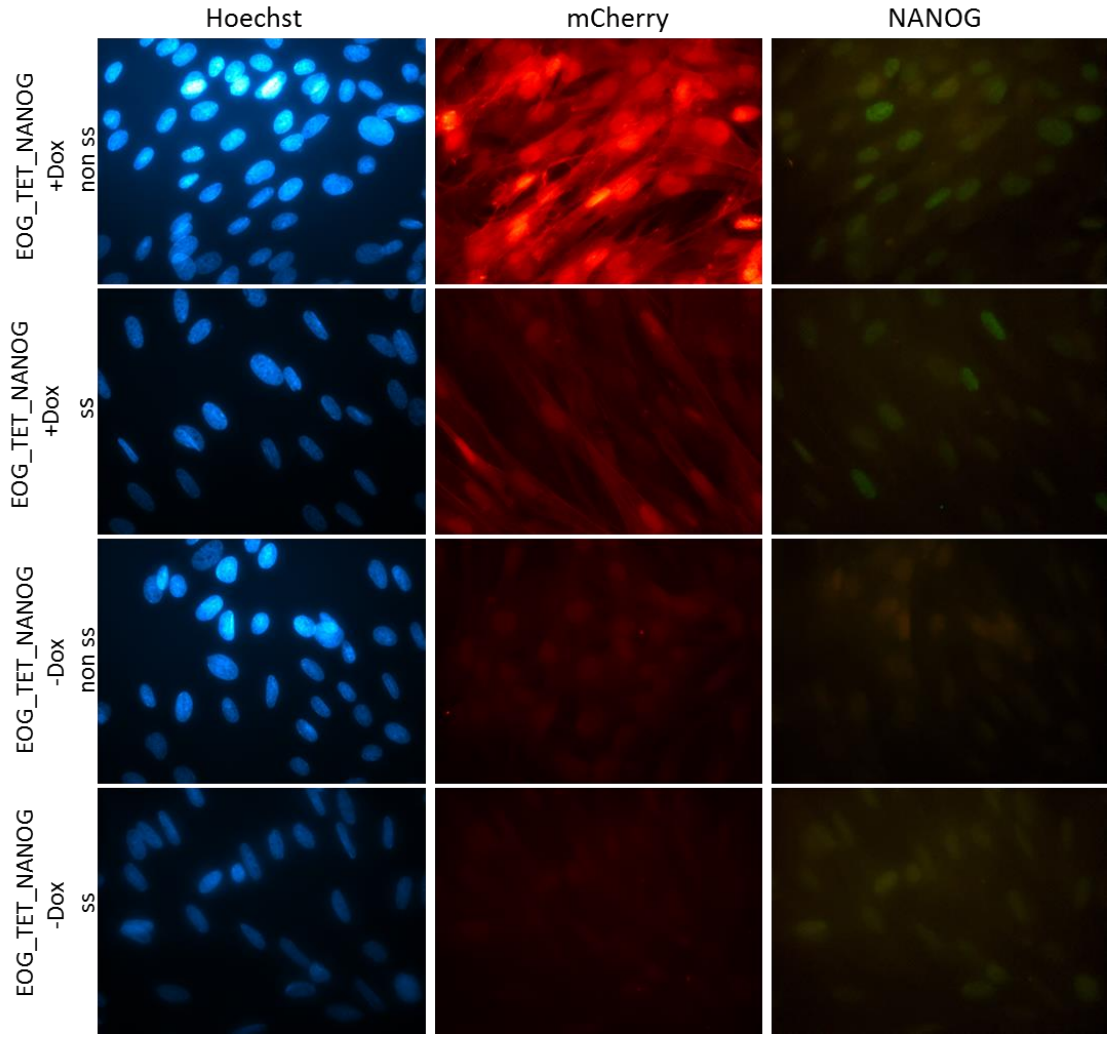

Figure 29: NANOG and mCherry protein show lower intensity of signal after serum starvation. ss denotes serum starved treatments. Blue and red images were pseudo coloured using ImageJ software. Green images were photographed in colour. Hoechst DNA stain (blue), mCherry signal (red) and NANOG indicated with Alexa Fluor 488 (green).

The NANOG protein is present in the induced serum starved treatment. However, the signal is weaker than what is seen in the induced non-starved treatment. A count of mCherry and NANOG antigen positive cells was conducted (Figure 30).

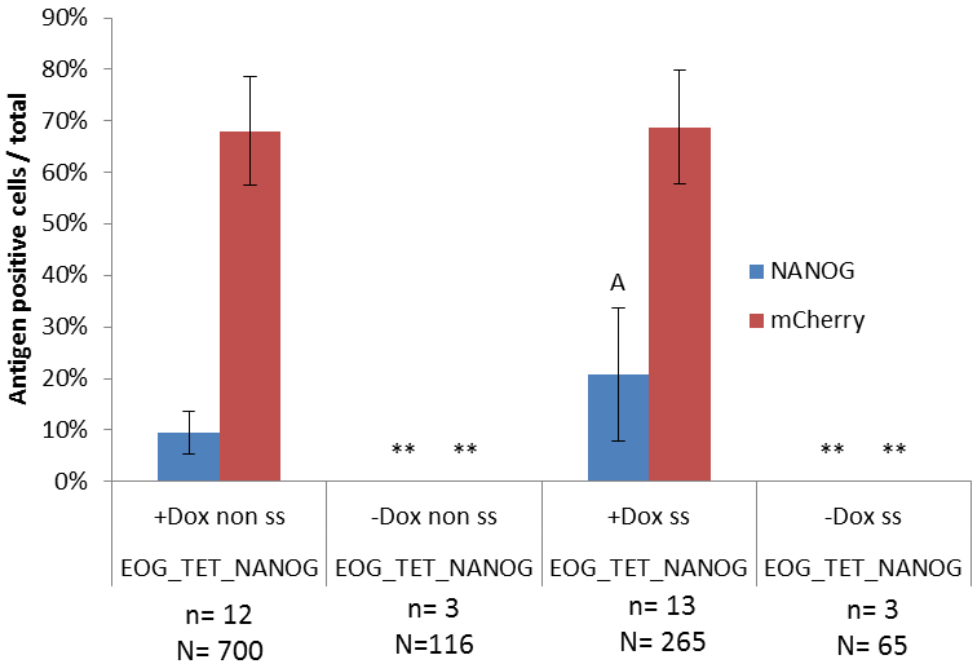

Figure 30: mCherry positive cells are not affected and NANOG positive cells increase by serum starvation over total cells. ss denotes serum starved treatments. Error bars represent ± SEM. Students t-tests were conducted to test significance ($P<0.05$). ** denotes $P<0.001$ from EOG_TET_NANOG +Dox equivalent treatment. A is significantly different from std +Dox (0.008).

There was around a 41 ± 17% survival rate in total cell number of the serum starved cells. When expressed as a percentage there was no significant difference between mCherry expression in the standard cell culture versus serum starved cells ($P = 0.862$). Also when expressed as a percentage the population of cells that are NANOG positive is significantly higher (0.008) in the serum starved cells than in the cells under standard culture.

3.5.3 Hygromycin resistance is doxycycline-inducible

In an attempt to enrich for mCherry positive cells, serum starved cells were cultured in hygromycin as this was the selection marker for the Tet system and should select for cells that contain it. Hygromycin was added to the serum starved cells at maintenance levels for the standard 6 day duration of serum starvation. A control was also prepared without hygromycin. Live images of this serum starvation culture were taken with the EVOS and can be seen in Figure 31.

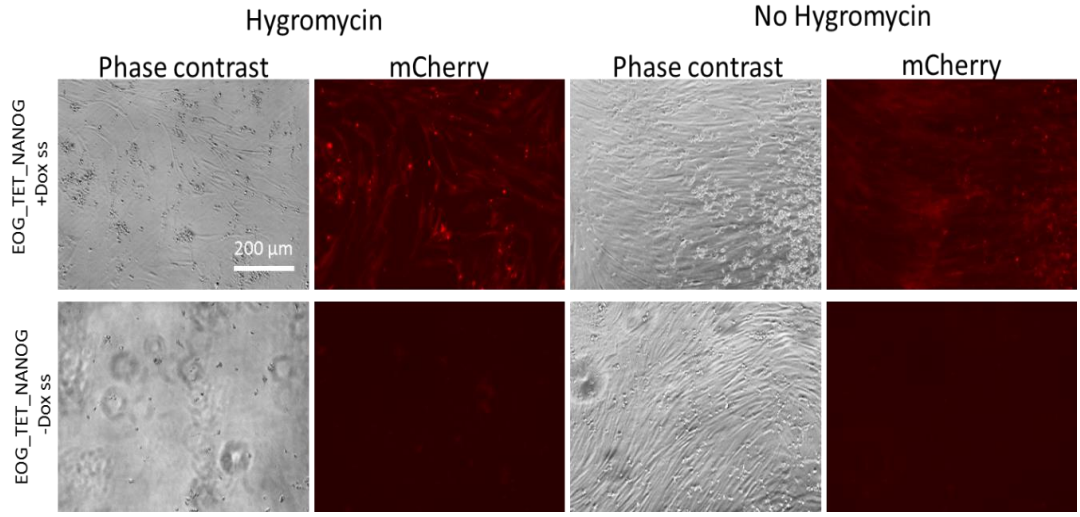

Figure 31: EOG_TET_NANOG –Dox ss has 100% mortality when cultured in hygromycin. ss denotes serum starved treatments. Live images of EOG_TET_NANOG +Dox ss and EOG_TET_NANOG –Dox ss cells treated with hygromycin with a no hygromycin control. Images taken on EVOS microscope.

Cells in the induced, serum starved, hygromycin treatment appear to have a more intense mCherry signal overall than those in the induced, serum starved, no hygromycin control. The non-induced hygromycin treatment had complete cell death where the non-induced no hygromycin treatment had a small percentage of death due to low serum conditions.

3.6 Characterisation of EOG_TET_NANOG NT embryos

There were 7 NT runs conducted on the EOG_TET_NANOG cell line after it was sorted against mCherry. The parameters for oocyte recovery and reconstruct numbers were the same as the NT runs conducted prior to FACS (Section 3.2). The development of embryos was recorded on day 7 and day 8 of each NT run using the grading protocol outlined in Appendix 4. The results of the blastocyst development can be seen in (Table 18 and Figure 33).

Table 18: Overexpression of NANOG has no effect on embryo development for day 8 embryos. [a] Embryos were cultured in medium containing doxycycline versus no doxycycline throughout embryo culture. N[b] number of independent runs. [C] Proportion placed into IVC (N) that developed into day 8 blastocysts grades 1-3 (B^{1-3}) [D] Proportion of all B^{1-3} that are B^{1-2}. Students t-tests were conducted (P<0.05).

Treatment [a]	n[b]	N	% Fused (% ± SD)	% B^{1-3} (% ± SD)[c]	% $^{B1-2}$ (% ±SD)[d]	Percentage (±SD) B^{1-2}/B^{1-3})
EOG_TET_NANOG +Dox	7	359	93.11 (±3.4)	36.53 (±18.4)	12.37 (±7.3)	7.75 (±18.6)
EOG_TET_NANOG -Dox	7	330	92.35 (±7.5)	42.15 (±11.1)	16.25 (±7.9)	.8 (± .5)

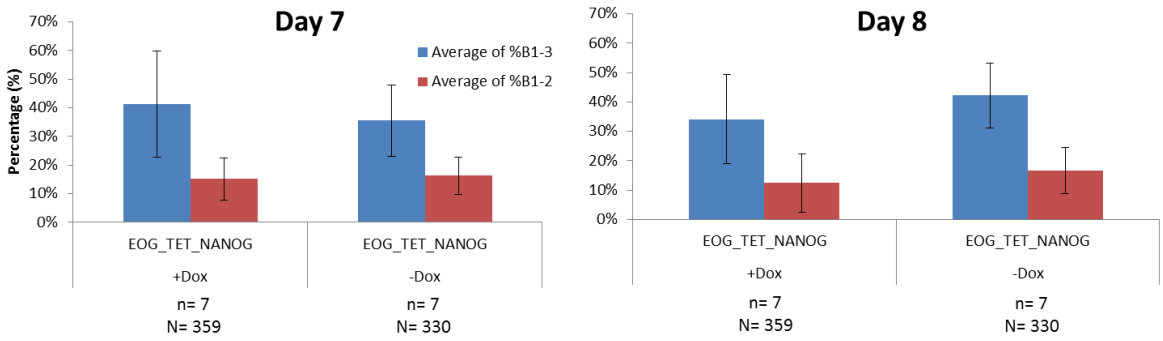

Figure 32: Blastocyst development for NT runs 1-7 of the EOG_TET_NANOG cell line on days 7 and 8. Grading criteria from Appendix 4 used. n= biological replicates, N= number of embryos analysed. Error bars represent ± SEM. Students t-tests were conducted to measure significance (P<0.05).

Over 7 consecutive NT runs there were no significant differences in development between induced and the non-induced treatments. There was also no significant difference in both treatments between day 7 and day 8 development. This is why only the day 8 data is presented in the table, as this is the developmental day in which this project is most interested. The mCherry and GFP data was recorded and embryos were graded using a fluorescence microscope, the embryo was recorded as positive if any cell within the embryo expressed mCherry or GFP (Figure 33).

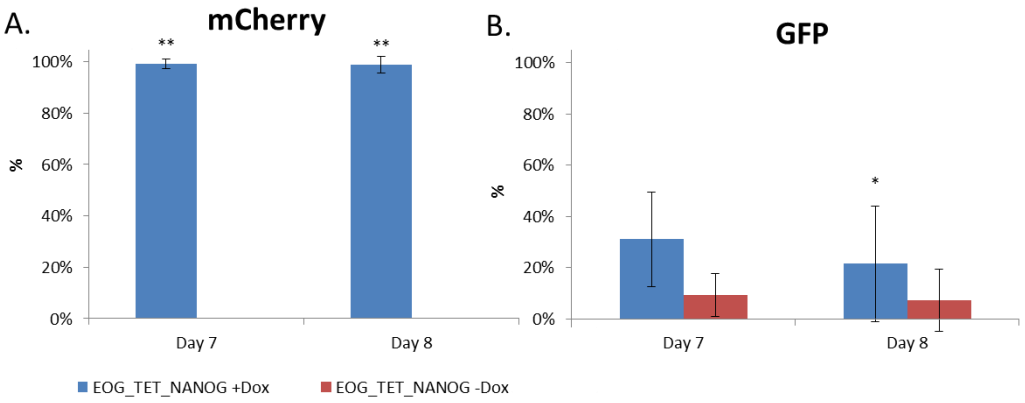

Figure 33: mCherry and GFP is higher than control on day 7 and day 8. n and N values (Figure 32). Visual analysis of mCherry and GFP signal. Error bars represent ± SEM. Fishers exact test was used to measure significance ($P<0.05$). * denotes significance $P<0.05$, ** denotes significance $P<0.001$ from control.

For mCherry expression on day 7 and day 8, induced treatment is significantly higher than non-induced. GFP expression was significantly higher in the induced treatment on day 8 ($P= 0.02$). This trend was also true on day 7. However, was not significant on this day ($P= 0.06$).

3.6.1 Significant increase in ectopic NANOG mRNA of FACS sorted NT embryos has no significant effects on pluripotency-related targets

The EOG_TET_NANOG NT embryos were analysed for ectopic *NANOG* expression in comparison to their endogenously expressed *NANOG*. Analysis of *XIST* was also conducted and the embryos were analysed for a series of pluripotency genes, to determine whether these were affected by the additional NANOG present. These were *SOX17*, *SOCS3*, *KLF4*, *FGF4*, *PDGFRα*, respectively (Figure 34).

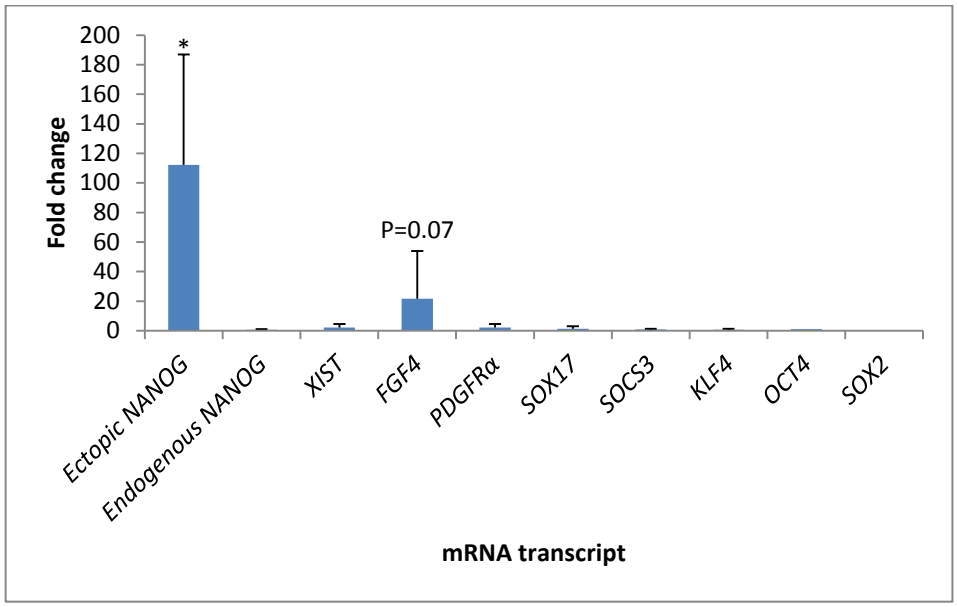

Figure 34: EOG_TET_NANOG embryos significantly overexpressed ectopic *NANOG* mRNA with no effects on pluripotency-related genes *XIST*, endogenous *NANOG, SOCS3, FGF4, PDGFRα, SOX17* and *KLF4*. Blastocysts (grades 1-2) derived from 7 NT runs, cultured with and without doxycycline were processed at day 8 via *RNA*GEM and cDNA synthesis in pools of 5-10 per sample. n= biological replicates N= number of embryos. EOG_TET_NANOG +Dox. n= 5 N= 33. EOG_TET_NANOG -Dox n= 7 N= 36.The values of target genes were normalised against *18S* in RU. These values were logged and averaged. Error bars indicate + SEM. Students t-test were conducted to measure significance ($P<0.05$). * denotes significance ($P = 0.05$)

The expression of ectopic *NANOG* showed a 100-fold significant increase in the induced against non-induced control ($P= 0.05$). Endogenous *NANOG* was not affected. *FGF4* was higher in the induced treatment by 20-fold but this was not significant ($P= 0.07$). *PDGFRα*, *SOX17*, *SOCS3*, *KLF4*, *OCT4* and *SOX2*, showed no difference between treatments. The absolute copy number of both ectopic and endogenous *NANOG* was calculated (Figure 35).

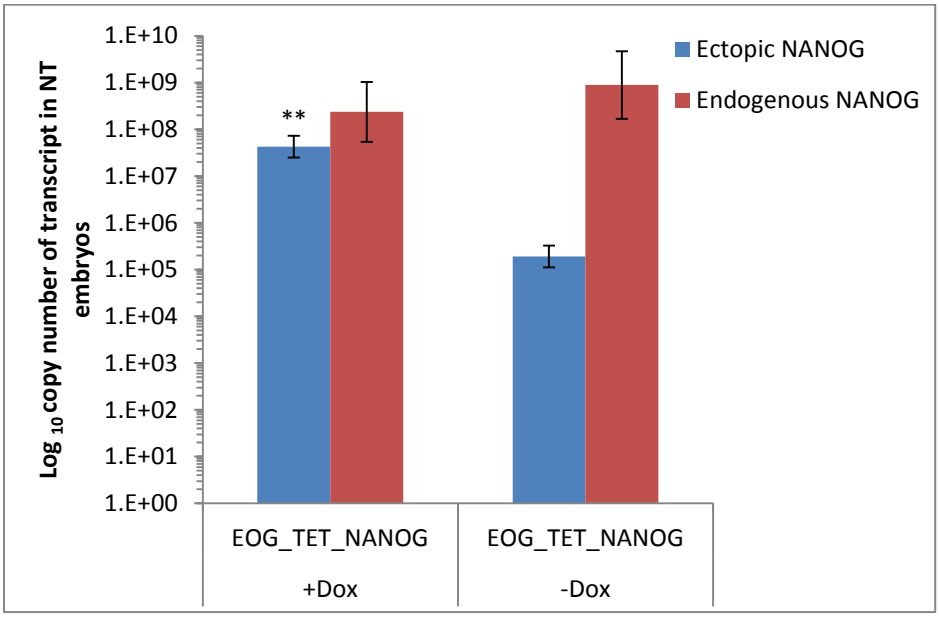

Figure 35: Copy number of endogenous and ectopic NANOG mRNA transcripts. Copy number was calculated using protocol outlined in section 2.2.11.1.4. Samples were normalised over embryo number. n= biological replicates n= number of embryos. EOG_TET_NANOG +Dox n= 3 N= 22 EOG_TET_NANOG –Dox n= 5 N= 27. Students t-test were conducted to evaluate significance. ** denotes P= <0.05.

For copy number analysis, there was no significant difference between induced and non-induced for endogenous *NANOG*. The ectopic *NANOG* was significantly higher in the induced treatment (P= 0.005). When combined, these two transcripts result in a two-fold increase in total *NANOG* expression.

3.6.2 Activation of the donor genome is initiated at day 3

Embryos were visualised throughout development and live images were captured on the EVOS microscope (Figure 36). Observations occurred on day 2, day 3, day 5, day 7 and day 8.

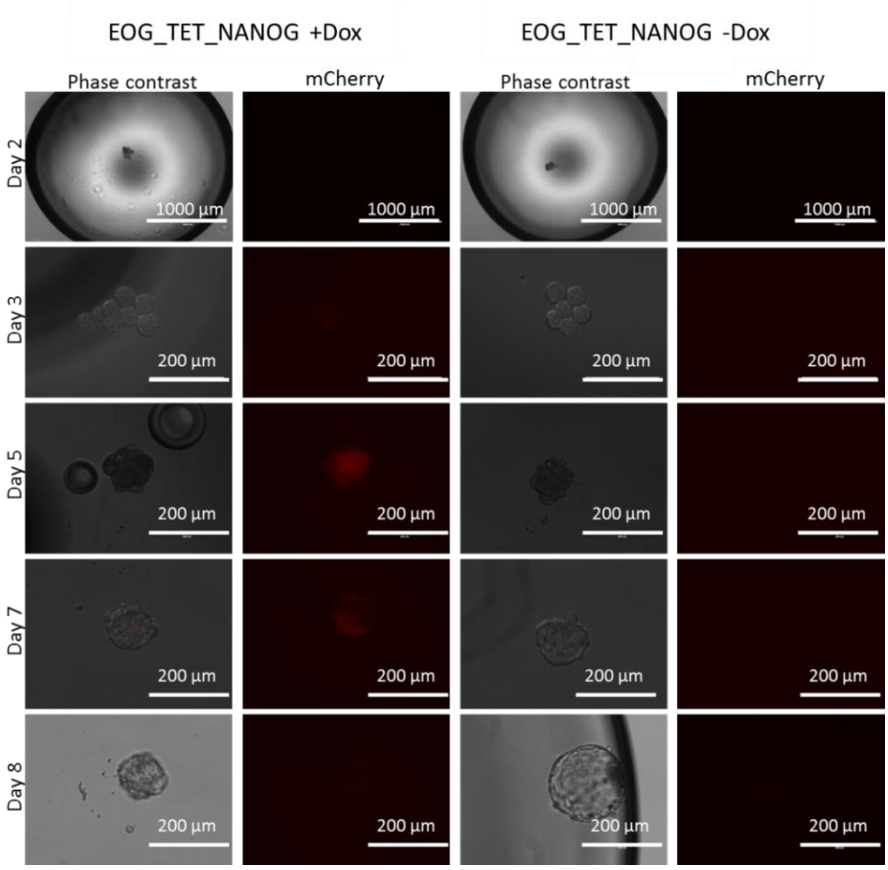

Figure 36: Live images of "+Dox" and "-Dox" embryos on days 2, 3, 5, 7, and 8 show activation of the donor genome at day 3. Images captured using EVOS microscope.

All non-induced embryos remained negative for the duration of culture. The mCherry signal only became visible on day 3 of culture and intensified from then on. All embryos were recorded for their GFP and mCherry expression throughout culture. This data can be seen in a bar graph (Figure 37).

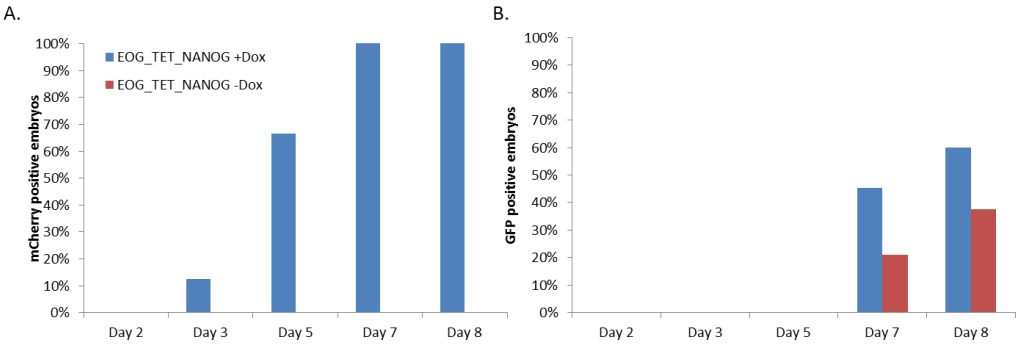

Figure 37: Bar graph of mCherry (A.) and GFP (B.) expression from day 2 to day 8 shown as a percentage (%) of viable embryos for NT run 7. n= biological replicates N= number of embryos. n= 1 EOG_TET_NANOG +Dox N= 10 EOG_TET_NANOG – Dox N= 18.

In the induced treatment the number mCherry positive embryos is 0% at day 2. Day 3 is the first day in which any mCherry positive embryo is visualised and at day 5 the percentage of positive embryos has increased. By day 7 the number of mCherry positive embryos is near 100% whereas no mCherry embryo is ever reported in the non-induced treatment. GFP is not observed up until day 7. The number of GFP embryos then increases at day 8 however, this difference is not significant (Figure 33). There is a significant increase in the induced and non-induced treatments for GFP expression on day 8 (Figure 33).

3.6.3 ICC for NT embryos could not detect increased NANOG protein although mCherry signal was detected throughout the embryo

Embryos from the first NT run were stained for NANOG using the ICC protocol (section 2.2.14). A Donkey anti Mouse Alexa Fluor® 488 (green) secondary was used for the secondary staining. Unfortunately, the stain was not successful but images of Hoechst and mCherry signal were captured.

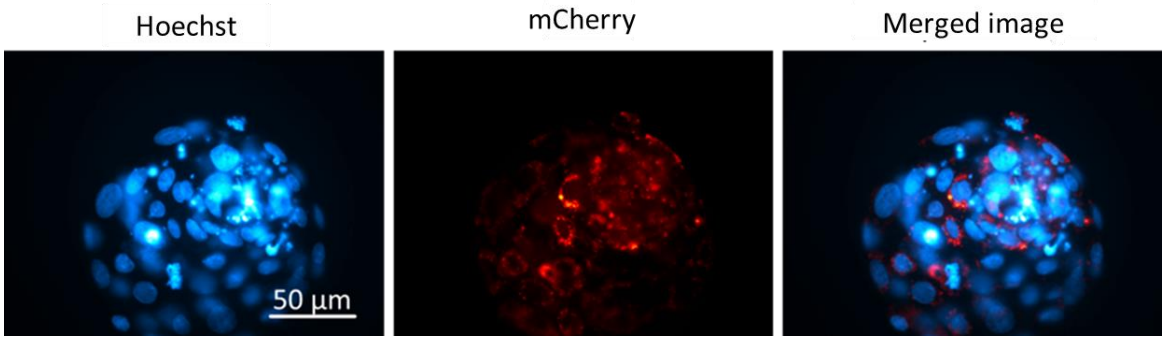

Figure 38: mCherry expression was visualised throughout the EOG_TET_NANOG + Dox embryo. Images were pseudo coloured using ImageJ software. Hoechst DNA stain (Blue), mCherry signal (Red) Merged image consist of mCherry and Hoechst merged channels using ImageJ software.

The mCherry signal is in the endoplasmic reticulum (ER) of the cell which is clearly seen in the merged image (Figure 38). The mCherry signal seems more intense in the inner cell mass but this may be an artefact of the ICM being a dense population of cells. Cells are positive for mCherry throughout the embryo.

3.6.4 mCherry analysis shows induction during serum starvation carries over into embryo culture

For NT run 2 cells were cultured with and without doxycycline and then were split into doxycycline and no doxycycline treatments during embryo culture. The first name of the treatment group relates to their treatment during serum starvation (+Dox or –Dox), the second name relates to their treatment during embryo culture (+Dox or –Dox). This was to see if there was any carryover of the mCherry signal from the serum starvation treatment into the embryo culture (Figure 39).

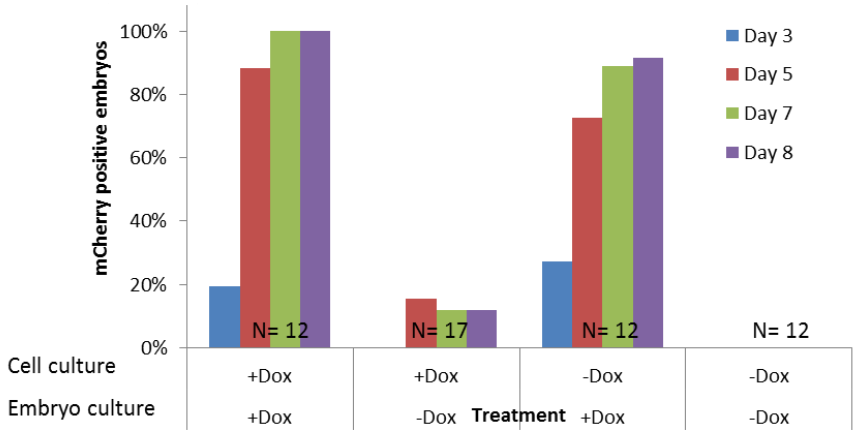

Figure 39: Carryover of mCherry from serum starvation induction. Column graph of percentage of mCherry positive embryos for four treatments in NT run 2. n= 1

Initially, mCherry signal was not detected in either population of embryos cultured without doxycycline. On day 5, there were positive embryos in the "+Dox, -Dox" treatment and still none in the "-Dox, -Dox" treatment. On day 3, the "+Dox, +Dox" treatment has a higher number of mCherry positive embryos but this trend is remains throughout embryo culture.

Embryos from NT run 2 were co-stained for NANOG with an Donkey anti Mouse Alexa Fluor® 488 (green) secondary and SOX2 with a Donkey anti Goat Alexa Fluor® 568 (red) secondary. They were also stained for DNA with Hoechst. A composite image of all three stains was compiled (Figure 40).

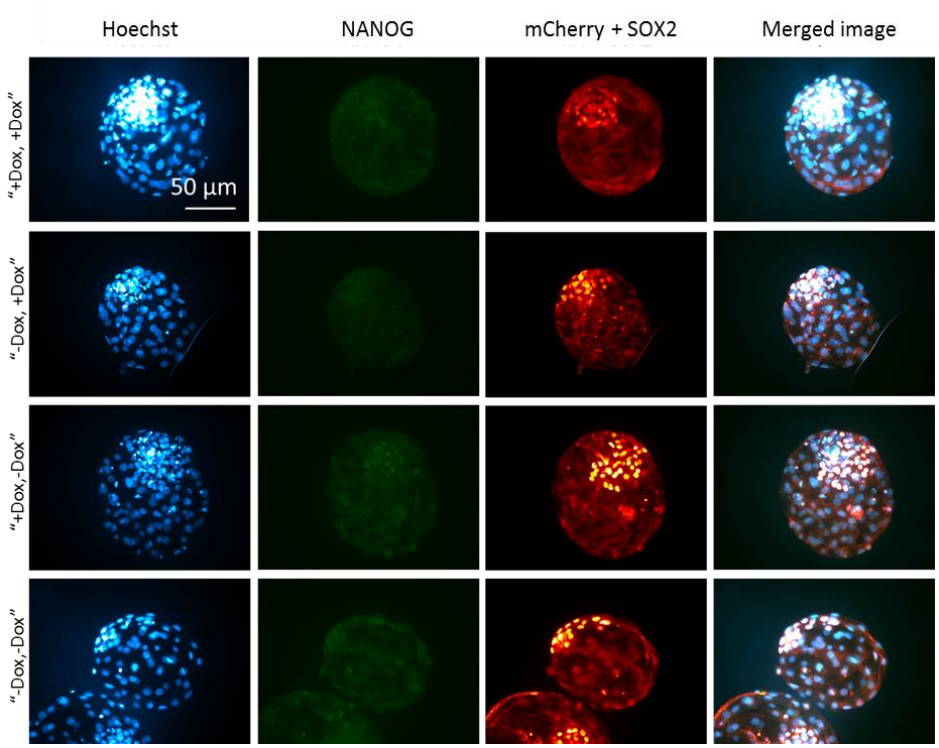

Figure 40: Representative embryos for all treatments from NT run 2 ICC for NANOG and SOX2. Images were pseudo coloured using ImageJ software. Hoechst DNA stain (blue), NANOG stain with Alexa Fluor 488 (green), SOX2 stain with Alexa Fluor 568 and mCherry signal (red), composite image compiled by merge channels using ImageJ software.

The green NANOG stain was not well defined and it was hard to determine a positive cell. NANOG cells were counted in a blind assay of three embryos per treatment. There were no significant differences between the treatments for the NANOG signal. The SOX2 stain worked well and is a good indicator for the number of ICM cells within the embryo (Figure 41). However, it did mask the mCherry signal which could not be analysed after this staining.

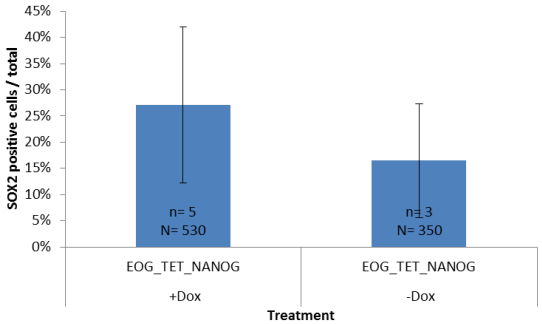

Figure 41: SOX2 is not affected by NANOG overexpression. Students t-tests were conducted to measure significance ($P<0.05$). Error bars represent ± SEM.

There was no significant difference between the "+Dox, +Dox" and "-Dox, -Dox" treatments for SOX2 positive cells.

3.6.5 GFP positive and GFP negative segregated embryos do not show different mRNA expression from pooled embryo analysis

Once it had been identified that there was a significantly higher number of GFP positive embryos in the induced embryos, the GFP positive embryos were kept separate from GFP negative embryos for qPCR analysis (Figure 42).

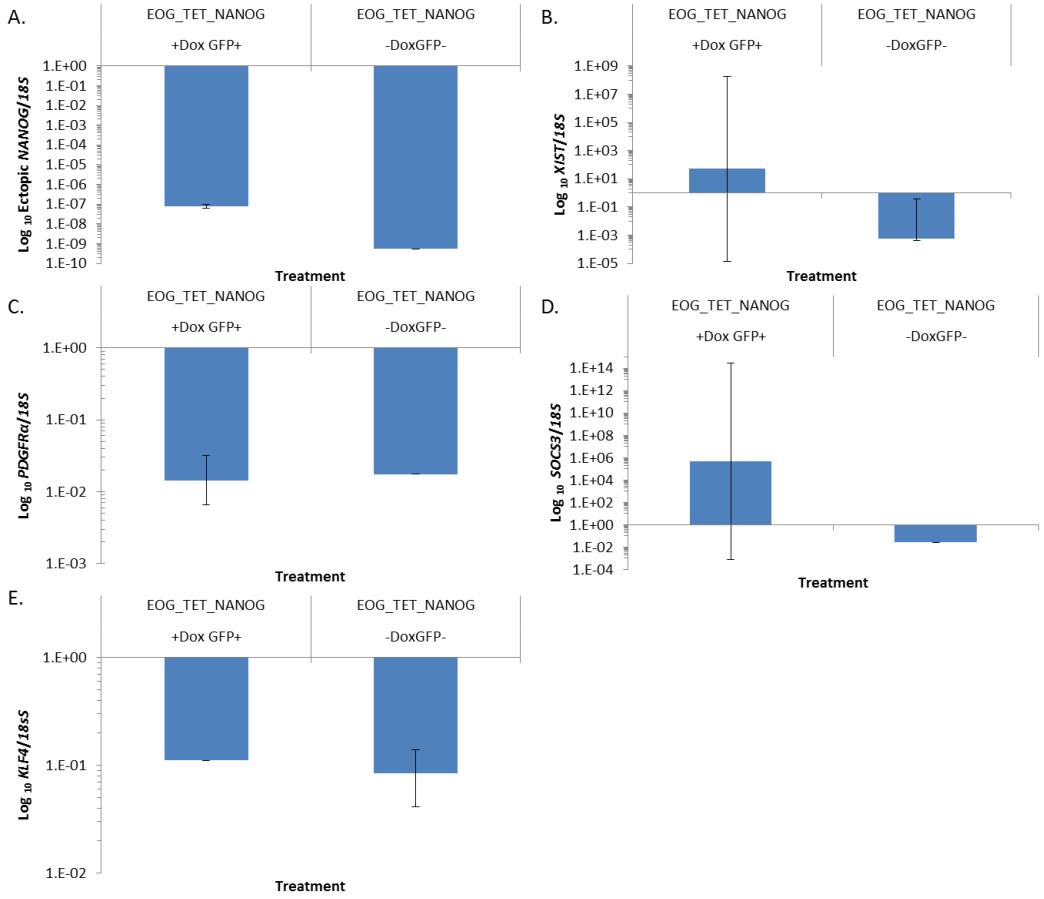

Figure 42: Analysis of cDNA of EOG_TET_NANOG +Dox separated into GFP positive and GFP negative treatments do not show differences in mRNA expression from pooled embryo analysis. cDNA was extracted from day 8 EOG_TET_NANOG +Dox GFP positive embryos and EOG_TET_NANOG +Dox GFP negative embryos in pools of 2-3 blastocysts per cDNA sample. n= biological replicates N= number of blastocysts. EOG_TET_NANOG +Dox GFP positive n=2 N= 8 EOG_TET_NANOG –Dox GFP- n= 2 N= 7. Target gene values were normalised against *18S* expression in RU. Results were logged and averaged. A. Ectopic *NANOG*, B. *XIST*. C. *PDGFRα*. D. *SOCS3* E. *KLF4*.

Unfortunately, this was only achieved in NT runs six and seven, meaning there were not enough samples for any statistical analysis. As a trend, there is two orders of magnitude lower expression of ectopic *NANOG* in the GFP negative embryos. No induced GFP negative embryos were able to produce an endogenous *NANOG* signal and could not be graphed. There was a higher expression of *XIST* in the GFP positive embryos by four orders of magnitude Figure 42 (B). *SOCS3* Figure 42 (D) was lower in the GFP negative treatment by eight orders of magnitude where *KLF4* and *PDGFRα* were similar between the two treatments Figure 42 (C and E).

Chapter 4: **Discussion**

4.1 **Introduction**

The aim of this research study was to investigate the role of *NANOG* overexpression and its effects on pluripotency-related genes, and X-chromosome inactivation in bovine fibroblasts and fibroblast derived NT embryos. The Tet-On 3G system was selected to induce this overexpression of *NANOG*. This system successfully overexpressed the ectopic *NANOG* sequence compared to controls in fibroblast and NT embryos. However, in terms of absolute copy number the increase was not sufficient to produce an effect on the eight pluripotency-related genes investigated or on the inactive X-chromosome.

4.2 **Objective 1: Investigation of the effects of overexpression of *NANOG* on pluripotency-related genes.**

4.2.1 Effects of NANOG overexpression on endogenous NANOG, OCT4, and SOX2 in fibroblast.

Previous studies in which *Nanog* was overexpressed within a pluripotency network have been conducted in other species such as pig [115]. In the research conducted for this thesis, a significant increase in ectopic *NANOG* was achieved in the induced treatment, compared to the non-induced EOG_TET_NANOG and EOG_TET controls by four and ten orders of magnitude, respectively (Figure 17). This held true when converted into absolute copy number where the induced EOG_TET_NANOG was significantly higher than the EOG_TET_NANOG and EOG_TET non-induced controls by five and ten orders of magnitude (Figure 18). Non-induced EOG_TET_NANOG was five orders of magnitude higher than the non-induced EOG_TET control.

Analysis of *OCT4* and *SOX2* via qPCR found that these were not affected in the fibroblasts (Figure 17). These results are in disagreement with a study which showed that porcine foetal fibroblasts transfected with *NANOG* overexpression vectors resulted in a five-fold increase in *OCT4* expression [115]. This may be because the absolute amount of *NANOG* that was produced pTRE3G-mCherry vector is insignificant to what is required to stimulate the pluripotency network. The increase of *NANOG* expression in the porcine study was 2000-fold higher

than that of the control. At this level of expression a morphology change was seen when the cells became round and small [115]. This observation was not identified during induction of the EOG_TET_NANOG cell line (Andria Green, unpublished data). The increase seen in this study could have been greater than that achieved here, unfortunately the porcine paper did not present copy number data and was therefore not comparable. An alternative theory is that the bovine fibroblast may have a stronger mechanism for maintaining its differentiated state than that of an ICM cell or porcine foetal fibroblast.

When the EOG_TET_NANOG cell line was originally FACS sorted for the mCherry signal, the resulting cell line was found to be 98% mCherry positive. When these were analysed via ICC it was found that the expression of mCherry was not homogeneous and there were only 55 ± 9 % mCherry positive cells (Figure 19 and Figure 20). The cell line analysed here is the same as what was initially tested after FACS, yet gives a lower level of mCherry positivity. This is theorised to be a result of the difference in technique as FACS can detect those cells that are only mildly positive for mCherry that the eye would ignore. It was also found that there were 58 ± 15% NANOG positive cells which were expressed heterogeneously. This difference between the two proteins is not significant but does show a discrepancy. NANOG is a quickly degraded protein which has a half-life of 120 minutes [44] which could cause NANOG to be misrepresented in the ICC analysis. This would suggest that the actual number of cells able to produce ectopic *NANOG* is higher than what was observed. In conclusion to this, NANOG is present in the fibroblast cell line in the induced treatment and is absent in the non-induced controls, though ICC is not an accurate quantitative measure of detecting NANOG or mCherry positivity. Investigation needs to be conducted into the homogeneity of the cell line.

4.2.2 Ectopic NANOG expression in serum starved fibroblast

The process of serum starvation does result in mortality of the cells. The EOG_TET_NANOG cell line survived serum starvation at a rate of 41 ± 17%. The cells also flattened as they transitioned into the G_0 cell cycle phase (Andria Green, unpublished data). The induction of NANOG did not affect the morphology of the cells during standard serum starvation conditions (Andria

Green, unpublished data). During the qPCR analysis of the serum starved cells it was found that there was significantly less ectopic *NANOG* in the induced serum starved treatment as opposed to the induced non-starved treatment by two orders of magnitude (P= 0.02) (Figure 28). This was expected as it has been characterised that cells in quiescence after serum starvation carry out less transcription and translation [131,132]. Although it does decrease the signal upon mRNA analysis, it is theorised that this decrease is homogenous throughout the population and does not actually decrease the percentage of cells that are capable of producing ectopic *NANOG*. Instead it decreases the amount each cell is capable of producing, overall lowering the total amount of ectopic *NANOG* in the cDNA sample.

This was confirmed in the ICC analysis of the serum starved versus non-starved cells (Figure 29). Both induced starved and induced non-starved treatments contained 68 % mCherry positive cells, which showed that the percentage of cells capable of transcribing the pTRE3G-mCherry vector was not changed by the serum starvation treatment. Unexpectedly, when expressed as a percentage the NANOG positive cells increase significantly after serum starvation. This may be because the process of serum starvation causes a large proportion of cell death. It may be that the cells that survive starvation treatment were those that were in a better condition and were therefore more likely to successfully transcribe and translate the pTRE3G-mCherry vector sequence. Overall, it was shown that the fibroblasts were able to successfully transcribe and translate the vector sequence under serum starvation conditions. This validates the cells in their use in NT cloning.

4.2.3 Effects of hygromycin selection on serum starved fibroblast

In an attempt to increase the number of NANOG positive cells within the EOG_TET_NANOG cell line under induction, the cells were cultured with the antibiotic hygromycin during serum starvation. It was thought that all transfected cells would contain hygromycin resistance, regardless of induction. Induced and non-induced treatments were expected to have some cell death as a result of the serum starvation and also a percentage of death from the presence of hygromycin. However, it was found that the cells in the non-induced treatment under

hygromycin selection had a 100 % mortality rate (Figure 31). This was unexpected as although the hygromycin resistance plasmid would have integrated into the same locus as the pTRE3G-mCherry plasmid, it should have not been doxycycline-inducible. Both hygromycin resistance and pTRE3G-mCherry plasmids contain the SV40 promotor. It was hypothesised that the induction of the pTRE3G-mCherry plasmid had a wider control of the entire locus, resulting in an inducible hygromycin resistance.

4.2.4 NANOG's effect within the NT embryo

It was hypothesised that the overexpression of *NANOG* would interact within the pluripotency network and would promote the pluripotency triumvirate *SOX2*, *OCT4* and *NANOG* itself. *NANOG* has a feedback loop in which it can promote or suppress its own expression. With the primers for ectopic and endogenous *NANOG* it was possible to analyse whether this feedback loop was stimulated by the ectopic *NANOG* causing expression or suppression of endogenous *NANOG*. It was also hypothesised that the additional NANOG would interact with other targets such as *SOX17*, *PDGFRα*, *FGF4*, *SOCS3*, and *KLF4*.

When the new series of NT experiments were conducted after FACS, the timeframe of the activation of the donor genome was investigated. This was easily monitored by the mCherry signal. On days 2, 3, 5, 7 and 8, all induced and non-induced embryos were visualised for their mCherry signal (Figure 36). The non-induced treatment remained negative for mCherry throughout the 8 days. The induced treatment was initially found to be mCherry negative on day 2 (4 cell). At day 3 (8 cell), the mCherry signal began and strengthened until it was its most intense signal at days 7 and 8 (blastocyst). This is consistent with literature showing that after fertilisation the oocyte carries out all transcription and translation until day 2 where it activates the donor genome [133]. However, it is still possible that residual mCherry produced during serum starvation could be concentrated during cleavages until it becomes visible on day 3 (8 cell) and then increases in strength with each cleave. To disprove this possible theory that the mCherry signal in the induced treatment could be residual from the induction during serum starvation, NT run 2 was conducted.

For the purposes of these experiments, the first name of the treatment group relates to their treatment during serum starvation (+Dox or –Dox), the second name relates to their treatment during embryo culture (+Dox or –Dox). The "+Dox, -Dox" treatment had low levels of residual mCherry expression throughout embryo culture; this was seen in less than 15% of embryos from days 3-8 (Figure 39). The "+Dox, +Dox" treatment had greater than 80% positive embryos from day 3 and by day 8 this was 100%. The "-Dox, +Dox" embryos were positive for mCherry at nearly the same rates as "+Dox, +Dox" (91% at day 8) which shows that this signal could only have been produced during embryo culture. To conclude, there is some signal that remains from induction during serum starvation but that the embryo is capable of producing mCherry.

The mCherry signal within the embryo was photographed in comparison to a DNA stain in Figure 38. When comparing that image to the images taken of the analysis of the fibroblast cells, some differences were observed. In the fibroblasts, mCherry signal was very strong in the nucleus and weak in the cytoplast (Figure 19) whereas the embryo's mCherry signal is absent from the nucleus and is highly concentrated in the ER (Figure 38). The results from NT run 2 show that the embryo is capable of producing mCherry during embryo culture. These images indicate that the mCherry protein is processed differently within the cells of the embryo compared to the fibroblast.

The developmental data of each EOG_TET_NANOG NT run was recorded and analysed. It was a possibility that the additional NANOG may increase the quality of embryos or the absolute numbers by helping them reach a naïve pluripotent state more easily. Alternatively, additional NANOG may have a detrimental effect on the embryo. NANOG is usually isolated to the ICM and cells of the trophoblast expressing NANOG may be incapable of normal formation. It was found that there was no significant difference between the induced and non-induced treatments in blastocyst number or quality (Figure 32 and Table 18). This indicates that the culture in doxycycline does not have an effect, which has been seen in previous studies [134]. It also means that the additional NANOG did not

have a beneficial or detrimental effect on the embryos development. This was also seen in the overexpression of *NANOG* in porcine [115].

In the NT embryo, when comparing just the expression of ectopic *NANOG* there was a 100-fold significant increase in the induced treatment compared to the non-induced control (Figure 34). However, when the copy number of endogenous *NANOG* and ectopic *NANOG* were calculated, the scale of the additional total *NANOG* was illuminated. The total amount of additional *NANOG* produced was increased at physiological by two-fold (Figure 35). This is comparable to what is seen when the bovine embryo was cultured in 2i, which saw a two-fold *NANOG* increase [37,38]. With the increase in total *NANOG* achieved here it could be assumed that a similar effect to 2i culture may result.

Using ICC, there was no clear NANOG staining of any NT embryo examined (Figure 40). Of the stainings that were achieved, there was no significant difference between induced and non-induced treatments. A successful SOX2 staining was conducted (Figure 40). SOX2 identifies the cells of the ICM [135]. With additional NANOG, it could be possible to observe an increase in the number of SOX2 positive cells by increasing the size of the ICM. This would indicate that the additional NANOG has interacted with the pluripotency network to increase its function. Results showed that there was no significant increase in the induced treatment in the number of SOX2 positive cells. This correlates with the qPCR data.

When the analysis of ectopic *NANOG*s was conducted it was found that there was no effect on the expression of endogenous *NANOG* (Figure 34). It was not suppressed nor was it up-regulated in the induced treatment compared to control. This indicates that the additional *NANOG* from the pTRE3G-mCherry vector does not stimulate or supress the feedback loop for endogenous *NANOG*. In addition, when *OCT4* and *SOX2* were investigated it was found that there was no effect on their expression (Figure 34). When *NANOG* was overexpressed in porcine embryos the NANOG was able to up-regulate the expression of endogenous *NANOG*, *SOX2* and *OCT4* [115]. This supports the theory that the increased

NANOG produced here, is either incapable of stimulating the function of the core pluripotency network or is too insignificant.

Pdgfrα and *Sox17* are markers differentiation and for the hypoblast [117,118]. These markers were hypothesised to decrease in expression after exposure to increased NANOG as the additional NANOG may decrease the size of the hypoblast [37]. After qPCR analysis of seven NT cDNA samples per treatment, it was found that there was no significant difference between the induced and non-induced treatments for both genes (Figure 34). This indicates that the increased NANOG did not have an effect of the fate of the cells. It could not prevent them from differentiating into hypoblast. This does not correlate with recent bovine studies where the use of 2i increased NANOG two-fold, and also down-regulated both *SOX17* and *PDGFRα* [37]. This could be a flow on effect from what is seen in the analysis of endogenous *NANOG, SOX2* and *OCT4*. Since the core pluripotency network was not affected it is unlikely that pluripotency-related genes would be effected either.

Klf4 binds directly to the promotor region of *Nanog* [116] and is one of the four factors required in the dedifferentiation of cells used in iPS cell generation [28,29]. It was theorised that the increase in NANOG would increase the expression of KLF4. However, it was found that there was no difference between the induced and non-induced treatments for *KLF4* expression (Figure 34). This again may be because of a lack of ability to increase the NANOG protein, ultimately making it impossible to increase NANOG function. Socs3 is a differentiation marker that negatively regulates the LIF pathway [120]. It is down-regulated by Nanog and results in an enhanced LIF signal transduction. Therefore, with the additional NANOG a decrease would be expected in SOCS3 expression. Yet like all other pluripotency-related genes investigated here, there was no change in SOCS3 expression between the induced and non-induced treatments (Figure 34).

The only gene investigated which did show a difference between treatment groups was *FGF4* (Figure 34). This was higher in the induced embryos by a 20-fold

increase compared to non-induced control. However, this was not significant (P= 0.07). This does correlate with 2i effects on bovine embryos where both *NANOG* and *FGF4* were up-regulated simultaneously [37]. This does indicate that there may be a effect of additional NANOG protein within the embryo, although.

There were a high proportion of GFP positive embryos in the induced treatment in comparison to non-induced control on day 7 of embryonic development. By day 8 this difference became significant (P= 0.02) (Figure 33). It was then theorised that those embryos that were successfully producing a large amount of ectopic *NANOG* were switching on the OCT4-GFP reporter system from the parental line EOG. GFP positive embryos were then analysed separately from GFP negative embryos. Due to time constraints, not enough NT runs could be conducted to produce the samples required for statistical analysis. However, some preliminary analysis was still conducted. When analysing the trends seen in the column graphs of Figure 42, the expression of ectopic *NANOG* does not change compared pooled GFP positive and negative samples. The endogenous *NANOG* could not be detected in the induced GFP negative embryos, which could be an interesting insight into their pluripotent state. There was an increase by four orders of magnitude in *XIST* and in *SOCS3* by eight orders of magnitude in GFP positive embryos compared to GFP negative controls. There is no change between the two treatments in the analysis of *PDGFRα* or *KLF4* (Figure 42) which indicates that the outer pluripotency network is again not affected. Although this data is not yet conclusive due to sample size, it does indicate that the theories of the OCT4-GFP reporter being stimulated by the additional NANOG are not valid.

In the experiments conducted for the purposes of this thesis, the mCherry signal was near 100% in induced embryos on day 8. This means that the pTRE3G-mCherry sequence was active in all embryos analysed. It has also been conclusively proven the mRNA of the total overexpression of *NANOG* was two-fold. What was unclear was whether the NANOG protein was overexpressed. The pTRE3G-mCherry vector construct encodes *mCherry* before *NANOG* (Figure 8). It has been identified that there are some issues with the IRES system, in that, it may fail to initiate separate protein production resulting in fusion proteins [136].

It can also cause unpredictability in the expression of the vector [136]. It may be possible that some mCherry positive embryos are not efficiently transcribing the NANOG section of the vector sequence. This would be the reason why the qPCR data indicates a significant overexpression of ectopic *NANOG* where no additional NANOG protein has been identified via ICC (Figure 40). This may be the cause the of lack of effect. The two effects identified in the induced embryos are the significantly increased GFP signal and the increase in *FGF4* expression which is not significant (P= 0.07). If the NANOG protein is not efficiently translated this may be the reason for such mild effects. Conclusive evidence for the overexpression of the NANOG protein needs to be achieved to verify if the NANOG protein is sufficiently overexpressed by the Tet-3G vector system.

4.3 Objective 2: NANOG's effect on *XIST* expression

It was also theorised that *NANOG* would have an effect on *XIST*. During the development of pluripotency in mouse, *Nanog* down-regulates *Xist*. It was proposed that this would hold true in the bovine system and would decrease the level of *XIST* detected via qPCR analysis. It could extend the period of double X-chromosome activation as well as potentially improving the removal of the *XIST* cloud.

When *XIST* was analysed via qPCR of eight cells lines, it was found that the female cell lines had significantly higher *XIST* expression in comparison to two male controls (Figure 24). *XIST* was found not to decrease in the presence of increased NANOG, which is not usually present within the fibroblast system. The induced treatment did not have significantly less *XIST* expression than the other female cell lines and remained significantly higher than the male controls. This shows that the additional NANOG achieved in these assays in the induced treatment does not down-regulate *XIST* in the fibroblasts at any measurable level. This may be because the X-chromosome dosage compensation is required to such a high level that the mechanisms that hold the inactive X-chromosome in place within the fibroblast are much stronger than that of the ICM.

There were many difficulties encountered during the analysis of *XIST* expression, many of which were a result of the fact that *XIST* is a lnc-RNA. There have been

many instances in which teams have achieved successful staining of *Xist* using techniques such as RNA *in situ* hybridisation and a standardised protocol in human pluripotent stem cells has been established [137]. Successful assays have also been achieved in bovine [130]. For the purposes of this research the ViewRNA^{TM} ISH Cell Assay for RNA FISH kit was used [138]. This technique had high sensitivity and could bind to a single RNA molecule. It also had the ability to perform multiplexing which was essential for these assays as the localisation of *NANOG* and *XIST* was required simultaneously. The positive controls provided by the kit produced some colour signal after conducting some preliminary experiments, but no signal was detected for the bovine cell line samples after multiple attempts. This method was then excluded from potential *XIST* visualisation options for the purposes of this thesis.

There are a number of protein stains that can evaluate the inactive X-chromosome. An Eed stain was conducted by Professor Austin Smith's team to produce the embryo images seen in Figure 5 [31] . Eed is a component of the Eed-Enx1 Polycomb group complex, which *Xist* recruits to attain methylation markers on the inactive X-chromosome [54], therefore staining for the Eed protein achieves a proxy stain to the inactive X-chromosome [31]. However, this method was not available as previous experiments conducted using this antibody showed that the Eed antibody did not reliably co-react with the bovine protein (Prasanna Kumar Kallingappa, Unpublished data). Instead, an equally valid $H_3K_{27}me_3$ staining was attempted. This also identifies the inactive X-chromosome as the *Xist* cloud collaborates the epigenetic silencing of the inactive X-chromosome through the use of methylations such as $H_3K_{27}me_3$ [55]. Because of this, $H_3K_{27}me_3$, although present throughout the nuclei is highly concentrated around the inactive X-chromosome [55].

The ICC assay has been successfully achieved in human and bovine for $H_3K_{27}me_3$ as a good proxy stain for the inactive X-chromosome [130]. In studies previously conducted in this group, this assay was successful using a specific antibody that recognises only one epitope of $H_3K_{27}me_3$ [139]. This polyclonal antibody was a finite resource and was no longer available by the time this project commenced.

Instead, two commercially available antibodies were analysed. Both of these produced a positive signal throughout the nuclei but neither were successful in the identification of the inactive X-chromosome (Figure 25)(Only the data of one antibody was presented). This assay was conducted on the induced and non-induced treatments of the EOG_TET_NANOG cell line. A series of controls were also run of confirmed female and male cell lines (section 3.4.1) this included the two parental cell lines, of EOG_TET_NANOG, EOG_TET and EOG as well as two unrelated female cell lines, LFC2 and EFC1B, and an unrelated male cell line, LJ801. The results of the staining showed some potential inactive X-chromosomes (Figure 26). Counting analysis of these potential inactive X-chromosome $H_3K_{27}me_3$ "clouds" showed that the female cells did not have significantly higher number of "clouds" than the male control group (Figure 27). This indicates that the spots which were thought to potentially be inactive X-chromosomes were just an artefact of the stain. Throughout this project there was never a confirmed inactive X-chromosome. This may be a result of the cell line used. After a review of the literature, it was confirmed that no studies have been conducted on fibroblasts as most are investigating the inactive X-chromosome were within the ES cell or embryo. It could be possible that the inactive X-chromosome is not present in the fibroblast.

XIST does not only interact with NANOG, it interacts with the entire pluripotency network [46]. It was hypothesised that the additional NANOG would be able to decrease *XIST* in the NT embryo, but for this to have been achieved an increase of the core pluripotency network may have been required. When *XIST* was investigated using qPCR in NT embryos it was found that *XIST* was not down-regulated by the additional NANOG (Figure 34). This was not surprising as the core pluripotency network (OCT4, SOX2 and endogenous NANOG) was not stimulated. When the NT embryos were separated into GFP positive and GFP negative embryos for qPCR analysis the trend seen in *XIST* expression did not change. NANOG does have a direct interaction with *XIST* and may be able to supress *XIST* on its own. However, it remains unclear how much additional NANOG protein was achieved in these assays and it may be possible that the

additional protein was incapable and/or too insignificant to produce a functional change.

4.4 Efficiency of the Tet-On-3G system

The Tet-On 3G system was the system selected for overexpression. One reason this system was chosen was its capability to be turned on or off in the presence or absence of doxycycline. This was essential for use in the embryo as it meant the transgene could be controlled temporally. The decision was made to induce throughout embryo culture after previous experiments (data not shown) had determined no effect on the time of induction.

There have been a number of instances in which the Tet-On 3G system has been used in fibroblasts and in NT embryos. In 2006, a proof-of-principle experiment was conducted in porcine [134] using a vector sequence containing enhanced GFP. The aim of this study was to show that a gene that may be detrimental to cells, or early embryos at different stages could be switched on or off depending on what was required. This experiment proved that the system could be controlled very tightly temporally, although there was some leaky expression which they could not control [134]. They suggest improvements to the leakiness of the system without compromising the expression of the gene of interest. In the analysis of the EOG_TET_NANOG fibroblasts there was a significant increase in expression in the non-induced EOG_TET_NANOG treatment when compared to EOG_TET. This suggested that the leaky expression of this system was still a problem. It may mean that the non-induced control was not a sufficiently silenced comparison for gene regulation in the NT embryo and that an EOG_TET NT embryo would be a more reliable control. It is also crucial that characterisation of the NANOG protein levels within the NT embryo occurs, as there is no evidence that NANOG protein was overexpressed.

4.5 Conclusion

In conclusion, the Tet-On 3G system could produce a significant increase in the expression of ectopic *NANOG* in bovine fibroblasts by four orders of magnitude. In NT embryos total *NANOG* was increased two-fold. There were no significant effects on the expression of the eight pluripotency-related genes investigated;

endogenous *NANOG*, *OCT4*, *SOX2*, *KLF4*, *FGF4*, *SOX17*, *PDGFRα*, and *SOCS3* in NT embryos. The expression of *XIST* was also not affected by the additional NANOG. No inactive X-chromosomes were detected via ICC, meaning that a direct comparison of localisation of expression of *XIST* and *NANOG* could not be achieved. There was no evidence for the presence of additional NANOG protein in induced embryos compared to controls.

4.6 Recommendations for future work

In the future, the clonality of the EOG_TET_NANOG cell line should be investigated. If one cell is strongly NANOG positive any daughter cell should also be strongly positive. Towards the end of this project some single cell colonies were derived from EOG_TET_NANOG. These cells should be stained for NANOG via ICC to see if they are homogeneously NANOG positive or if the resemble the results produced from the current EOG_TET_NANOG cell line. This will give insight into the function of the pTRE3G-mCherry vector and if it is stably expressed. Also, the expression of the pTRE3G-mCherry vector throughout the embryo needs to be investigated. Analysis of the trophectoderm in comparison to the ICM will illuminate issues that may arise with *NANOG* expression in tissues that it is not commonly expressed in. These tissues may possess alternative *NANOG* processing or the presence of NANOG could be detrimental to them. Effects of the temporal expression of *NANOG* should also be evaluated as it is only transiently expressed within the ICM and a thorough investigation of its constant expression will also reveal *NANOG* processing and or functional aspects. Further investigation should be conducted into the expression of the pTRE3G-mCherry vector and its IRES, because there was no evidence that there was any additional NANOG protein in the induced NT embryos.

There have been recent advances in the methods used for establishing genetic modifications. Some of these entail cytoplasmic injection which avoids the artefacts of NT cloning, but need to be carefully characterised for their efficiency of dispersal throughout the embryo before they can be used effectively. The most promising of these is the clustered regularly interspaced short palindromic repeats (CRISPR)/Cas9 system. This is an aspect of the bacterial immune system which evolved to defend against phages and plasmids [140]. It works by creating double

stranded breaks at a specific site in the genome. This system could be utilised by adapting the genetic sequence used to target specific sites in the genome. These breaks can then be used to genetically modify the sequence [141]. This CRISPR/Cas9 system has been investigated in livestock and has provided efficient new means of derivation of transgenic animals. [141]. Over other methods this technique has many advantages. The CRISPR/cas9 system is easy to use and has a fast protocol, it also has high-specificity DNA recognition [142]. A protocol has been established for using CRISPR/Cas9 in the generation of overexpression systems [143]. It can target the promotor of a gene and modulate endogenous gene expression. Human cancer cells were transfected with single-guide RNAs which targeted the promotor of *Nanog*. They were able to achieve a two-fold increase in *Nanog* expression [143]. This systems can also be applied in a multiplex, overexpressing or suppressing the expression of multiple genes simultaneously [143]. This will aid the understanding of complex molecular systems such as the pluripotency network. Future work similar to what was conducted in this thesis should be via the use of this system.

Another improvement would be in the genetic analysis of mRNA. The *RNA*GEM, cDNA synthesis protocols result in 21 µL. The current method of qPCR analysis requires between 1-2 µL of sample per gene analysed. This severely limits the number of genes that can be analysed. If a robust overexpression of *NANOG* was successfully established, single embryo analysis would be a better form of evaluation. There have been advances in the field of genetic analysis, for example the development of next generation sequencing. This has increased the rate at which experiments can be conducted, by analysing huge numbers of genes from just one sample. Soon this technology will become more available and could be more widely applied. Recent studies in New Zealand have used new technologies [37] such as the Nanostring nCounter technique. This offers gene expression analysis of up to 800 genes on one sample with a sensitivity that can detect one molecular copy per cell. For the NT embryo system this would identify target genes more efficiently from small sample numbers [144].

Chapter 5: **References**

1. Oback B., Huang B. (2014) Pluripotent stem cells from livestock. In: Calegari F., Waskow C., editors. Stem cells: From basic research to therapy, Volume two: Tissue homeostasis and regeneration during adulthood, applications, legislation and ethics. Boca Raton:FL: CRC Press; Taylor & Francis Group. pp. 305-346.
2. Thomson J., Itskovitz-Eldor J., Shapiro S., Waknitz M., Swiergiel J., et al. (1998) Embryonic stem cell lines derived from human blastocysts. Science 282: 1145-1147.
3. Stachelscheid H., Wulf-Goldenberg A., Eckert K., Jensen J., Edsbagge J., et al. (2013) Teratoma formation of human embryonic stem cells in three-dimensional perfusion culture bioreactors. Journal of Tissue Engineering and Regenerative Medicine 7: 729-741.
4. Martin G. (1981) Isolation of a pluripotent cell line from early mouse embryos cultures in medium conditioned by teratocarcinoma stem cells. Proceedings of the National Academy of Science of the United States of America 78: 7634-7638.
5. Smith A., Heath J., Donaldson D., Wong G., Moreau J., et al. (1988) Inhibition of pluripotential embryonic stem cell differentiation by purified polypeptides. Nature 336.
6. Williams R., Hilton D., Pease S., Willson T., Stewart C., et al. (1988) Myeloid leukaemia inhibitory factor maintains the developmental potential of embryonic stem cells. Nature 336: 684-687.
7. Ying Q., Nichols J., Chambers I., Smith A. (2003) BMP induction of Id proteins suppresses differentiation and sustains embryonic stem cell self-renewal in collaboration with STAT3. Cell 115: 281-292.
8. Buehr M., Meek S., Blair K., Yang J., Ure J., et al. (2008) Capture of authentic embryonic stem cells from Rat blastocysts. Cell 135: 1287-1298.
9. Li P., Tong C., Mehrian-Shai R., Jia L., Wu N., et al. (2008) Germline competent embryonic stem cells derived from Rat blastocysts. Cell 135: 1299-1310.
10. Smith A. (2001) Embryo derived stem cells: Of Mice and Men. Cell and Developmental Biology 17: 435-462.
11. Ying Q., Wray J., Nichols J., Batlle-Morera L., Doble B., et al. (2008) The ground state of embryonic stem cell self-renewal. Nature 453: 519-523.
12. Murray J., Campbell D., Morrice N., Auld G., Shpiro N., et al. (2004) Exploitation of KESTREL to identify NDRG family members as physiological substrates for SGK1 and GSK3. The Biochemical Journal 384: 477-488.
13. Mohammadi M., McMahon G., Sun L., Tang C., Hirth P., et al. (1997) Structures of the tyrosine kinase domain of fibroblast growth factor receptor in complex with inhibitors. Science 276: 955-960.
14. Davies S., Reddy H., Caivano M., Cohen P. (2000) Specificity and mechanism of action of some commonly used protein kinase inhibitors. The Biochemical Journal 351: 95-105.

15. Avilion A., Nicolis S., Pevny L., Perez L., Vivian N., et al. (2003) Multipotent cell lineages in early mouse development depend on SOX2 function. Genes and Development 17: 126-140.
16. Nichols J., Zevnik B., Anastassiadis K., Niwa H., Klewe-Nebenius D., et al. (1998) Formation of pluripotent stem cells in the mammalian embryo depends on the POU trasncription factor Oct4. Cell 95: 379-391.
17. Saunders A., Faiola F., Wang J. (2013) Pursuing self-renewal and pluripotency with the stem cell factor Nanog. Stem Cells 31: 1227-1236.
18. Chambers I., Colby D., Robertson M., Nichols J., Lee S., et al. (2003) Functional expression cloning of nanog, a pluripotency sustaining factor in embryonic stem cells. Cell 113: 643–655.
19. Mitsui K., Tokuzawa Y., Itoh H., Segawa K., Murakami M., et al. (2003) The homeoprotein Nanog is required for maintenance of pluripotency in mouse epiblast and ES cells. Cell 113: 631-642.
20. Chickarmane V., Troein C., Nuber U., Sauro H., Peterson C. (2006) Transcriptional dynamics of the embryonic stem cell switch. PLoS Computational Biology 2.
21. Zhang J., Li L. (2005) BMP signaling and stem cell regulation. Developmental Biology 284: 1-11.
22. Lanner F., Rossant J. (2010) The role of FGF/Erk signaling in pluripotent cells. Development 137: 3351-3360.
23. Kunath T., Saba-El-Leil M., Almousailleakh M., Wray J., Meloche S., et al. (2007) FGF stimulation of the Erk1/2 signalling cascade triggers transition of pluripotent embryonic stem cells from self-renewal to lineage commitment. Development 134: 2895-2902.
24. Nichols J., Smith A. (2009) Naive and primed pluripotent states. Cell: Stem Cell 4: 487-492.
25. Quinlan L. (2011) Signaling pathways in mouse embryo stem cell self-renewal. In: Kallos M., editor. Embryonic stem cells- Basic biology to bioengineering. Croatia: In Tech Europe. pp. 283-304.
26. Pereira L., Yi F., Merrill B. (2006) Repression of Nanog gene transcription by Tcf3 limits embryonic stem cell self-renewal. Molecular and Cellular Biology 26: 7479-7491.
27. Loh Y., Wu Q., Chew J., Vega V., Zhang W., et al. (2006) The Oct4 and Nanog transcription network regulates pluripotency in mouse embryonic stem cells. Nature Genetics 38.
28. Takahashi K., Yamanaka S. (2006) Induction of pluripotent stem cells from mouse embryonic and adult fibroblast cultures by defined factors. Cell 126: 663-676.
29. Takahashi K., Tanabe K., Ohnuki M., Narita M., Ichisaka T., et al. (2007) Induction of pluripotent stem cells from adult human fibroblasts by defined factors Cell 131: 861-872.
30. Pan G., Thomson J. (2007) Nanog and transcriptional networks in embryonic stem cell pluripotency. Cell Research 17: 43-49.
31. Silva J., Nichols J., Theunissen T., Guo G., van Oosten A., et al. (2009) Nanog is the gateway to the pluripotent ground state. Cell 138: 722-737.
32. Yates A., Chambers I. (2005) The homeodomain protein Nanog and pluripotency in mouse embryonic stem cells. Biochemical Society Transactions 33: 1518-1521.

33. Darr H., Mayshar Y., Benvenisty N. (2006) Overexpression of NANOG in human ES cells enables feeder-free growth while inducing primitive ectoderm features. Development 133.
34. Pant D., Keefer C. (2009) Expression of pluripotency-related genes during bovine inner cell mass explant culture. Cloning Stem Cells 11: 355-365.
35. Yang Q., Sarah F., Zhang K., Ozawa M., Johnson S., et al. (2011) Fibroblast growth factor 2 promotes primitive endoderm development in bovine blastocyst outgrowths. Biology of Reproduction 85: 946-953.
36. Kuijk E., Puy L., Van-Tol H., Oei C., Haagsman H., et al. (2008) Differences in early lineage segregation between mammals. Developmental Dynamics 237 918-927.
37. McLean Z., Meng F., Henderson H., Turner P., Oback B. (2014) Increased MAP kinase inhibition enhances epiblast-specific gene expression in bovine blastocysts. Biology of Reproduction 49.
38. Harris D., Huang B., Oback B. (2013) Inhibition of MAP2K and GSK3 signaling promotes bovine blastocyst development and epiblast-associated expression of pluripotency factors. Biology of Reproduction 88: 28.
39. Loh Y., Wu Q., Chew J., Vega V., Zhang W., et al. (2006) The Oct4 and Nanog transcription network regulates pluripotency in mouse embryonic stem cells. Nature Genetics 38: 431-440.
40. Jauch R., Leng Ng C., Saikatendu K., Stevens R., Kolatkar P. (2008) Crystal structure and DNA binding of the homeodomain of the stem cell transcription factor Nanog. Journal of Molecular Biology 376: 758-770.
41. Hart A., Hartley L., Ibrahim M., Robb L. (2004) Identification, cloning and expression analysis of the pluripotency promoting Nanog genes in mouse and human. Developmental Dynamics 230: 187-198.
42. Pan G., Pei D. (2003) Identification of two distinct transactivation domains in the pluripotency sustaining factor Nanog. Cell Research 13: 499-502.
43. Uniprot (2014) Homeobox protein NANOG.
44. Ramakrishna S., Suresh B., Lim K., Cha B., Lee S., et al. (2011) PEST motif sequence regulating human NANOG for proteasomal degradation. Stem Cell Development 20: 1511-1519.
45. Pan G., Thomson J. (2007) Nanog and transcriptional networks in embryonic stem cell pluripotency. Cell Research 17: 42-49.
46. Navarro P., Avner P. (2009) When X-inactivation meets pluripotency: An intimate rendezvous. FEBS Letters 583: 1721-1727.
47. Lyon M. (1961) Gene action in the X-chromosome of the mouse (Mus musculus L.). Nature 190: 372-373.
48. Heard E., Disteche C. (2006) Dosage compensation in mammals: fine-tuning the expression of the X chromosome. Genes and Development 20: 1848-1867.
49. Wrenzycki C., Lucas-Hahn A., Herrmann D., Lemme E., Korsawe K., et al. (2002) In Vitro production and nuclear transfer affect dosage compensation of the X-Linked gene transcripts G6PD, PGK, and Xist in preimplantation bovine embryos. Biology of Reproduction 66: 127-134.
50. Clerc P., Avner P. (2003) Multiple elements within the Xic regulate random X inactivation in mice Seminars in Cell & Developmental Biology 14: 85-92.
51. Froberg J., Yang L., Lee J. (2013) Guided by RNAs: X-Inactivation as a model for lncRNA function. Journal of Molecular Biology 425: 3698-3706.
52. Clemson C., McNeil J., Willard H., Lawrence J. (1996) XIST RNA paints the inactive X chromosome at interphase: evidence for a novel RNA involved

in nuclear/chromosome structure. Journal of Cellular Biology 132: 259-275.
53. Graeme P., Graham K., Sheardown S., Rastan S., Brockdorff N. (1996) Requirement for Xist in X chromosome inactivation. Nature 379: 131-137.
54. Silva J., Mak W., Zvetkova I., Appanah R., Nesterova T., et al. (2003) Establishment of histone h3 methylation on the inactive X chromosome requires transient recruitment of Eed-Enx1 polycomb group complexes. Developmental Cell 4: 481-495.
55. Marks H., Chow J., Denissov S., Françoijs K., Brockdorff N., et al. (2009) High-resolution analysis of epigenetic changes associated with X inactivation. Genome Research 19: 1361-1372.
56. Lee J., Davidow L., Warshawsky D. (1999) Tsix, a gene antisense to Xist at the X-inactivation centre. Nature Genetics 21: 400-404.
57. Sado T., Hoki Y., Sasaki H. (2005) Tsix silences Xist through modification of chromatin structure. Development of the cell 9: 159-165.
58. Ohhata T., Hoki Y., Sasaki H., Sado T. (2008) Crucial role of antisense transcription across the Xist promoter in Tsix-mediated Xist chromatin modification. Development 135: 227-235.
59. Ohhata T., Wutz A. (2013) Reactivation of the inactive X chromosome in development and reprogramming. Cell and Molecular Life Science 70: 2443-2461.
60. Jonkers I., Monkhors K., Rentmeester E., Grootegoed A., Frank Grosveld F., et al. (2008) Xist RNA is confined to the nuclear territory of the silenced X chromosome throughout the cell cycle. Molecular and Cellular Biology 28: 5583-5594.
61. Suraniemail M., Hayashi K., Hajkova P. (2007) Genetic and epigenetic regulators of pluripotency. Cell 128: 747-762.
62. Okamoto I., Otte A., Allis C., Reinberg D., Heard E. (2004) Epigenetic dynamics of imprinted X inactivation during early mouse development. Science 303: 644-649.
63. Navarro P., Chambers I., Karwacki-Neisius V., Chureau C., Morey C., et al. (2008) Molecular coupling of Xist regulation and pluripotency. Science 321: 5896.
64. Pasque V., Tchieu J., Karnik R., Uyeda M., Dimashkie A., et al. (2014) X chromosome reactivation dynamics reveal stages of reprogramming to pluripotency. Cell 159: 1681–1697.
65. Schulz E., Meisig J., Nakamura T., Okamoto I., Sieber A., et al. (2014) The two active X chromosomes in female ESCs block exit from the pluripotent state by modulating the ESC signaling network. Cell: Stem Cell 14: 203-216.
66. Dorret Boomsma D. ABLP (2002) Classical twin studies and beyond. Nature Reviews Genetics 3: 872-882.
67. Meissner A., Jaenisch R. (2006) Mammalian nuclear transfer. Developmental Dynamics: Mouse Development Special Issue 235: 2460-2469.
68. Spemann H. (1938) Embryonic development and induction. Yale Journal of Biology and Medicine 11: 95-96.
69. Briggs R., King T. (1952) Transplantation of living nuclei from blastula cells into enucleated frogs' eggs *. Proceedings of the National Academy of Science of the United States of America 38: 455-463.

70. Gurdon J, Elsdale T, Fischberg M (1958) Sexually mature individuals of Xenopus laevis from the transplantation of single somatic nuclei. Nature 182: 64–65.
71. Gurdon J. (1962) The developmental capacity of nuclei taken from intestinal epithelium cells of feeding tadpoles. Journal of Embryology and Experimental Morphology 10: 622-640.
72. Campbell K., McWhir J., Ritchie W., Wilmut I. (1996) Sheep cloned by nuclear transfer from a cultured cell line. Nature 380: 64-66.
73. Meng L., Ely J., Stouffer R., Wolf D. (1997) Rhesus monkeys produced by nuclear transfer. Biology of Reproduction 57.
74. Wakayama T., Perry A., Zuccotti M., Johnson K., Yanagimachi R. (1998) Full-term development of mice from enucleated oocytes injected with cumulus cell nuclei. Nature 394: 369-373.
75. Wakayama T., Rodriguez I., Perry A., Yanagimachi R., Mombaerts P. (1999) Mice cloned from embryonic stem cells. Proceedings of the National Academy of Science of the United States of America 96: 14984-14989.
76. Baguisi A., Behboodi E., Melican D., Pollock J., Destrempes M., et al. (1999) Production of goats by somatic cell nuclear transfer. Nature Biotechnology 17: 456-461.
77. Polejaeva I., Chen S., Vaught T., Page R., Mullins J., et al. (2000) Cloned pigs produced by nuclear transfer from adult somatic cells. Nature 407: 86-90.
78. Shin T., Kraemer D., Pryor J., Liu L., Rugila J., et al. (2001) A cat cloned by nuclear transplantation. Nature 415: 859.
79. Loi P., Ptak G., Barboni B., Fulka J., Cappai P., et al. (2001) Genetic rescue of an endangered mammal by cross-species nuclear transfer using post-mortem somatic cells. Nature Biotechnology 19: 962-964.
80. Lanza R., Cibelli J., Diaz F., Moraes C., Farin P., et al. (2000) Cloning of an endangered species (Bos gaurus) using interspecies nuclear transfer. Cloning 2: 79-80.
81. Chesné P., Adenot P., Viglietta C., Baratte M., Boulanger L., et al. (2002) Cloned rabbits produced by nuclear transfer from adult somatic cells. Nature Biotechnology 20: 366-369.
82. Galli C., Lagutina I., Crotti G., Colleoni S., Turini P., et al. (2003) Pregnancy: a cloned horse born to its dam twin. Nature 424: 635.
83. Lee B., Kim M., Jang G., Oh H., Yuda F., et al. (2005) Dogs cloned from adult somatic cells. Nature 436: 641.
84. Li Z., Sun X., Chen J., Liu X., Wisely S., et al. (2006) Cloned ferrets produced by somatic cell nuclear transfer. Developmental Biology 293: 439-448.
85. Zhou Q., Renard J., Le Friec G., Brochard V., Beaujean N., et al. (2003) Generation of fertile cloned rats by regulating oocyte activation. Science 302: 1179.
86. Cibelli J., Stice S., Golueke P., Kane J., Jerry J., et al. (1998) Cloned transgenic calves produced from nonquiescent fetal fibroblasts. Science 280: 1256-1258.
87. Kato Y., Tani T., Sotomaru Y., Kurokawa K., Kato J., et al. (1998) Eight calves cloned from somatic cells of a single adult. Science 282: 2095-2098.
88. Strachan T. (1999) Genetic manipulation of animals. New York, NY: Wiley-Liss.
89. Lai L., Prather R. (2003) Creating genetically modified pigs by using nuclear transfer. Reproductive Biology and Endocrinology 1.

90. Cho J., Bhuiyan M., Shin S., Park E., Jang G., et al. (2004) Development potential of transgenic somatic cell nuclear transfer embryos according to various factors of donor cell. The Journal of Veterinary Medical Science/ The Japanese Society of Veterinary Science 66: 1567-1573.
91. Clontech Laboratories Inc (2013) Tet-On® 3G inducible expression system. User Manual.
92. Krafft C., Hinrichs W., Orth P., Saenger W., Welfle H. (1996) Interaction of Tet repressor with operator DNA and with Tetracycline studied by infrared and raman spectroscopy. Biophysical Journal 74: 63-71.
93. Baron U., Schnappinger D., Helbl V., Gossen M., Hillen W., et al. (1999) Generation of conditional mutants in higher eukaryotes by switching between the expression of two genes. Proceedings of the National Academy of Science of the United States of America 96: 1013-1018.
94. Hellen C., Sarnow P. (2001) Internal ribosome entry sites in eukaryotic mRNA molecules. Genes and Development 15: 1593-1612.
95. The Bovine Genome Sequencing and Analysis Consortium, Elsik C., Tellam R., Worley K. (2009) The genome sequence of Taurine cattle: A window to ruminant biology and evolution. Science 324: 522-528.
96. Saito S., Strelchenko N., Nieman H. (1992) Bovine embryonic stem cell-like cell lines cultured over several passages. Roux's Archives of Developmetal Biology 201: 134-141.
97. Talbot N., Powell A., Rexroad C. (1995) In vitro pluripotency of epiblasts derived from bovine blastocysts. Molecular Reproduction and Development 36: 35-52.
98. Rexroad C., Powell A. (1998) Culture of blastomeres from in vitro-matured, fertilized, and cultured bovine embryos. Molecular Reproduction and Development 48: 238-245.
99. Vejlsted M., Avery B., Gjorret J., Maddox-Hyttel P. (2005) Effect of leukemia inhibitory factor (LIF) on in vitro produced bovine embryos and their outgrowth colonies. Molecular Reproduction and Development 70: 445-454.
100. Pant D., Keefer C. (2009) Expression of pluripotency-related genes during bovine inner cell sass explant culture. Cloning and Stem Cells 11: 355-365.
101. Anderson G., BonDurant R., Goffa L., Groffc J., Moyer A. (1996) Development of bovine and porcine embryonic teratomas in athymic mice. Animal Reproductive Science 45: 231-240.
102. Cibelli J., Stice S., Golueke P., Kane J., Jerry J., et al. (1998) Trasgenic bovine chimeric offspring produced from somatic cell-derived stem-like cells. Nature Biotechnology 16: 642-646.
103. Capecchi M. (2005) Gene targeting in mice: Functional analysis of the mammalian genome for the twenty-first century. Nature Reviews, Genetics 6: 507-512.
104. Behboodi E., Lam L., Gavin W., Bondareva A., Dobrinski I. (2013) Goat embryonic stem-like cell derivation and characterization. Methods in Molecular Biology 1074: 51-67.
105. Saito S., Ugai H., Sawaid K., Yamamotod Y., Minamihashid A., et al. (2002) Isolation of embryonic stem-like cells from equine blastocysts and their differentiation in vitro. FEBS Letters 531: 389-396.
106. Evans M., Notarianni E., Lauriea S., R. M (1990) Derivation and preliminary characterization of pluripotent cell lines from porcine and bovine blastocysts. Theriogenology 33: 125-128.

107. Piedrahita J., Anderson G., BonDurant R. (1990) On the isolation of embryonic stem cells: Comparative behavior of murine, porcine and ovine embryos. Theriogenology 34: 879-901.
108. Strojek R., Reed M., Hoover J., Wagner T. (1990) A method for cultivating morphologically undifferentiated embryonic stem cells from porcine blastocysts. Theriogenology 33: 901-913.
109. Wattiaux M. (2014) Reproduction and genetic selection. Dairy Essentials: Babcock institute.
110. Shin M. (2011) Mus musculus: Genetic portrait of the house mouse. Portraits of Model Organisms: McGraw-Hill Higher Education.
111. Jabed A., Wagner S., McCracken J., Wells D., Laible G. (2012) Targeted microRNA expression in dairy cattle directs production of β-lactoglobulin-free, high-casein milk. Proceedings of the National Academy of Science of the United States of America 109: 16811-16816.
112. Wal J. (1998) Cow's milk allergens. Allergy 53: 1013-1022.
113. Høst A. AAAI, Suppl 1):33–37 (2002) Frequency of cow's milk allergy in childhood. Annals of Allergy, Asthma and Immunology 89: 33-37.
114. Garrick D., Snell R. (2005) Emerging technologies for identifying superior dairy cows in New Zealand. New Zealand Veterinary Journal 53: 390-399.
115. Zhang L., Luo Y., Bou G., Kong Q., Huan Y., et al. (2011) Overexpression NANOG activates pluripotent genes in porcine fetal fibroblasts and nuclear transfer embryos. Developmental Biology 294: 1809-1817.
116. Zhang P., Andrianakos R., Yang Y., Liu C., Lu W. (2010) Kruppel-like factor 4 (Klf4) prevents embryonic stem (ES) cell differentiation by regulating Nanog gene expression. The Journal of Biological Chemistry 285: 9180-9189.
117. Niakan K., Ji H., Maehr R., Vokes S., Rodolfa K., et al. (2010) Sox17 promotes differentiation in mouse embryonic stem cells by directly regulating extraembryonic gene expression and indirectly antagonizing self-renewal. Genes and Development 24: 312-326.
118. Artus J., Panthier J., Hadjantonakis A. (2010) A role for PDGF signaling in expansion of the extraembryonic endoderm lineage of the mouse blastocyst. Development and Stem Cells 137: 3361-3372.
119. Krawchuk D., Honma-Yamanaka N., Anani S., Yamanaka Y. (2013) FGF4 is a limiting factor controlling the proportions of primitive endoderm and epiblast in the ICM of the mouse blastocyst. Developmental Biology 384: 65-71.
120. Stuart H., van Oosten A., Radzisheuskaya A., Martello G., Miller A., et al. (2014) NANOG amplifies STAT3 activation and they synergistically induce the naive pluripotent program. Current Biology 24: 340-346.
121. Wells D., Misica P., Tervit R. (1999) Production of Cloned Calves Following Nuclear Transfer with Cultured Adult Mural Granulosa Cells 1. Biology of Reproduction 60: 996-1005.
122. Berg D., Smith C., Pearton D., Wells D., Broadhurst R., et al. (2011) Trophectoderm lineage determination in cattle. Developmental Cell 20: 244-255.
123. Wells D., Misica P., Tervit H., Vivanco W. (1998) Adult somatic cell nuclear transfer is used to preserve the last surviving cow of the Enderby Island cattle breed. Reproduction, Fertility and Development 10: 369-378.

124. Oback B., Wiersema A., Gaynor P., Laible G., Tucker F., et al. (2003) Cloned cattle derived from a novel zona-free embryo reconstruction system. Cloning and Stem Cells 5: 3-12.
125. Life technologies Cell Culture Basics Handbook.
126. Wells D., Laible G., Tucker F. (2003) Coordination between donor cell type and cell cycle stages improves nuclear clining efficiency in cattle. Theriogenology 59: 45-59.
127. Miyoshi K., Rzucildo S., Pratt S. (2003) Improvements in cloning efficiencies may be possible by increasing uniformity in recipient oocytes and donor cells Biology of Reproduction 68: 1079-1086.
128. Piedrahita J., Wells D., Miller A. (2002) Effects of follicular size of cytoplast donor on the efficiency of cloning in cattle. Molecular Reproduction and Development 61: 317-326.
129. Oback B., Wells D. (2003) Methods paper: Cloning cattle. Cloning and stem cells 5: 243-256.
130. Coppola G., Pinton A., Joudrey E., Basrur P., King W. (2008) Spatial distribution of histone isoforms on the bovine active and inactive X chromosomes. Sexual Development 2: 12-23.
131. Gelehrter T., Tomkins G. (1969) Control of tyrosine aminotransferase synthesis in tissue culture by a facto in serum. Proceedings of the National Academy of Science of the United States of America 64: 723-730.
132. Rudlang P. (1974) Control of translation in cultured cells: Continued synthesis and accumulation of messenger RNA in nondividing cultures. Proceedings of the National Academy of Science of the United States of America 71: 750-754.
133. Graf A., Krebs S., Zakhartchenko V., Schwalb B., Blum H., et al. (2014) Fine mapping of genome activation in bovine embryos by RNA sequencing. Proceedings of the National Academy of Science of the United States of America 111: 4139-4144.
134. Choi B., Koo B., Ahn K., Kwon M., Kim J., et al. (2006) Tetracycline-inducible gene expression in nuclear transfer embryos derived from porcine fetal fibroblasts transformed with retrovirus vectors. Molecular Reproduction and Development 73: 1221-1229.
135. Avilion A., Nicolis S., Pevny L., Perez L., Vivian N., et al. (2003) Multipotent cell lineages in early mouse development depend on SOX2 function. Genes and Development 17: 126-140.
136. Mansha M., Wasim M., Ploner C., Hussain A., Latif A., et al. (2012) Problems encountered in bicistronic IRES-GFP expression vectors employed in functional analyses of GC-induced genes. Molecular Biology Reports 39: 10227-10234.
137. Erwin J., Lee J. (2013) Characterization of X-Chromosome Inactivation Status in Human Pluripotent Stem Cells. Current Protocols in Stem Cell Biology 12: B.6.1-1B.6.11.
138. Affymetrix I (2014) ViewRNATM ISH Cell Assay for Fluorescence RNA In Situ Hybridization (RNA FISH).
139. Verma V., Huang B., Kallingappa P., Oback B. (2013) Dual kinase inhibition promotes pluripotency in finite bovine embryonic cell Lines. Stem Cells and Development 22: 1728-1742.
140. Barrangou R., Fremaux C., Deveau H., Richards M., Boyaval P., et al. (2007) CRISPR provides acquired resistance against viruses in prokaryotes. Science 315: 1709-1712.

141. Ran F., Hsu P., Wright J., Agarwala V., Scott D., et al. (2013) Genome engineering using the CRISPR-Cas9 system. Nature Protocols 8: 2281-2308.
142. Cong L., Ran F., Cox D., Lin S., Barretto R., et al. (2013) Multiplex genome engineering using CRISPR/Cas systems. Science 339: 819-823.
143. Konermann S., Brigham M., Trevino A., Joung J., Abudayyeh O., et al. (2015) Genome-scale transcriptional activation by an engineered CRISPR-Cas9 complex. Nature 517: 583-588.
144. Kulkarni M. (2011) Digital multiplexed gene expression analysis using the NanoString nCounter system. Current Protocols in Molecular Biology 94: 1-25.

Appendices

Appendix 1: Fusion record sheet.

FBA Zona-Free **Experiment:**_____

Date:_____

Cell Data:_____

Drop No.	No. Cytos	Time Fused	No. Fused	No. not fused	Comments
1					
2					
3					
4					
5					
6					
7					
8					
9					
10					

Fusion Parameters

	Parameter 1	Parameter 2	Parameter 3
Amplitude			
µsec			

Fusion Rate

	No. fused	Total	Percent
1st Fusion			
Total			

	No. into ESOF –Ca	Time into ESOF –Ca	No. for Activation	Time HSOF + 1mg/ml	Time Ionomycin	Time into DMAP	No. into DMAP	Time into IVC	No. into IVC
1									
2									
3									
4									
5									
6									
7									
8									
9									
10									

Appendix 2: mCherry and GFP embryo grading sheet.

NT Run Number:

Treatment:

Embryo Number:	RFP	GFP	Embryo grade	Embryo Number:	RFP	GFP	Embryo grade
1				31			
2				32			
3				33			
4				34			
5				35			
6				36			
7				37			
8				38			
9				39			
10				40			
11				41			
12				42			
13				43			
14				44			
15				45			
16				46			
17				47			
18				48			
19				49			
20				50			
21				51			
22				52			
23				53			
24				54			
25				55			
26				56			
27				57			
28				58			
29				59			
30				60			

Appendix 3: Embryo grading record sheet.

Grading

Grader:	Run :	Experiment :	Date :

drop	total		1-cells	cDNA #
1. w-drop				
2. w-drop				

drop	total		1-cells	cDNA #
1. w-drop				
2. w-drop				

drop	total		1-cells	cDNA #
1. w-drop				
2. w-drop				

drop	total		1-cells	cDNA #
1. w-drop				
2. w-drop				

Grading

Grader:	Run :	Experiment :	Date :

drop	total		1-cells	cDNA #
1. w-drop				
2. w-drop				

drop	total		1-cells	cDNA #
1. w-drop				
2. w-drop				

drop	total		1-cells	cDNA #
1. w-drop				
2. w-drop				

drop	total		1-cells	cDNA #
1. w-drop				
2. w-drop				

Grading

Grader:	Run :	Experiment :	Date :

drop	total		1-cells	cDNA #
1. w-drop				
2. w-drop				

drop	total		1-cells	cDNA #
1. w-drop				
2. w-drop				

drop	total		1-cells	cDNA #
1. w-drop				
2. w-drop				

drop	total		1-cells	cDNA #
1. w-drop				
2. w-drop				

Appendix 4: Embryo grading regulations

Images from “Manual of the International Embryo Transfer Society” (3rd edition). Edited by David A. Stringfellow and Sarah M. Seidel. Published April 1988, International Embryo Transfer Society, 1111 North Dunlap Ave, Savoy, IL, USA.

When applied for the purposes of this research; 4= Tight Morula (TM), 5= Early blastocyst (EM), 6= Blastocyst (B), 7= expanded blastocyst (EB) and 8= hatched blastocyst (HB). The cycle day is the equivalent day at which the stage code would develop after fertilisation. Quality code or grade (1-3) is based on morphological characteristics depicted in each corresponding image. Comments about reasoning of morphological grade identified by the manual are presented as stated below.

Comments:

d) Single or small blastomeres comprise less than 15% of the total cellular material and the embryo is consistent with the expected stage of development.

e) Sperm on zona pellucida.

f) Embryos with many extruded cells or debris must be carefully rolled over to determine the presence and quality of any viable embryo mass.

g) Quality code 3 embryos have an embryo mass that is less than 50% of all cellular material within the zona pellucida.

h) This embryo has a nice but very small mass. If the embryo mass is less than 25% of all cellular material, it should be given a code 4 (non-viable).

i) Irregular shape is a common variation in blastocoel development.

j) Collapsing of the blastocoel is considered a normal physiological process that does not lower the quality grade.

k) Extruded cells in stage code 6, 7, and 8 embryos are often pressed against the zona pellucida and not obvious unless the embryo has collapsed due to normal physiological processes or when cryoprotective additive is introduced.

l) This embryo has a flat (even concave) surface of the zona pellucida that can cause the embryo to stick to the petri dish or straw. This defect alone keeps the embryo from being classified as quality grade 1 and should not be utilised in international commerce unless agreements allow for other than quality code 1 embryos.

m) Cellular debris on the surface of the zona pellucida shows that this embryo has not been washed by proper procedures.

n) This embryo has a cracked zona pellucida at the top of the picture. Embryos that do not have an intact zona pellucida should not be utilised in international commerce.

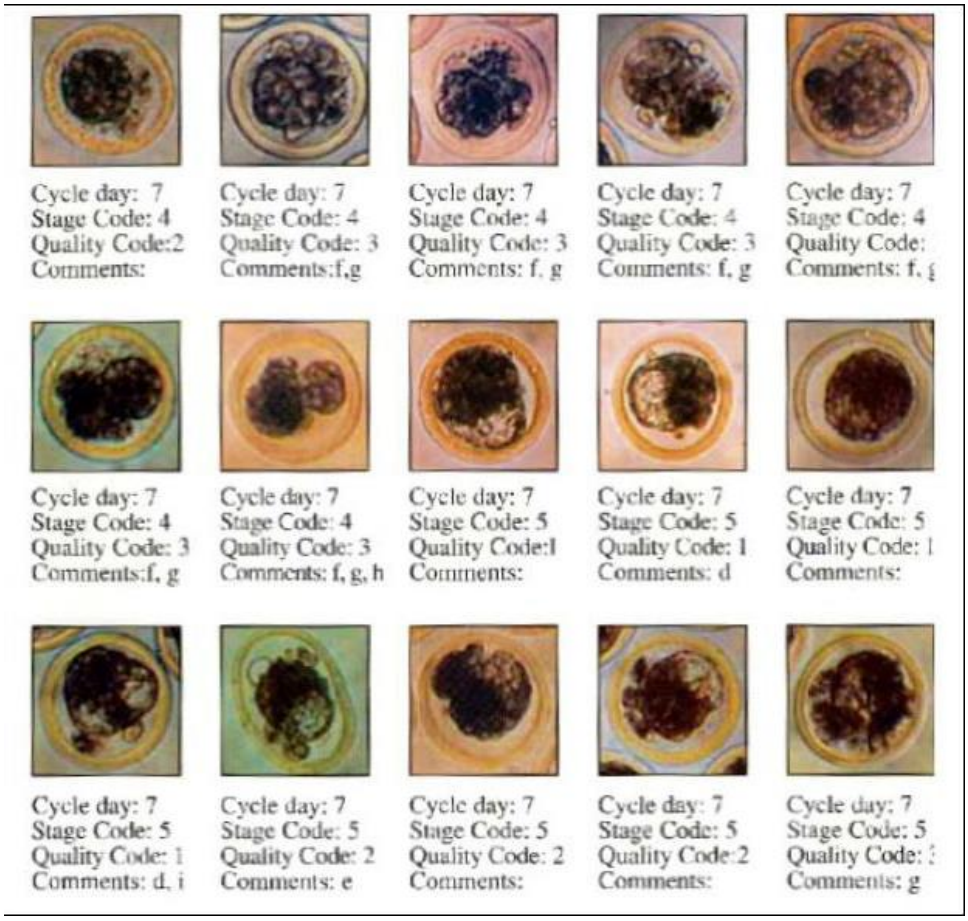

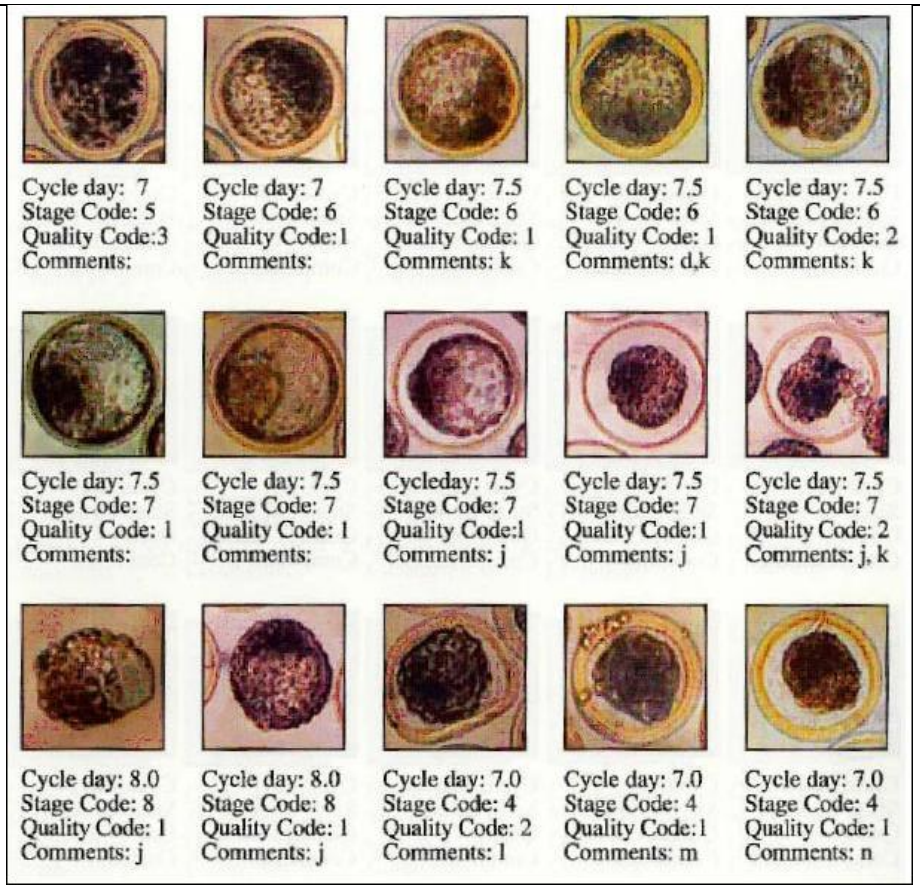
Cycle day: 7
Stage Code: 5
Quality Code:3
Comments:
Cycle day: 7
Stage Code: 6
Quality Code:1
Comments:
Cycle day: 7.5
Stage Code: 6
Quality Code: 1
Comments: k
Cycle day: 7.5
Stage Code: 6
Quality Code: 1
Comments: d,k
Cycle day: 7.5
Stage Code: 6
Quality Code: 2
Comments: k
Cycle day: 7.5
Stage Code: 7
Quality Code: 1
Comments:
Cycle day: 7.5
Stage Code: 7
Quality Code: 1
Comments:
Cycleday: 7.5
Stage Code: 7
Quality Code:1
Comments: j
Cycle day: 7.5
Stage Code: 7
Quality Code:1
Comments: j
Cycle day: 7.5
Stage Code: 7
Quality Code: 2
Comments: j, k
Cycle day: 8.0
Stage Code: 8
Quality Code: 1
Comments: j
Cycle day: 8.0
Stage Code: 8
Quality Code: 1
Comments: j
Cycle day: 7.0
Stage Code: 4
Quality Code: 2
Comments: l
Cycle day: 7.0
Stage Code: 4
Quality Code:1
Comments: m
Cycle day: 7.0
Stage Code: 4
Quality Code: 1
Comments: n